Open access to orbit and runaway space debris growth

Akhil Rao[1] and Giacomo Rondina[2*]

[1]Middlebury College[†]

[2]University of California, San Diego

January 16, 2022

Abstract

As Earth's orbits fill with satellites and debris, debris-producing collisions between orbiting bodies become more likely. Runaway space debris growth, known as Kessler Syndrome, may render Earth's orbits unusable for centuries. We present a dynamic physico-economic model of Earth orbit use under rational expectations with endogenous collision risk and Kessler Syndrome. When satellites can be destroyed in collisions with debris and other satellites, the open-access equilibrium manifold allows for multiple steady states. When debris can collide to produce more debris, at least one steady state may be a tipping point and Kessler Syndrome can occur along equilibrium paths. We show open access is increasingly and inefficiently likely to cause Kessler Syndrome as satellites become more profitable. Calibrated simulations reveal Kessler Syndrome is expected to occur in low-Earth orbit around 2048 under recent historical sectoral growth trends, and may occur as early as 2035 if the space economy grows consistent with projections by major investment banks. These results highlight the urgent need for modeling and policy approaches which incorporate open access and positive feedbacks in debris growth.

JEL codes: Q20, Q54, Q57, D62

Keywords: open-access commons, satellites, space debris, dynamic externality, tipping point

*We are grateful to Dan Kaffine, Jon Hughes, Martin Boileau, Miles Kimball, Alessandro Peri, Matt Burgess, Sami Dakhlia, Sébastien Rouillon, Martin Abel, David Munro, Derek Lemoine, participants at the University of Colorado Environmental and Resource Economics, Macroeconomics, and Applied Microeconomics seminars, and participants at the CU Boulder Environmental Economics workshop and the Western Economic Association International 2018 AERE sessions for helpful comments and feedback. We are especially grateful to Aditya Jain for excellent research assistance. Funding for this research was generously provided by Center for Advancement of Teaching and Research in Social Science and the Reuben A Zeubrow Fellowship in Economics. The latest version is available here. All errors are our own.

[†]Department of Economics, Warner Hall, 303 College Street, Middlebury College, 05753; akhilr@middlebury.edu

1 Introduction

Satellite services are increasingly important in the modern world. As humans launch more satellites, the risk of collisions between orbiting objects increases. Such collisions can destroy satellites and produce orbital debris, further increasing the risk of future collisions, threatening active satellites and the future of human use of outer space. The worst-case scenario is runaway debris growth, known as Kessler Syndrome, wherein the production of debris due to collisions between orbiting bodies becomes self-sustaining and irreversible. In such a scenario valuable regions of orbital space may become unusable and impassable for decades, centuries, or longer. While a social planner may wish to avoid such a scenario, the current legal and institutional regime is one of open access: anyone with a suitable rocket can place a satellite in any orbit they choose.

How will open access to orbit affect orbital debris accumulation, satellite collision risk, and the occurrence of Kessler Syndrome? How do short-run economic dynamics transition to long-run outcomes in orbit? If current institutions persist, when is Kessler Syndrome likely to occur? These questions are underexplored in economics and in the engineering and legal literatures.[1] In this paper, we build a quantitative dynamic economic model of satellite launching and conduct theoretical and numerical analysis to explore the consequences of open access to orbit. Our model is "fully coupled", allowing satellite and debris stocks to interact with themselves and each other. This feature is critical to understanding how and when economic behavior may cause or avoid Kessler Syndrome.

We highlight three main findings about open-access orbit use. First, we show the open-access equilibrium collision probability is determined by the excess rate of return on a satellite. This generates an equilibrium manifold as long as satellites can be destroyed by debris or other satellites. Open-access paths lead to the manifold, subject to initial conditions and launch rate constraints. Second, when collisions between debris produce more debris, Kessler Syndrome can occur along open-access paths. We show conditions under which open-access orbit users will cause Kessler Syndrome. We also derive the social planner's solution, decompose the steady-state marginal external cost, and numerically illustrate the inefficiency of open-access Kessler Syndrome. Third, we calibrate our model to an important region of low-Earth orbit and show that sectoral growth projections from investment banks and industry associations are consistent with open-access Kessler Syndrome occurring as early as 2035.

To contextualize our results and motivate our core model features, we offer some physical and institutional detail on orbit use. Satellites produce debris over their lifecycle. Launching

[1] Wienzierl (2018) highlights several issues in the development of a space economy, from space debris to coordination problems and market design, which economists are uniquely positioned to address.

satellites produces orbital debris (spent rocket stages, separation bolts), satellites can produce some debris while in orbit (paint chips, lost tools, etc.), and satellites which are not deorbited or shifted to disposal orbits at the end of their life become debris. Satellites struck by debris can shatter into thousands of hazardous debris fragments.[2] Compounding the problem, collisions between debris objects can generate even more hazardous high-velocity debris. Debris accumulation can cause a cascading series of collisions between orbital objects, creating a growing field of debris which can render an orbital region unusable and impassable for decades, centuries, or longer. Engineers call this phenomenon "collisional cascading" or "Kessler Syndrome" (Kessler and Cour-Palais, 1978). Kessler Syndrome can cause large economic losses, both directly from damage to active satellites and indirectly from limiting access to space (Bradley and Wein, 2009; Schaub et al., 2015). Existing estimates of debris growth indicate that the risk of Kessler Syndrome is highest in low-Earth orbit (LEO), where it threatens current and future imaging and telecommunications satellites and can reduce access to higher orbits (Kessler et al., 2010; Lewis, 2020). In the worst-case scenario Kessler Syndrome could completely block human access to space, marking an eventual end to services like GPS and satellite imaging. In 2019, the cost of a temporary GPS outage to the US private sector alone was estimated to be on the order of $1 billion per day, and as much as 50% higher if it occurred during the critical planting season (O'Connor et al., 2019). Long-run disruption of satellite services will make it harder to measure economic activity, reduce weather-related uncertainty, measure environmental degradation and respond to natural disasters, monitor environmental policy compliance, and meet conservation goals (Donaldson and Storeygard, 2016; Sullivan and Krupnick, 2018; Baragwanath et al., 2019; Jain, 2020; Cooke and Golub, 2020; Stroming et al., 2020; Bernknopf, Steinkruger, and Kuwayama, 2021). Further, development of the space economy is expected to contribute to terrestrial growth globally (Crane et al., 2020). Some estimates show debris production due to debris-debris collisions in higher reaches of LEO has already crossed the self-sustaining growth threshold (Liou and Johnson, 2008).

Existing legal frameworks for orbit use such as the Outer Space Treaty (OST) complicate the process of establishing orbital property rights and hinder debris cleanup efforts.[3] We offer a new perspective on how these institutions interact with orbital mechanics to make Kessler Syndrome possible, and a model environment in which alternative management institutions

[2]Objects in orbit move at velocities higher than 5 km/s, so debris as small as 10 cm in diameter can be hazardous to active satellites. Debris as low as 900 km above the Earth's surface can take centuries to deorbit naturally, while debris at 36000 km can take even longer (Weeden, 2010). Currently, there are more than 2,000 operating satellites in orbit, up to 600,000 pieces of debris large enough to cause satellite loss, and millions of smaller particles that can degrade satellite performance (Ailor et al., 2010). Over 80% of currently-active satellites are in low-Earth orbit, a share which is projected to grow in the near future (Union of Concerned Scientists, 2021).

[3]For example, Article 2 of the OST forbids national appropriation or claims of sovereignty over outer space, which is often interpreted as prohibiting national authorities from unilaterally establishing orbital property rights (Gorove, 1969).

can be explored quantitatively.[4]

As Stavins (2011) notes, management of the commons is among the central issues of economics. While open access problems have been well-studied in terrestrial settings such as fisheries, forests, climate, oil fields, traffic, and invasive species management (Gordon, 1954; Scott, 1955; Nordhaus, 1982; Libecap and Wiggins, 1985; Bohn and Deacon, 2000; Duranton and Turner, 2011; Huang and Smith, 2014), open access to orbital resources is not as well understood. Though results from these other settings provide some helpful intuition, open access and the orbital mechanics governing collision risk and debris production create unique physico-economic feedback loops. We extend the literature on how open access and a lack of property rights affects resource use and management to a new, increasingly-relevant context.

Commons problems, particularly in biophysical commons, often involve dynamic externalities and nonconvexities (Haveman, 1973; Brown Jr, 1974; Levhari and Mirman, 1980; Reinganum and Stokey, 1985; Farzin, 1996; Sherstyuk et al., 2016). Such issues also occur in arms races, growth, lake management, climate management, industrial development, and other settings with strategic or dynamic interactions and tipping points (Simaan and Cruz, 1975; Boldrin, 1992; Henderson, 1997; Mäler, Xepapadeas, and de Zeeuw, 2003; Hein, 2006; Lemoine and Traeger, 2014; Chavas, Grainger, and Hudson, 2016; Beaudry, Galizia, and Portier, 2020). Though results from other settings again offer helpful intuition, the unique physical properties of orbits create a novel dynamic externality problem which illuminates the natures of congestion and pollution more generally, particularly in the face of tipping points. We add to the literature on decentralized and optimal responses to interacting dynamic externalities by showing how profit-maximizing responses to congestion can limit pollution production, and biophysical conditions under which profit maximization leads to runaway pollutant accumulation due to a fold bifurcation. The bifurcation emerges due to fragment-generating collisions between debris objects (i.e. autocatalytic pollutant production), but is modulated by the degree to which debris reduces satellite profitability in the short run (i.e. pollution-induced congestion). We also identify an important difference between resource-use dynamics when the relevant capital stock is provided by nature (e.g. fish in fisheries) and when it is provided by humans (e.g. satellites in orbits): while increases in the discount rate make optimal resource collapse more likely for natural capital, they have the opposite effect for artificial capital.

Active satellites provide services to individuals, firms, governments, research agencies,

[4] Ostrom et al. (1999) provides some insight into why decentralized orbit management may face challenges. Orbit users are a diverse and international group, ranging from national militaries and intelligence agencies to corporations, universities, and wealthy individuals. Excluding potential users from orbital regions without creating additional debris is difficult, and the relevant conflict resolution mechanisms can be unclear. National regulatory regimes must also contend with "launch leakage", which has happened at least once already (Selk, 2017). Weeden and Chow (2012) discuss some of these issues in more detail.

and other entities. They tend to be information services like mobile broadband, images of the Earth, and positioning/timing. Adilov, Alexander, and Cunningham (2015) account for orbital product differentiation in a two-period setting. To focus on the dynamics of collisions and debris, we ignore such differentiation. Our paper bridges the short-term and long-term physical and economic dynamics of perfectly-competitive open-access and socially-optimal orbit use in a physically-general environment where Kessler Syndrome can occur over multiple periods, and is the first to provide economically-grounded estimates of the time until Kessler Syndrome occurs. While Sandler and Schulze (1981) account for collision risk when studying geostationary belt position allocation, debris accumulation and general orbital regions are not considered. Our analysis generalizes those presented in Macauley (2015); Adilov, Alexander, and Cunningham (2015, 2018), Grzelka and Wagner (2019), and Rouillon (2020) in the physical dimensions by allowing non-stationary dynamics and runaway debris growth, and clarifies the sources of external effects by explicitly considering the economics of general forms of couplings between physical state variables. While our model is most similar to that of Rouillon (2020), we generalize the analysis by considering a planner who owns both the current stock of satellites in orbit as well as the rights to launch to that orbit in perpetuity, and by allowing debris to collide with other debris. The former generalization allows us to decompose the marginal external cost of satellites into three channels (congestion, pollution, and debris persistence), while the latter generalization is relevant for analyzing long-run orbit use (Lewis, 2020). Unlike Rao (2018), Grzelka and Wagner (2019), Rao, Burgess, and Kaffine (2020), and Béal, Deschamps, and Moulin (2020), we focus primarily on economic dynamics rather than policy instrument design. However, as is the case with climate management, the positive feedbacks we incorporate are likely important for optimal orbital-use policy design (Lemoine and Traeger, 2016; Daniel, Litterman, and Wagner, 2019; Dietz et al., 2021b,a). Because we explicitly model the physical processes leading to Kessler Syndrome, we are able to calibrate our model to an important region of LEO and estimate the time when Kessler Syndrome occurs under continued open-access management and historically-plausible sectoral growth patterns.

Though prior work has established that the open-access launch rate exceeds the socially-optimal launch rate and results in excess collision risk and debris production (Adilov, Alexander, and Cunningham, 2015; Rouillon, 2020), our framework yields the novel insight that an open-access equilibrium manifold can exist due to couplings between satellites and debris in the collision risk function. This manifold contains all of the steady states and, combined with initial conditions and launch rate constraints, determines the steady-state approach paths. Under certain conditions open-access paths can cause Kessler Syndrome, in which case a steady state will never be reached. Our results contrast with those in Adilov, Alexander, and Cunningham (2018), where open access is found to never cause Kessler Syndrome as orbits become economically unprofitable before they become physically unusable ("economic Kessler Syn-

drome"). The contrast is due to our differing definitions of Kessler Syndrome and degrees of physical generality. Adilov, Alexander, and Cunningham (2018) consider a definition of Kessler Syndrome where satellites are destroyed with probability one ("unusable orbits") and disallow collisions between debris objects—as long as the collision probability is below one this definition states Kessler Syndrome has not occurred, and as long as launch activity ceases the debris stock eventually decays. We define Kessler Syndrome as states where the debris stock diverges to infinity ("runaway debris growth") and allow collisions between debris objects. Both features are critical for understanding orbit-use dynamics, as collisions between debris are becoming increasingly likely and are expected to dominate the long-run dynamics of the orbital environment (Davenport, 2020; Lewis, 2020). Once runaway debris growth occurs in our model, the collision probability will eventually reach one (runaway debris growth eventually renders orbits unusable), but it may only happen over a span of decades or centuries. Though launch activity may cease before orbits are unusable, if the Kessler threshold has been crossed this will not stop ongoing debris accumulation. Thus, our definition encompasses the one in Adilov, Alexander, and Cunningham (2018) while allowing Kessler Syndrome to occur over time due to dynamic feedbacks. Finally, the physical detail of our model allows us calibrate parameters to an important region of LEO and estimate the likely time when Kessler Syndrome will occur under continued open-access management. As in Rouillon (2020); Rao, Burgess, and Kaffine (2020), and Béal, Deschamps, and Moulin (2020), we use constant payoffs and costs per satellite to derive theoretical results. However, to calibrate the model and estimate the time till Kessler Syndrome occurs we allow both to vary over time and allow the per-period payoff to depend on the satellite stock. We find that the average growth of returns to operating a satellite and the "orbital occupancy elasticity of satellite payoffs" are key economic parameters determining whether and when Kessler Syndrome occurs under open access.

This paper is organized as follows. In section 2 we describe the core physical model. In section 3 we describe the core economic model. In section 4 we derive dynamic properties of open-access equilibria. In section 5 we pose the planner's problem, decompose the marginal external cost of a satellite, and study cases where Kessler Syndrome is inefficient. In section 6 we generalize our core physico-economic model and calibrate it to the 600-650 km orbital region. We use the calibrated model to simulate open-access LEO use and estimate the time until Kessler Syndrome occurs under alternate space economy growth projections. We discuss our results in context of other natural resource management problems in section 7, and conclude in section 8.

2 Physical model

Consider a spherical shell around the Earth, say the region between 600-650 km above mean sea level. Active satellites and debris move through the orbital shell ("orbit") in elliptical paths. Influences from the Earth and other celestial bodies perturb their motion and may cause their paths to intersect, upon which the colliding bodies shatter into debris fragments. The stock of active satellites in the orbit is periodically replenished by new launches, which may bring with them more debris. While active satellites expend fuel to counteract the perturbations they face, debris do not and eventually fall back to Earth and burn up in the atmosphere. If the supply of satellites is high enough for long enough, the production of debris from collisions may become self-sustaining.[5]

The number of active satellites in orbit in period $t+1$ (S_{t+1}) is the number of launches in the previous period (X_t) plus the number of satellites which survived the previous period ($S_t(1-L(S_t,D_t))$). The amount of debris in orbit in $t+1$ (D_{t+1}) is the amount from the previous period which did not decay ($D_t(1-\delta)$), plus the number of new fragments created in collisions ($G(S_t,D_t)$), plus the amount of debris in the shell created by new launches (mX_t).[6] The laws of motion for the satellite and debris stocks formalize this:

$$S_{t+1} = S_t(1-L(S_t,D_t)) + X_t \tag{1}$$

$$D_{t+1} = D_t(1-\delta) + G(S_t,D_t) + mX_t. \tag{2}$$

$L(S_t,D_t)$ is the proportion of orbiting active satellites which are destroyed in collisions, and $G(S_t,D_t)$ is the number of new fragments created by collisions between orbiting bodies. Since we assume active satellites are identical, $L(S_t,D_t)$ is also the probability an individual satellite is destroyed in a collision. We assume that the collision probability is twice continuously differentiable, nonnegative, increasing in each argument, and bounded below by 0 and above by 1.[7] $\delta > 0$ is the rate of orbital decay for debris, and $m \geq 0$ is the amount of launch

[5] This "shell of interest" approach is frequently used in debris modeling, e.g. Rossi et al. (1998) and Bradley and Wein (2009), though higher fidelity models use large numbers of small regions to track individual objects, e.g Liou et al. (2004), Liou and Johnson (2008), and Liou and Johnson (2009b). Paths which span shells are possible and useful for some applications, but highly elliptical orbits (such as Molniya orbits) are the exception rather than the rule. A Molniya orbit has a low perigee over the Southern Hemisphere and a high apogee over the Northern Hemisphere. Molniya orbits require less power to cover regions in the Northern Hemisphere (e.g. former Soviet Union countries) than geosynchronous orbits, due to the low incidence angles of rays from the Northern Hemisphere to geosynchronous positions.

[6] Satellites eventually cease being productive and their orbits eventually decay without fuel expenditure to maintain their path, features we abstract from in the main model. This abstraction makes some results a little clearer but does not qualitatively affect them. Rouillon (2020) includes these features in the main model and derives qualitatively similar results, albeit in a continuous-time setting. We include limited lifetimes, time-varying payoffs and costs, and state-dependent satellite payoffs in our calibrated simulations in section 6.

[7] Satellite operators try to avoid collisions by maneuvering their satellites when possible; the collision probability in this model should be thought of as the probability of collisions which could not be avoided, with easily avoided

debris created by new satellites.

We assume the new-fragment function G is twice continuously differentiable, nonnegative, strictly increasing in each argument, zero when there are no objects in orbit ($G(0,0) = 0$), and unbounded above ($\lim_{S\to\infty} G(S,D) = \lim_{D\to\infty} G(S,D) = \infty$). We also assume the effect of the first satellite or debris fragment on new fragment formation is negligible, i.e. $G_S(0,D) = G_D(S,0) = 0$ (letting subscripts denote partial derivatives).

Definition 1. *(Launch policy) The launch policy $X(S_t,D_t) \equiv X_t$ is a mapping from orbital states at time t to a launch rate at time t, where $X : \mathbb{R}^2_+ \to \mathbb{R}$.*

Definition 2. *(Fragment autocatalysis rate) The fragment autocatalysis rate is the net rate of fragment growth due to marginal debris objects. Formally,*

$$G_D(S,D) - \delta.$$

Positive fragment autocatalysis rates are a necessary condition for existence of unstable fixed points of long-run orbit use under open access (described precisely in Proposition 3), and are associated with Kessler Syndrome. Figure 3 illustrates this connection. We allow the fragment autocatalysis rate to become positive if the object stocks are large enough, but at low levels the rate is naturally negative.[8] Formally, we assume that for any value of S, there exists a value of D such that $G_D(S,D) > \delta$.

Definition 3. *(Kessler Syndrome) The Kessler region for a launch policy X is the set of states (satellite and debris levels) such that under X the debris stock will grow to infinity, i.e.*

$$\kappa_X \equiv \{(S,D) : \lim_{\tau\to\infty} D_{\tau+1} = \infty \mid S_t = S, D_t = D, X_t = X(S_t,D_t), \tau \geq t\}$$

Kessler Syndrome occurs when the satellite and debris stocks enter the Kessler region, i.e. $(S_t,D_t) \in \kappa_X$.

This definition of Kessler Syndrome can accommodate open access, optimal management, or any other type of orbital management institution.[9] Continued collision activity will eventually reduce the size of debris objects until they no longer pose a threat, but such reductions

collisions optimized away. Collisions which could have been avoided but were not due to human error are included in L. Implicitly we are assuming operators are imperfect cost-minimizers when maneuvering satellites. Even when operators can maneuver their satellites and are aware of impending collisions, coordination can be challenging and plagued by technical glitches (Brodkin, 2017).

[8] This assumption is consistent with long-run engineering studies of the evolution of the orbital environment, e.g. Liou (2006a); Lewis (2020).

[9] In Kessler and Cour-Palais (1978), collisional cascading is defined as one of the "possible consequences of continuing unrestrained launch activities". "Unrestrained launch activities" is not defined precisely, though that paper and other engineering studies of the debris environment typically assume either continuation of historical trends indefinitely or continuation with total launch cessation at an arbitrary date (Rossi et al., 1998; Liou, 2006b; Bradley and Wein, 2009). Open-access launch behavior is consistent with "unrestrained launch activities", current legal institutions

may take a very long time given the high energies involved. We define the *unavoidable Kessler region*, where Kessler syndrome will occur even if there are no new launches, as the Kessler region under a never-launch policy, i.e.

$$\kappa_0 \equiv \{(S,D) : \lim_{\tau\to\infty} D_{\tau+1} = \infty \mid S_t = S, D_t = D, X_t \equiv 0, \tau \geq t\}.$$

The unavoidable Kessler region is a subset of the Kessler region for any launch policy constrained to have nonnegative numbers of launches ($\kappa_0 \subseteq \kappa_X \ \forall X : X_t \geq 0 \ \forall t$), i.e. a policy without satellite and debris removal technologies.

Using the definition of the Kessler region for a launch policy, we define the *Kessler threshold* of a launch policy, D_X^κ. The Kessler threshold of a launch policy is the maximum sustainable debris level given that policy:

$$D_X^\kappa \equiv \sup\{D : (S,D) \notin \kappa_X\}. \tag{3}$$

We characterize D_X^κ analytically for open access, and compute examples of the Kessler regions under open access and optimal management.

Finally, we define the *Kessler time* under a launch policy, T_X^κ. The Kessler time of a launch policy is the time at which the Kessler threshold is crossed under that policy:

$$T_X^\kappa \equiv \inf\{t : (S_t, D_t) \in \kappa_X\}. \tag{4}$$

We calibrate our model to the 600-650 km shell and estimate the open-access Kessler time.

For orbits where the fragment autocatalysis rate is negative for all satellite and debris levels, Kessler Syndrome is impossible. Our assumption that the new fragments function G is monotonically increasing in both arguments, and the lack of debris removal technologies, imply that Kessler Syndrome is an absorbing state. Intuitively, the Kessler threshold is increasing in the decay rate, making lower-altitude orbits (where drag from the Earth's atmosphere makes debris decay faster than higher orbits) physically less vulnerable to Kessler Syndrome than higher-altitude orbits.

around orbit use, and economic behavior. In Kessler et al. (2010), "runaway debris growth" is defined in terms of a launch policy which holds the stock of "intact objects" (active satellites and unfragmented debris objects) constant. Such a policy is less consistent with rational economic behavior—eventually the required rate of replacement should make launchers prefer to invest their funds elsewhere. In any case, our definition encompasses all such definitions and makes the dependence on the launch policy explicit.

2.1 Three types of physical couplings

We use "physical coupling" to refer to ways that variables in the laws of motion for satellite and debris stocks are connected to each other. These couplings give structure to the laws of motion and drive the physical dynamics of orbit use. There are five economically-relevant physical couplings between objects in orbit, which we group into three types: the collision probability satellite coupling and collision probability debris coupling (the first type); the new fragment formation satellite coupling and new fragment formation debris coupling (the second type); and the launch debris coupling (the third type). If all five couplings were turned off, there would be no problems of excess satellite congestion or debris accumulation. The strength of a coupling between X and $f(\cdot)$ is the value of $\frac{\partial f}{\partial X}$, with $\frac{\partial f}{\partial X} = 0$ when there is no coupling. Principles of orbital mechanics imply any non-zero coupling is positive.

The collision probability couplings The collision probability couplings refer to the arguments of the collision probability function, L. When these couplings are turned off, the collision probability is exogenous: $L(\cdot) = L$. If the collision probability is exogenous, there is no congestion externality even when the probability varies over time. Even if open access causes Kessler Syndrome due to other couplings, the open-access launch rate is efficient in the sense that the planner would produce the same outcome.

If the collision probability is coupled with the satellite stock ($L(\cdot) = L(S)$), then there can be a "steady state" congestion externality. Despite any other couplings and their effects on debris growth, the only source of inefficiency is that open access results in too many satellites in orbit relative to the optimal plan. This describes a world where debris is harmless but active satellites aren't perfectly coordinated to avoid collisions with each other. If the collision probability is coupled with the debris stock ($L(\cdot) = L(D)$) but not the satellite stock, there can be a "dynamic" congestion externality. Due to debris accumulation and the coupling, there can be persistent consequences for specific launch histories. This describes a world where active satellites are perfectly coordinated to avoid collisions with each other, but debris are hazardous and not always successfully avoided. Such a function might be a good representation of the situation in the geostationary belt, where active satellites are coordinated to have virtually no motion relative to each other but debris objects are not. The "fully coupled" case links collision probability to both the satellite and debris stocks ($L(\cdot) = L(S,D)$). In this world, active satellites face collision risk from debris and each other. Adilov, Alexander, and Cunningham (2015, 2018) focus on a collision probability function with only a debris coupling. Rouillon (2020) focuses on the steady state and abstracts from the details of the collision probability couplings. The existence of both collision probability couplings allows us to define the marginal rate of technical substitution between satellites and debris in producing collision probability, $\frac{L_D}{L_S}$, which we show in Proposition 3 to be important in determining to the stability of open-access

steady states.

The launch debris coupling The launch debris coupling refers to the amount of launch debris created by a new launch, i.e. the parameter m in the debris law of motion $\left(\frac{\partial D_{t+1}}{\partial X_t} = m\right)$. When collision probability is coupled with the debris stock, the launch debris coupling reduces the equilibrium and optimal number of launches per period, since launches themselves produce debris. Thus, the launch debris coupling can "stabilize" open-access orbit use by forcing operators to internalize some of the persistent effects of their launches, shown in Proposition 3.

The new fragment formation couplings The new fragment formation couplings refer to the arguments of the new fragment function, $G(\cdot)$. If the new fragment function is coupled to the satellite stock, $G(\cdot) = G(S)$ (a world where only active satellites fragment upon collision), then there can be persistent consequences of excess satellite levels. When the new fragment function is coupled to the debris stock, $G(\cdot) = G(D)$ (a world where only debris fragment upon collision), there can be multiple open-access steady states and Kessler Syndrome becomes possible. This multiplicity will exist independent of the collision probability and launch debris couplings. When the collision probability is only coupled to the satellite stock or uncoupled ($L(\cdot) = L(S)$ or $L(\cdot) = L$), the multiplicity is only in debris levels. When the collision probability is fully coupled ($L(\cdot) = L(S,D)$) and the new-fragment function is coupled with only the debris stock, multiple open-access steady states in both satellites and debris can exist: one with low debris and high satellites, and one with high debris and low satellites. In both cases, only the low-debris equilibrium is stable. Adilov, Alexander, and Cunningham (2015, 2018) focus on new-fragment formation functions coupled only to the satellite stock.

For simulations and figures, we use the following fully-coupled functional forms:

$$L(S,D) = 1 - e^{-\alpha_{SS}S - \alpha_{SD}D} \tag{5}$$

$$G(S,D) = \beta_{SS}(1 - e^{-\alpha_{SS}S})S + \beta_{SD}(1 - e^{-\alpha_{SD}D})S + \beta_{DD}(1 - e^{-\alpha_{DD}D})D, \tag{6}$$

where $\alpha_{SS}, \alpha_{SD}, \alpha_{DD}, \beta_{SS}, \beta_{SD}, \beta_{DD}$ are all positive physical parameters. We derive these forms and give some physical intuition about the parameters in Appendix A.3. We describe how we calibrate these parameters for simulations and estimation of the open-access Kessler time in section 6 and Appendix A.3.2. The functional forms do not affect our qualitative results.

3 Economic model

In our model satellites are identical, infinitely lived unless destroyed in a collision, and produce a single unit of output per period. The net payoff from this output is $\pi > 0$, and each satellite costs $F > \pi$ to plan, build, and launch.[10,11] The market for satellite output is perfectly competitive, and the private marginal benefit of satellite output is the same as its social marginal benefit.[12] Costs and payoffs are constant over time. While these assumptions facilitate theoretical analysis and intuition, we relax them for the calibrated simulations in section 6, allowing for finite satellite lifetimes, time-varying costs and payoffs, and payoffs which depend on the current stock of active satellites in the shell.

We consider two scenarios: open access by profit-maximizing firms which can own up to one satellite at a time—or equivalently that all firms are choosing whether or not to launch identical constellations of satellites at any given time, changing the units of S_t from individual satellites to constellations—and launching controlled by a fleet planner who owns all satellites.[13] We focus on the open-access problem in this section and the following, deferring discussion of the social planner's problem until section 5.

The value of a satellite, $Q(S_t, D_t)$, is the sum of present payoffs and the expected discounted value of its remaining lifetime payoffs:

$$Q(S_t, D_t) = \pi + \frac{1}{1+r}(1 - L(S_t, D_t))Q(S_{t+1}, D_{t+1}), \tag{7}$$

[10] This is a simplification to focus on the margin of launch decisions. Operational costs like managing receiver stations on the ground or monitoring the satellite to perform stationkeeping are incurred each period, and may push $\pi \leq 0$. We assume that the firms have correctly forecasted $\pi > 0$ before deciding to launch. This also allows us to abstract from the margins of decisions to sell or deorbit satellites, or to purchase already-orbiting satellites.

[11] Assuming $F > \pi$ allows us to ignore the uninteresting case where satellites are always profitable to launch even if they only survive for a single period.

[12] In reality, satellites generate both external costs and external benefits, e.g. GPS is provided for free. We abstract from the external benefits to focus on the dynamics of managing the negative externalities from debris and collision probability.

[13] Our assumption that each firm is identified with a single satellite is equivalent to assuming that either the marginal satellite in an equilibrium is launched by such a firm, or that firms may own multiple satellites but ignore their inframarginal satellites in launching. In either case we could obtain the same equilibrium condition given by equation 11 below. Rouillon (2020) uses the latter interpretation and arrives at an equivalent equilibrium condition (the condition in Rouillon (2020) is the continuous-time limit of ours with finite satellite lifetimes). We maintain our stricter interpretation to avoid the complications of solving the dynamic satellite inventory management problem facing a constellation owner outside the steady state, with the attendant assumptions about when and how they choose to refresh their constellation. See Adilov et al. (2019) for a model of GEO satellite inventory management. Versions of those orbital warehousing issues are also relevant to LEO constellation management, with additional dynamic and strategic complications through the collision probability and debris growth functions. The constellation management problem is eminently important to study, but given the complications we leave it to future research. As long as there exists a marginal potential launcher who is considering the profitability of a single satellite, our results hold.

where X_t is the aggregate launch rate based on each potential launcher's entry decision $x_{it} \in \{0,1\}$, and $r > 0$ is the discount rate. Firms cannot choose to deorbit satellites.[14] The maximum number of launches possible in one period is $\bar{X}$.[15]

A firm which does not own a satellite in period t decides whether to pay F to plan, build, and launch a satellite which will reach orbit and start generating payoffs in period $t+1$, or to wait and decide again in period $t+1$.[16] All potential launchers are risk-neutral profit maximizers, and the value of potential launcher i at the beginning of period t is

$$V_i(S_t, D_t, X_t) = \max_{x_{it} \in \{0,1\}} \{(1-x_{it}) \frac{1}{1+r} V_i(S_{t+1}, D_{t+1}, X_{t+1}) + x_{it} \left[\frac{1}{1+r} Q(S_{t+1}, D_{t+1}) - F \right] \} \tag{8}$$

$$\text{s.t. } S_{t+1} = S_t(1 - L(S_t, D_t)) + X_t \tag{1}$$

$$D_{t+1} = D_t(1-\delta) + G(S_t, D_t) + mX_t \tag{2}$$

While firms may choose to launch or not, all satellites earn *ex-ante* identical payoffs.

3.1 Open-access equilibrium

An open-access equilibrium is a launch rate such that, given the current state and laws of motion, launching firms earn zero profits. We define this formally below.

Definition 4. *(Open-access equilibrium) An open-access equilibrium is a launch rate $X_t \in [0, \bar{X}]$ and a state (S_t, D_t) such that the marginal potential launcher i in period t earns zero profits ($V_i(S_t, D_t, X_t) = 0$), subject to the laws of motion of the satellite and debris stocks (equations 1 and 2) at the current state (S_t, D_t). Formally, an open-access equilibrium is a vector*

[14] This assumption does not matter in our setting, where satellite payoffs and launch costs are common to all firms and constant over time: if it is ever profitable to launch in this setting, it is never profitable to deorbit. Generating nontrivial dynamics from the option to deorbit requires heterogeneous and time-varying payoffs or costs. We abstract from this to keep the dynamical analysis manageable but this is an interesting avenue for future research.

[15] For theoretical analysis we assume the launch rate constraint does not bind except in scenarios where we illustrate those effects specifically.

[16] Physical interactions in orbit occur continuously while launch decisions do not. Historically, the median time to build for a geostationary satellite has been 3.5 years (TelAstra, Inc., 2017). While LEO satellites take less time to build, launches to LEO are still constrained by the availability of launch windows. Globally, launch windows are typically available in clusters no closer than two weeks apart, and launches may be postponed for days or weeks at the last minute due to inclement weather (Union of Concerned Scientists, 2020). We include the one-period lag from the decision to launch to the beginning of a satellite's productive life to capture this gap in timescales. We describe the importance of accounting for the difference in timescales when calibrating the model in Appendix A.3.

(X_t, S_t, D_t) *such that*

$$V_i(S_t, D_t, X_t) = 0 \tag{9}$$

$$s.t.\ \ S_{t+1} = S_t(1 - L(S_t, D_t)) + X_t \tag{1}$$

$$D_{t+1} = D_t(1-\delta) + G(S_t, D_t) + mX_t. \tag{2}$$

An open-access equilibrium is interior if $X \in (0, \bar{X})$.

Using definition 4, we obtain the interior-equilibrium present value of owning a satellite in period $t+1$:

$$X_t \in (0, \bar{X}) :\ V_i(S_t, D_t, X_t) = 0 \tag{10}$$

$$\implies \frac{1}{1+r} Q(S_{t+1}, D_{t+1}) = F. \tag{11}$$

Equation 11 is the condition which defines an interior open-access equilibrium. The resulting value of a satellite is the period profit plus the expected value of its survival under open access (substituting equation 11 into equation 7),

$$Q(S_t, D_t) = \pi + (1 - L(S_t, D_t))F. \tag{12}$$

Equations 11 and 12 can be rewritten to show that in an interior equilibrium the flow of benefits generated by a satellite is equated with the flow of opportunity costs and expected collision costs (the marginal private costs of satellite ownership):

$$F = \frac{1}{1+r} Q(S_{t+1}, D_{t+1}) \tag{13}$$

$$\implies \pi = rF + L(S_{t+1}, D_{t+1})F. \tag{14}$$

Using equation 14 we define $\rho(X_t, S_t, D_t) = \frac{\pi}{F} - r - L(S_{t+1}, D_{t+1})$ as the collision-risk-adjusted return on a satellite.[17] Then given a state (S_t, D_t), the open-access launch rate in t is $\hat{X}_t$, where

$$\hat{X}_t \in (0, \bar{X}) \text{ if } \rho(S_t, D_t, \hat{X}_t) = 0, \tag{15}$$

with $\hat{X}_t = 0$ if $\rho(S_t, D_t, 0) < 0$ and $\hat{X}_t = \bar{X}$ if $\rho(S_t, D_t, \bar{X}) > 0$.

An open-access path is a sequence of launch rates such that an open-access equilibrium holds in each period.

[17] The expected collisions cost term in equation 14, $L(S_{t+1}, D_{t+1})F$, is analogous to a default premium required by satellite operators to compensate them for the probability that their asset will "default" through destruction. In this way, satellites can be thought of as risky assets similar to corporate bonds, e.g. Fons (1987).

Definition 5. *(Open-access paths) An open-access path is a sequence of launch rates,* $\{X_t\}_{t=1}^{T}$*, such that, for* $t = 1, \ldots, T$*,*

$$V_i(S_t, D_t, X_t) = 0 \tag{9}$$

$$s.t.\ \ S_{t+1} = S_t(1 - L(S_t, D_t)) + X_t \tag{1}$$

$$D_{t+1} = D_t(1-\delta) + G(S_t, D_t) + mX_t. \tag{2}$$

An open-access path is interior if $\rho(S_t, D_t, \hat{X}_t) = 0$ *at every period in the sequence.*

Given that $L(S,D) \in [0,1]\ \forall (S,D)$ since L is a probability, equation 14 provides existence conditions for interior open-access paths: $\pi \leq (1+r)F$ and $\pi \geq rF$. The first condition, $\pi \leq (1+r)F$, requires a satellite to produce less profit in a single period than the total cost of launching it inclusive of opportunity costs. If $\pi > (1+r)F$, then there can exist no nonnegative value of X_t which makes the marginal potential launcher indifferent—any marginal potential launcher will strictly prefer launching over not launching. The second condition, $\pi \geq rF$, requires a satellite to cover at least the opportunity cost of funds. If $\pi < rF$, potential launchers will always strictly prefer not launching over launching. We define the one-period rate of return on a satellite as $\pi/F \equiv r_s \geq 0$ and the excess return on a satellite as $r_s - r$. The existence conditions then become $r_s - r \leq 1$ and $r_s - r \geq 0$.

When the collision probability function is fully coupled with satellites and debris (i.e. $L = L(S,D)$), there exists a manifold containing the set of states that interior open-access paths traverse.

Definition 6. *(Equilibrium manifold) The open-access equilibrium manifold is the set*

$$\{(S,D) : L(S,D) = r_s - r\}.$$

As long as the economic parameters π, F, r are not state-dependent functions, the equilibrium manifold is also the isoquant where the collision probability is equal to the excess return on a satellite. Increases in the excess return on a satellite lead open-access operators to become indifferent at a higher isoquant, increasing the equilibrium collision probability. We establish this in Proposition 1.

Proposition 1 (Equilibrium collision probability)**.** *Given that an open-access equilibrium exists and the collision probability function is coupled with both the satellite and debris stocks, there are multiple vectors* (X_t, S_t, D_t) *such that*

$$L(S_{t+1}, D_{t+1}) = r_s - r.$$

Increases in the excess return on a satellite cause S_{t+1}, D_{t+1}, and $L(S_{t+1}, D_{t+1})$ to increase.

In cases where the economic parameters π, F, r are time-varying, Proposition 1 implies that the equilibrium collision probability in period t under open access will be determined by the values of the economic parameters in period $t-1$, i.e. the period when the newest satellites in orbit were launched. This is consistent with equilibrium collision probability being driven by marginal launchers. Interior open-access paths will then move between equilibrium manifolds as the economic parameters vary over time. When the per-period payoff function depends on the satellite and debris stocks, e.g. $\pi = \pi(S)$ or $\pi = \pi(S,D)$, the equilibrium manifold is no longer an isoquant of the collision probability function but can still be expressed as the discount-rate-isoquant of the expected per-period return. That is, letting $r^S(S,D) = \pi(S,D)/F$, the interior equilibrium condition is

$$\rho(\hat{X}_t, S_t, D_t) = 0 \iff \underbrace{r^s(S_{t+1}, D_{t+1}) - L(S_{t+1}, D_{t+1})}_{\substack{\text{Expected per-period} \\ \text{return}}} = \underbrace{r}_{\substack{\text{Opportunity} \\ \text{cost of funds}}} \tag{16}$$

In general, the payoff function may depend on the satellite stock due to internal economies (e.g. applications which require a minimum number of satellites), market competition between firms, radio frequency spectrum congestion, and collision avoidance maneuvers. Except for internal economies, all of these factors would make $\pi(S)$ a decreasing function. Similarly, the payoff function may depend on the current debris stock due to the need for collision avoidance maneuvers, again making $\pi(D)$ a decreasing function. These modifications to π will affect quantitative analysis, but under conditions of open access and competitive markets for satellite output they will not affect the qualitative results we focus on here. Consequently, we abstract from these modifications to derive our theoretical results.[18]

The condition in Proposition 1 shows that increases in the excess return on a satellite will shift the equilibrium collision probability isoquant outwards. Since every point on the excess-return isoquant of the collision probability function is an open-access equilibrium, initial conditions and physical dynamics will determine the open-access path along the isoquant. This is an implication of the physics of orbit use—as long as the collision probability function is coupled with the satellite and debris stocks, the same collision probability level can be realized by different combinations of satellite and debris levels. Figure 1 illustrates these results. In panels a, b, c, d, e, the unconstrained trajectory from the origin ($X_t < \bar{X} \ \ \forall t$) takes a most-rapid approach path (MRAP) to the equilibrium isoquant, while the constrained trajectory attains the maximum possible launch rate $\bar{X}$ until it reaches the equilibrium isoquant. Both trajectories have identical economic parameters; the only difference is that the constrained path has a lower

[18] While a decreasing $\pi(S)$ makes it more difficult for open access to cause Kessler Syndrome, we show in section 6 that it is still possible.

value of $\bar{X}$. The MRAP for the unconstrained trajectory appears in panel a as a straight line from the origin to the isoquant. Both paths then traverse the equilibrium isoquant until they reach a steady state. In panel f, the equilibrium isoquant shifts outward when the excess return increases. This shift increases the equilibrium collision risk as well as the equilibrium satellite and debris levels.

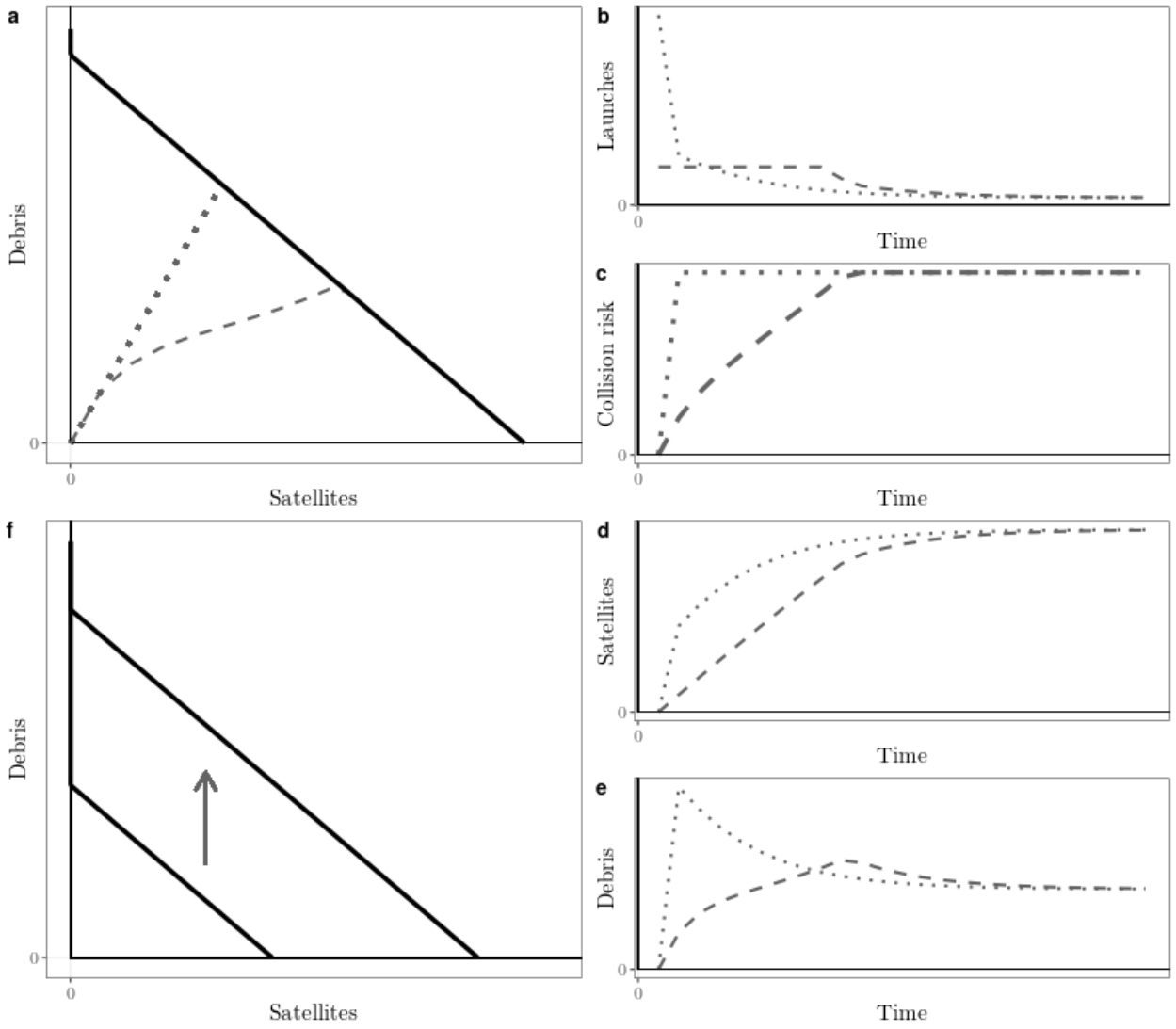

Figure 1: Panel a shows two approach paths from the same initial condition: one which reaches the equilibrium isoquant immediately (dotted straight line), the other with a binding launch rate constraint ($\bar{X}$) which takes multiple periods to reach the equilibrium isoquant (dashed curving line). Panels b, c, d, e show the time evolution of the launch rate, collision probability, satellite stock, and debris stock from panel a. Panel f shows the equilibrium isoquant shifting outwards when the excess return on a satellite increases.

4 Dynamic properties of open access

When the system is fully coupled, there can be multiple open-access steady states. Removing period t subscripts and letting $'$ superscripts denote period $t+1$ variables, open-access steady states are defined by the collision probability equaling the excess return on a satellite ($L(S,D) = L(S',D') = r_s - r$) along with the usual stationarity conditions on the state variables:

$$(S,D) : L(S,D) = r_s - r, \tag{17}$$

$$\begin{aligned} S' = S &\implies S = (1 - L(S,D))S + X \\ &\implies X = L(S,D)S, \end{aligned} \tag{18}$$

$$\begin{aligned} D' = D &\implies D = (1-\delta)D + G(S,D) + mX \\ &\implies \delta D = G(S,D) + mX. \end{aligned} \tag{19}$$

The following lemma simplifies our analysis in the rest of this section, allowing us to reduce the system of equations 17, 18, and 19 to two equations.

Lemma 1 (Reduction)**.** *Given a fully-coupled collision probability function, the steady states of an open-access equilibrium are defined by solutions to*

$$\mathscr{Y}(D) = -\delta D + G(\hat{S},D) + m(r_s - r)\hat{S} = 0, \tag{20}$$

where $\hat{S} = S(r_s - r, D) \geq 0$ *is defined from*

$$L(\hat{S},D) = r_s - r \tag{21}$$

when such an S exists and 0 *otherwise.*

Intuitively, the open-access condition links the steady-state satellite and debris stocks and reduces the system's degrees of freedom. Using Lemma 1, we establish the existence of multiple steady states when the collision probability function is fully coupled and the new fragment debris coupling exists.

Proposition 2 (Multiplicity)**.** *Given a positive excess return on a satellite and a fully-coupled collision probability function, multiple open-access steady states can exist if the new-fragment-debris coupling exists (i.e.* $G = G(S,D)$*).*

This multiplicity is possible in part because open access makes the equilibrium satellite stock a decreasing function of the debris stock. Increases in the steady-state debris stock initially cause the number of new fragments created to fall as open-access launchers respond by

launching fewer satellites. Eventually, the fragment-reducing effect of fewer satellites is dominated by the fragment-producing effect of additional debris through the new fragment debris coupling. The number of open-access steady states will depend on the shapes of L and G. For example, if L is strictly increasing and G is strictly convex, there can be up to two open-access solutions to equation 20. Intuitively, strict convexity of G suggests that putting more objects in orbit strictly increases the expected number of fragments generated by collisions in each period, e.g. due to fragments from one collision propagating and increasing the likelihood of fragment-generating collisions during that period.

Figure 2 illustrates Proposition 2 in the space of equation 20 and the accompanying phase diagram of the satellite-debris system. Proposition 3 connects the stability of these steady states to the fragment autocatalysis rate and the marginal rate of technical substitution of satellites for debris in producing collision probability. Convexity of G (strict somewhere but not necessarily everywhere) generates the upward slope in the curve B. The equilibrium manifold (reflected in $\hat{S}$) generates the positive intercept and the initial relative flatness of curve B.

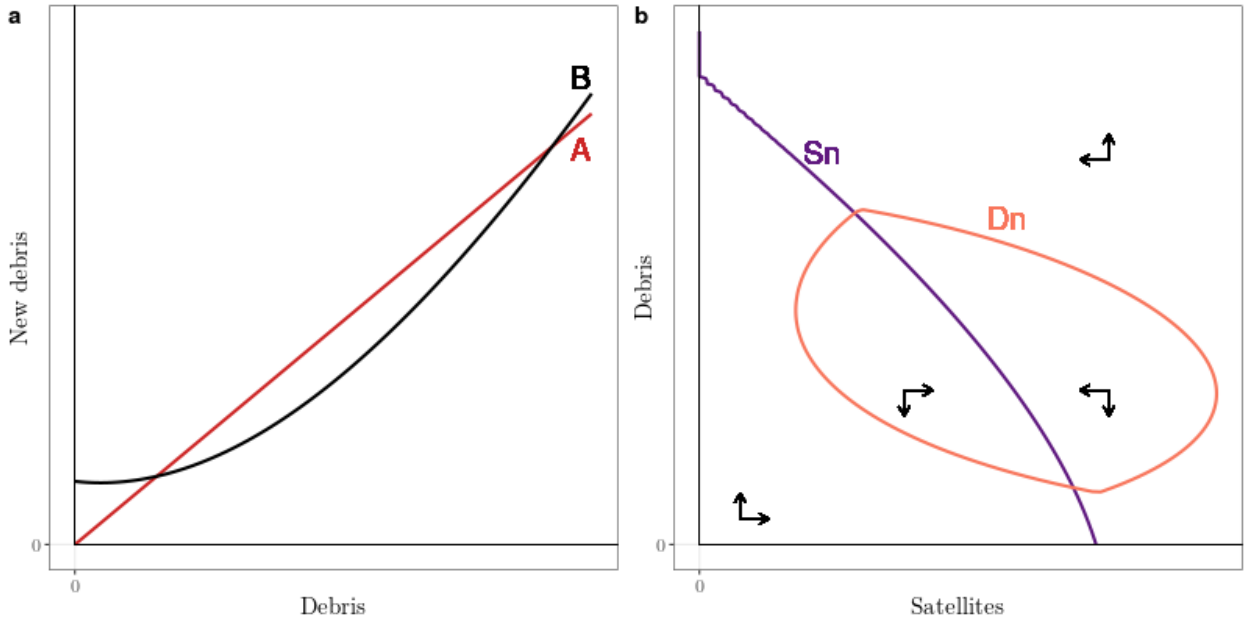

Figure 2: Panel a shows equation 20 for a parameterization with two steady states. The red line (line A) shows δD, while the black line (curve B) shows $G(\hat{S},D)+m(r_s-r)\hat{S}$. Panel b shows the phase diagram of the same parameterization, with the purple curve (Sn) showing the satellite nullcline and the orange curve (Dn) showing the debris nullcline. Only the lower-debris steady state is stable.

Proposition 3 (Local stability)**.** *Given a positive excess return on a satellite, new fragment satellite coupling, and launch debris coupling, open-access steady states will be locally stable if and only if the fragment autocatalysis rate is small enough, or the marginal rate of technical*

substitution of satellites for debris in collision probability is high enough, i.e.

$$(G_D(S^*,D^*)-\delta) < \frac{L_D(S^*,D^*)}{L_S(S^*,D^*)}(G_S(S^*,D^*)+m(r_s-r)). \tag{22}$$

When G is strictly convex in both arguments and two steady states exist, the higher-debris steady state is unstable.

The key equation from the proof is the first derivative of the reduction from Lemma 1,

$$\frac{\partial \mathscr{Y}}{\partial D}(D^*) = (G_D(S^*,D^*)-\delta) - \frac{L_D(S^*,D^*)}{L_S(S^*,D^*)}(G_S(S^*,D^*)+m(r_s-r)), \tag{23}$$

where $S^* \equiv S(r_s - r, D^*)$. If a steady-state debris level D^* is such that $\frac{\partial \mathscr{Y}}{\partial D}(D^*) < 0$, then it will be stable.[19] The stability of an open-access steady state depends on two factors, shown on the right hand side of equation 23. The first term is the fragment autocatalysis rate, $G_D - \delta$, which can ensure stability if it is close enough to negative infinity. This has a clear physical intuition: higher decay rates indicate regions with greater natural renewability, while stronger new fragment debris couplings indicate stronger positive feedbacks between debris stocks.

The second term is the equilibrium effect of new satellites on debris growth. This term is increasing in the marginal rate of technical substitution (MRTS) of satellites for debris in collision probability, as a larger MRTS indicates the collision probability function is more sensitive to debris fragments than to satellites. A larger MRTS incentivizes profit-maximizing satellite launchers to be more responsive to debris stocks than they would be with a smaller MRTS, thus stabilizing the steady state. The effect of the MRTS is scaled by the strength of the new fragment satellite coupling, the launch debris coupling, and the excess return on a satellite. The new fragment satellite and launch debris couplings are both byproducts of putting satellites into orbit, and force satellite operators to account for additional risks they face in orbit.

When there are only two solutions to equation 20, say if L is strictly increasing and G is strictly convex, then the higher-debris solution is a repelling fixed point. The debris level associated with this fixed point is then the Kessler threshold defined earlier in equation 3, D_X^κ. D_X^κ was defined as the maximum sustainable debris level for this reason—if the larger fixed point is repelling, any debris level at or beyond it will eventually diverge to infinity. This is formalized in Lemma 2.

Lemma 2 (Open-access Kessler threshold)**.** *When G is strictly convex in both arguments and two steady states exist, let*

$$\underline{D} = \min\{D : \mathscr{Y}(D) = 0\}$$

[19] This condition arises from application of the Hartman-Grobman Theorem to the reduction in Lemma 1.

be the stable steady state, and

$$\bar{D} = \max\{D : \mathscr{Y}(D) = 0\}$$

be the unstable steady state. Then

$$\bar{D} = D_X^{\kappa}.$$

The connection between the Kessler threshold and the unstable steady state allows us to characterize the Kessler region as the complement of the stable steady state's basin of attraction. Intuitively, interior open-access paths from an initial condition must be governed by the attracting or repelling behavior induced by one of the steady states. So initial conditions which do not lead to the stable steady state must be governed by the unstable one, which will drive the debris stock to infinity and the satellite stock to zero.[20]

Given the potential for an unstable steady state, it is natural to wonder whether open access can lead to Kessler Syndrome. There are two cases where this can occur:

1. the initial condition is inside the Kessler region;
2. the fragment autocatalysis rate or rate of excess return is high enough no stable steady state exists.

The first case can occur due to non-economic factors, such as changes in environmental parameters (e.g. space weather) or military activity in space (e.g. anti-satellite missile tests which create debris). The second can occur due to economic or non-economic factors, with examples of the former including reductions in launch costs. Figure 3 illustrates this example. As long as Kessler Syndrome is possible, open access is "more likely" to cause Kessler Syndrome as the excess return on a satellite increases (in the sense that the Kessler basin is expanding in the excess return on a satellite), and certain to cause Kessler Syndrome if the excess return exceeds the maximum sustainable level. We define the maximum sustainable excess return below and then state the result.

[20] Since our stability results come from the Hartman-Grobman Theorem they are local to neighborhoods of the steady states. However, the reduction in Lemma 1 enables a global characterization for interior open-access paths. The argument follows from the following observations:

1. By definition interior open-access paths move along the equilibrium manifold, so the dynamics along such paths are effectively one-dimensional in a modified coordinate system defined on the equilibrium manifold.
2. Steady states of one-dimensional systems partition the state space into disjoint regions.
3. Initial conditions from each region of a one-dimensional system are governed by the dynamics associated with the relevant steady state.

Thus, local stability analysis of the steady states has a "more global" flavor *for interior open-access paths*, in the sense that it applies to all open-access paths traversing the equilibrium manifold.

Definition 7. *The maximum sustainable excess return, R^{max}, is the maximum rate of excess return on a satellite such that a stable open-access steady state exists. That is, R^{max} is a nonnegative number which solves*

$$\begin{aligned} &\textit{(Stationarity):} \quad -\delta D_X^\kappa + G(S_X^\kappa, D_X^\kappa) + mR^{max} S_X^\kappa = 0, \\ &\textit{(Weak stability):} \quad G_D(S_X^\kappa, D_X^\kappa) - \frac{L_D(S_X^\kappa, D_X^\kappa)}{L_S(S_X^\kappa, D_X^\kappa)}(G_S(S_X^\kappa, D_X^\kappa) + mR^{max}) = \delta, \end{aligned}$$

$$\implies R^{max} : -\delta D_X^\kappa + G(S_X^\kappa, D_X^\kappa) + mR^{max} S_X^\kappa = G_D(S_X^\kappa, D_X^\kappa) - \frac{L_D(S_X^\kappa, D_X^\kappa)}{L_S(S_X^\kappa, D_X^\kappa)}(G_S(S_X^\kappa, D_X^\kappa) + mR^{max}) - \delta,$$

where $S_X^\kappa \equiv \hat{S}(D_X^\kappa)$, $\hat{S}(D)$ is as defined in Lemma 1, and D_X^κ is the open-access Kessler threshold.

Proposition 4 (Open-access Kessler Syndrome)**.** *When the rate of excess return is positive and the new fragment function is fully coupled and strictly convex in both arguments,*

1. *open access will cause Kessler Syndrome if the excess return on a satellite exceeds the maximum sustainable excess return R^{max};*
2. *the open-access Kessler region will expand as the excess return approaches R^{max}.*

Intuitively, as the rate of excess return on a satellite increases the two steady states are squeezed closer to each other.[21] When the excess rate of return is equal to the maximum sustainable level, the two steady states collide. When the rate of excess return exceeds the maximum sustainable excess return ($r_s - r > R^{max}$), Kessler Syndrome is the only long-run possibility under open access. If $R^{max} < 1$, then Kessler Syndrome will occur before open access drives the collision probability to one. If $R^{max} \geq 1$, then Kessler Syndrome under open access is inconsistent with the existence of an open-access steady state; since existence of an interior open-access equilibrium requires the excess rate of return to be less than one, the maximum sustainable level will not be crossed.[22]

Figure 3 illustrates Proposition 4. The lower-debris intersection of the satellite and debris nullclines marks the stable open-access steady state (point "Oa" in panel a), while the higher-debris intersection marks the maximum sustainable debris level D_X^κ (the unstable steady state).

[21] This is similar to a sub-critical fold bifurcation in the excess rate of return, though the unstable steady state is not annihilated when the two steady states collide. Making the per-period payoff a decreasing function of the total satellite stock would not remove the bifurcation; it would require restrictions on the new fragment function, e.g. removing the new fragment debris coupling.

[22] Note that if an open-access path will cause Kessler Syndrome then that open-access path cannot be interior for every t. However, causing Kessler Syndrome will still be an equilibrium outcome as long as $V_t(S_t, D_t, X_t) = 0$ in all periods. Given the conditions of Proposition 4, existence of a future period T where launchers have the option to exit the launch market and collect a payoff of 0 is sufficient to ensure existence of open-access paths where Kessler Syndrome occurs.

The yellow shaded region shows the basin of attraction for the stable steady state.[23] As the rate of excess return on a satellite increases, the stable basin of attraction shrinks and D_X^κ decreases while the stable open-access steady state debris level increases, squeezing the two fixed points closer to each other. Eventually, the stable steady state crosses the boundary where the fragment autocatalysis rate becomes positive (the red dashed line)—a necessary condition for Kessler Syndrome to occur.

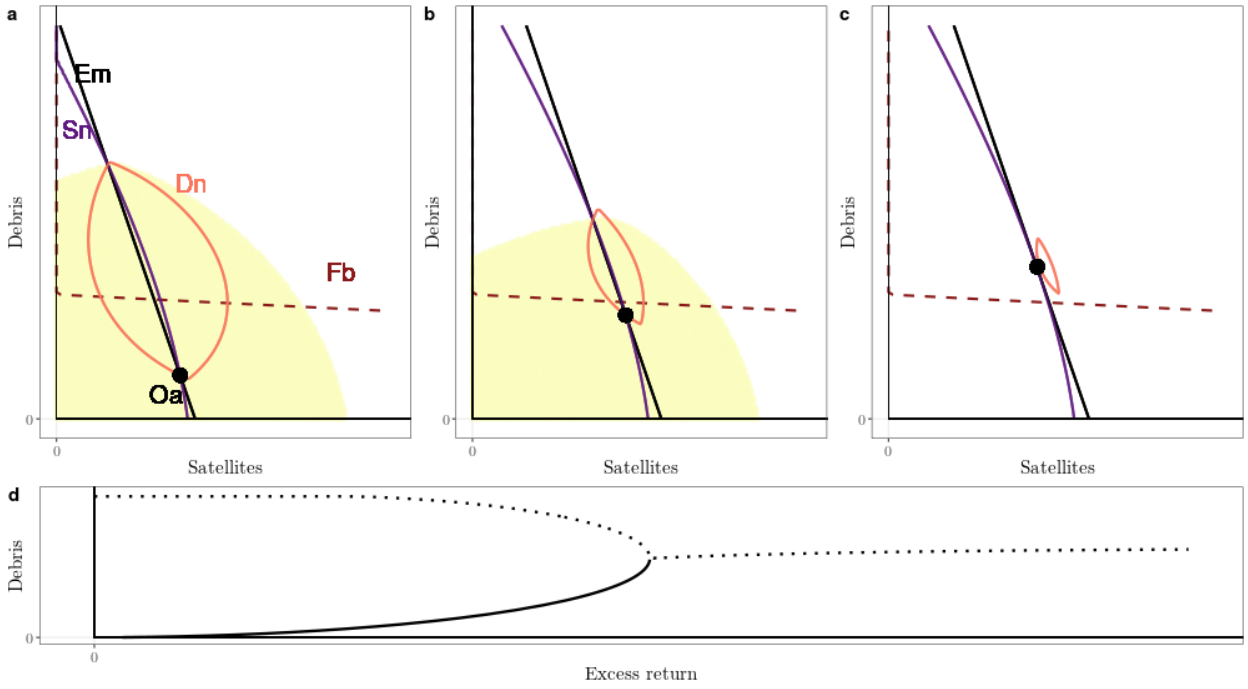

Figure 3: An illustration of how increases in the rate of excess return on a satellite can cause Kessler Syndrome. In panels a-c, the shaded yellow region shows the basin of attraction of the stable open-access steady state, and the dashed red line (curve *Fb* in panel a) shows the boundary where the fragment autocatalysis rate becomes positive. The solid black line (*Em* in panel a) shows the equilibrium isoquant, and the purple and orange curves (*Sn* and *Dn* in panel a) show the satellite and debris nullclines. The black dot (point *Oa* in panel a) shows the stable (in panels a and b) or only (in panel c, where it is unstable) open-access steady state. From panel a to c the rate of excess return steadily increases, shrinking the basin of attraction of the stable open-access steady state or equivalently increasing the size of the open-access Kessler region. When the stable open-access steady state crosses the fragment autocatalysis rate boundary, it loses stability and its basin of attraction vanishes. Panel d shows the stable (solid line) and unstable (dotted line) open-access steady-state debris levels colliding as the rate of excess return on a satellite increases.

Provided there is a stable open-access steady state to approach, it is important to understand the open-access approach paths. If open access monotonically approaches stable steady states,

[23] The stable basin of attraction is determined by computing open-access paths beginning at each state in a fine grid. If an open-access path from a state (S,D) ever causes the debris stock to exceed the maximum sustainable level, D_X^κ, then it is excluded from the stable basin. Repeating this calculation at every state in the grid determines the stable basin.

then parameter changes which shift the steady state may not cause costly spikes in the debris stock. Such parameter changes include technological advances (e.g. better-shielded satellites), policy guidelines (e.g. encouragement to use frangibolts instead of exploding bolts for booster separation), environmental processes (e.g. sunspot activity which causes δ to vary), or economic changes (e.g. increases in the excess return on a satellite).

Proposition 5 shows it is unlikely monotonic approach paths occur when the launch rate is unconstrained. Initial conditions which result in smooth approach paths to a stable steady state form a set of Lebesgue measure zero. Almost all initial conditions instead overshoot the steady state in at least one state variable.

Proposition 5 (Overshooting)**.** *Suppose the new fragment formation function is strictly convex in both arguments and the launch rate constraint does not bind. Except on a set of measure zero, open access paths from initial conditions with positive launch rates will overshoot the stable open-access steady state in at least one state variable.*

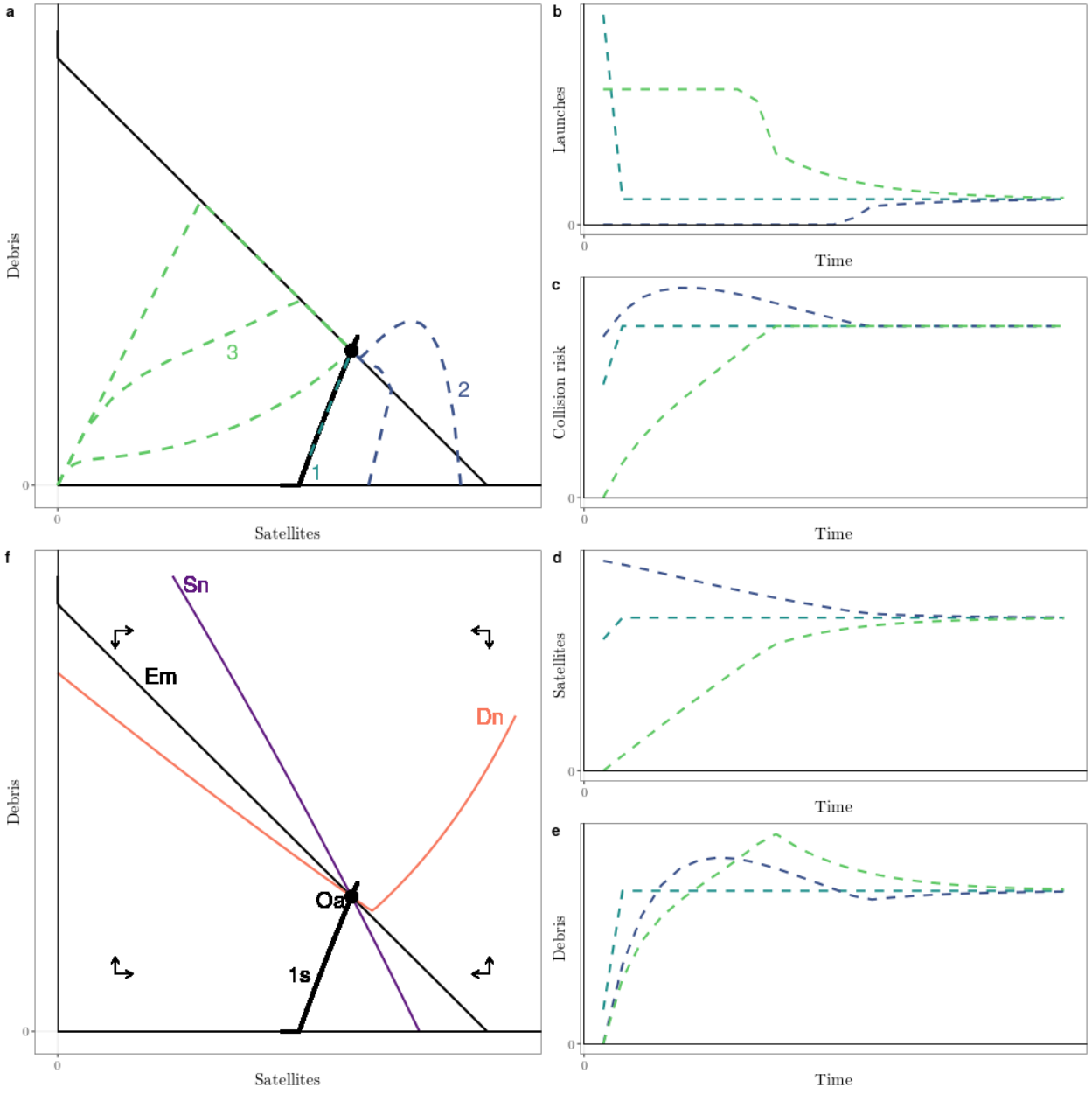

Figure 4: In panels a and f, the thin black line shows the equilibrium isoquant (curve *Em* in panel f). The thick black point in panels a and f on the equilibrium isoquant is the stable open-access steady state (point *Oa* in panel f). The thick black line in panels a and f connecting the steady state to the y-axis is the manifold of points which can converge to the stable steady state in one step (the "one-step set", curve *1s* in panel f). Panel a illustrates Proposition 5 with sample paths. The teal dashed line (labeled 1) along the thick black line shows a path converging to the steady state in one step. The green dashed lines (including the line labeled 3) show paths which overshoot in debris, all of which converge to the steady state along the equilibrium isoquant. The purple dashed lines (including the line labeled 2) show paths which overshoot at least in satellites. These paths follow the equilibrium isoquant to the steady state whenever possible, though the physical dynamics force two of the five paths shown to approach the steady state from outside the action region. Panels b-e show the launch rate, collision probability, and satellite and debris stocks for sample paths 1-3 over time. Panel f shows the equilibrium isoquant (thin black), the one-step set (thick black), and the satellite (purple, curve *Sn* in panel f) and debris nullclines (pink, curve *Dn* in panel f).

Proposition 5 suggests some scope for orbit-use stabilization policies which impose a cap on the number of launches per period, since slowing the rate at which firms approach the equilibrium isoquant can reduce the amount of overshooting. Even if the cap does not change the open-access steady state (i.e. the cap is greater than the replacement launch rate required at the steady state), reducing overshooting can make the steady state approach path smoother. This can be seen in figure 4. For example, an unconstrained path from the $(0,0)$ initial condition (the dashed green straight line from $(0,0)$) immediately reaches the equilibrium isoquant by overshooting the steady-state debris level. The overshooting is reduced when the launch rate is constrained (e.g. path 3, as shown in figure 4b-e), with the most tightly-constrained (green) path showing no overshooting.

5 The planner's problem

The fleet planner has exclusive rights in perpetuity to the orbit and all satellites in it. The planner therefore controls launches to maximize the net present value of the satellite fleet, equating the per-period marginal benefit of another satellite with its per-period social marginal cost. Firms which do not own exclusive orbital rights internalize only the opportunity cost of funds and the risk to their satellite, ignoring the costs the satellite imposes on the rest of the fleet.

The fleet planner solves

$$W(S_t, D_t) = \max_{X_t \in [0,\bar{X}]} \{\pi S_t - F X_t + \frac{1}{1+r} W(S_{t+1}, D_{t+1})\} \tag{24}$$

$$\text{s.t. } S_{t+1} = S_t(1 - L(S_t, D_t)) + X_t \tag{25}$$

$$D_{t+1} = D_t(1-\delta) + G(S_t, D_t) + mX_t. \tag{26}$$

The planner's optimal interior launch rate equates the flow of marginal benefits and costs, such that

$$\pi = rF + L(S_{t+1}, D_{t+1})F + \xi(S_{t+1}, D_{t+1}) \tag{27}$$

$$\implies L(S_{t+1}, D_{t+1}) = r_s - r - \mu(S_{t+1}, D_{t+1}). \tag{28}$$

where $\xi(S_{t+1}, D_{t+1})$ is obtained from the planner's optimality condition and is defined as the marginal external cost of another launch in t. The marginal external cost is calculated as the additional terms in the planner's first-order condition which do not appear in the interior open-access equilibrium condition, equation 14. $\mu(S_{t+1}, D_{t+1}) = \xi(S_{t+1}, D_{t+1})/F$ is the rate of external cost incurred per dollar spent on a launch in t. The per-period social marginal cost is the sum of the opportunity cost and collision risk ($rF + L(S_{t+1}, D_{t+1})F$), plus the effect of

the marginal satellite on the fleet through future collisions and debris growth ($\xi(S_{t+1}, D_{t+1})$). We derive equation 27 and $\xi(S,D)$ in the general (non-interior, non-stationary) case in Appendix A.2.

Similar to the open-access case, we define $\rho^*(X_t, S_t, D_t) = \frac{\pi}{F} - r - L(S_{t+1}, D_{t+1}) - \mu(S_{t+1}, D_{t+1})$ as the risk-and-externality-adjusted excess return on a satellite.[24] Given the bounds on launches, the planner's launch policy is then

$$X_t^* \in (0, \bar{X}) \text{ if } \rho^*(X_t^*, S_t, D_t) = 0, \tag{29}$$

with $X_t^* = 0$ if $\rho^*(0, S_t, D_t) < 0$ and $X_t^* = \bar{X}$ if $\rho^*(\bar{X}, S_t, D_t) > 0$.

While the full expression is lengthy, analyzing the interior steady state reveals the core intuition for the marginal external cost. Suppressing function arguments, the marginal external cost in an interior steady state is

$$\xi(S,D) = \underbrace{L_S SF}_{\substack{\text{“congestion” channel:} \\ \text{marginal cost of satellites colliding} \\ \text{with each other due to crowding}}} + \underbrace{\frac{1}{1+r}\left(G_S + m(L + SL_S)\right) L_D SF + (1 - \frac{1}{1+r}) m L_D SF}_{\substack{\text{“pollution hazard” channel:} \\ \text{marginal cost of satellites colliding} \\ \text{with new fragments and launch debris}}}$$
$$+ \underbrace{\frac{1 - \delta + G_D}{1+r}\left(\pi - rF - (L + L_S S)F\right)}_{\substack{\text{“pollution persistence” channel:} \\ \text{marginal cost of persistent debris} \\ \text{and debris growth}}} \tag{30}$$

The first term of $\xi(S_{t+1}, D_{t+1})$, the congestion channel, represents the cost of additional satellite collision probability due to satellite crowding. As long as the collision probability is coupled with the satellite stock and new satellites weakly increase the probability of satellite-destroying collisions ($L_S \geq 0$), this term is nonnegative.

The second term, the pollution hazard channel, is the cost of additional collisions with debris. There are two components of this channel, reflecting debris costs incurred over time and immediately. The first component, $\left(G_S + m(L + SL_S)\right) L_D SF$, represents the marginal cost of colliding with fragments generated by collisions involving other satellites (including fragments from collisions between satellites and launch debris). This component reflects the long-run risk to the fleet created by the marginal satellite, as it may be destroyed in a collision and generate

[24] Continuing the intuition of satellites as risky assets, the planner can be viewed as internalizing not only the risk the asset stops producing payoffs ($L(S_{t+1}, D_{t+1})$) but also the effect of each additional asset acquired on their portfolio as a whole ($\mu(S_{t+1}, D_{t+1})$).

additional fragments. The second component, mL_DSF, represents the marginal cost of the new satellite's launch debris—an immediate hazard to the fleet. As the discount factor approaches one only the long-run debris cost matters, while as it approaches zero only the immediate debris cost matters. As the number of launch debris fragments from the marginal satellite goes to zero, this channel reduces to the discounted marginal cost of collisions from fragments of satellite-debris collisions ($\frac{1}{1+r}G_SL_DSF$, a long-run cost) only. As long as the new fragment satellite and collision probability debris couplings are weakly positive, i.e. having more satellites in orbit weakly increases the number of fragments produced in collisions and having more objects in orbit weakly increases the probability of a collision, this term is nonnegative.

The third term, the pollution persistence channel, is the cost of debris which does not decay and new fragments produced in collisions between debris objects. If all debris in orbit decayed at the end of each period and the debris coupling in the new fragment function was inactive ($\delta = 1$ & $G_D \equiv 0$), this channel would disappear. The cost associated with this channel is the forgone discounted payoff from a satellite net of collision risk (L), congestion costs (L_SSF), and the opportunity cost of the funds used to deploy the asset (rF). As long as the excess rate of return weakly exceeds the collision probability and marginal rate of congestion costs ($r_s - r \geq L(S,D) + L_S(S,D)S$), this term is nonnegative.

Proposition 6 establishes that the marginal external cost in an interior steady state is nonnegative as long as the excess rate of return on a satellite weakly exceeds the collision probability and marginal rate of congestion costs.

Proposition 6 (Negative externality)**.** *If the excess rate of return on a satellite weakly exceeds the collision probability and marginal rate of congestion costs in an optimal interior steady state, then the marginal external cost is weakly positive and the optimal collision probability is weakly lower than the open-access collision probability, i.e.*

$$r_s - r \geq L(S,D) + L_S(S,D)S \implies \xi(S,D) \geq 0, \tag{31}$$

and

$$\xi(S,D) \geq 0 \implies L(S^*,D^*) \leq L(\hat{S},\hat{D}). \tag{32}$$

As long as the marginal external cost is positive, the planner will maintain a lower collision probability in an interior steady state than open-access operators would. Kessler Syndrome therefore seems less likely under the planner's management than under open access. While full analysis of the dynamics of the optimal launch plan is beyond our scope here, we calculate numerical examples under illustrative parameterizations (shown in figure 5) to develop some intuition for how the optimal launch plan manages the risk of Kessler Syndrome.

In the first set of scenarios (shown in the top row of figure 5, panels a.1-3) we increase the excess return on a satellite by lowering the cost to build and launch a satellite. This corresponds to technological changes such as reusable rockets or more efficient satellite manufacturing processes. In the second set of scenarios (shown in the middle row of figure 5, panels b.1-3), we increase the discount rate while holding the payoff generated and costs incurred by a satellite constant. This corresponds to improved outside investment options and a lower excess return. In the third set of scenarios (shown in the bottom row of figure 5, panels c.1-3), we increase the discount rate while decreasing launch costs such that the excess return is held constant. This corresponds to improved outside investment options and technological improvements in satellite launching.

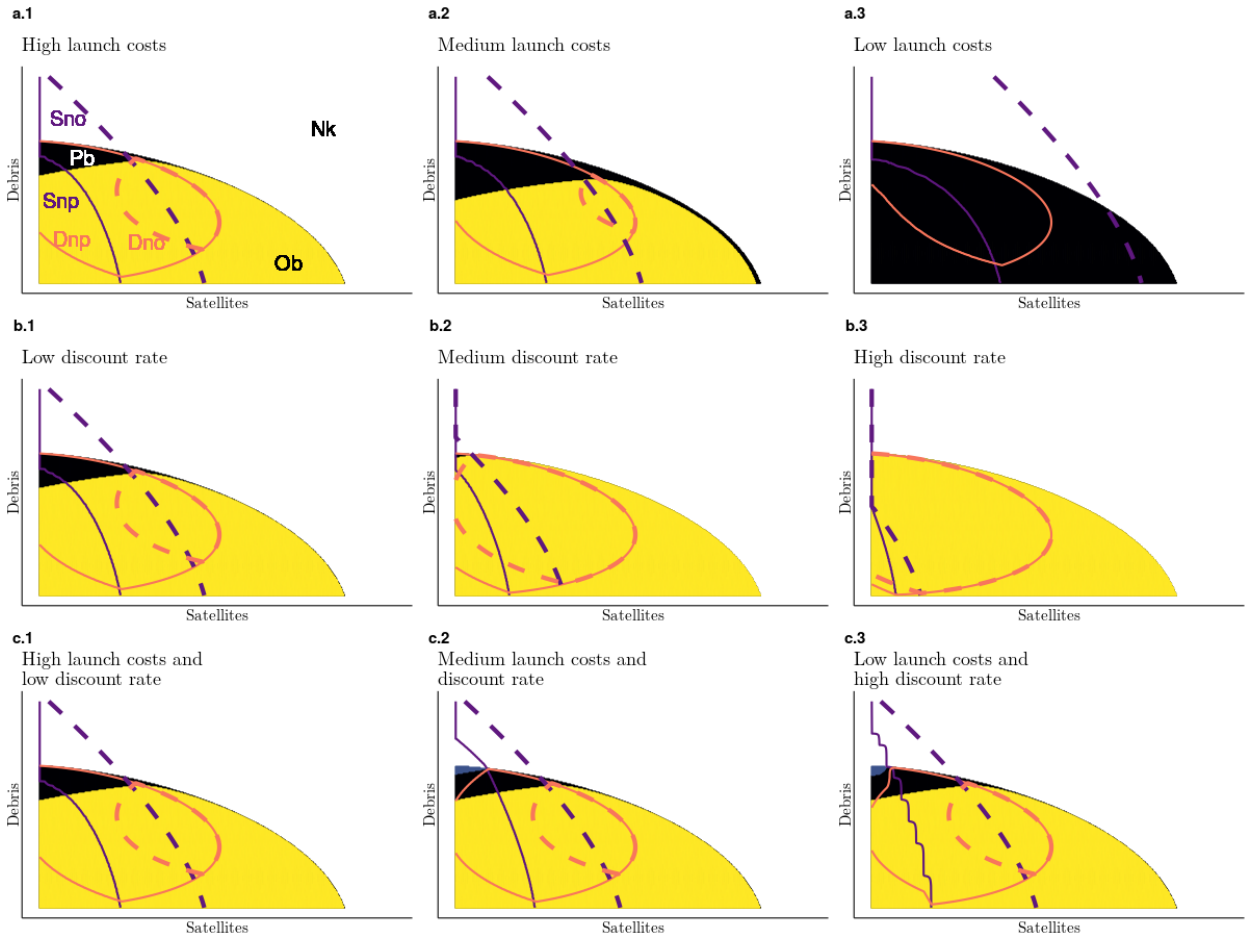

Figure 5: The unshaded area labeled *Nk* in panel a.1 marks the unavoidable Kessler region, the black shading labeled *Pb* marks the basin of attraction to the planner's stable steady state, and the yellow shading labeled *Ob* marks the basin of attraction to the open-access stable steady state. The solid orange and purple lines labeled *Dnp* and *Snp* show the debris and satellite nullclines under the planner's launch policy, while the dashed lines labeled *Dnp* and *Snp* show the nullclines under the open-access launch policy. From panels a.1-3, the excess rate of return on a satellite is increasing due to decreases in launch costs, holding the discount rate constant. From panels b.1-3, the discount rate rises, holding launch costs constant (implying lower excess return). From panels c.1-3, the launch costs fall and discount rate rises such that the excess return is held constant. The jagged lines in panel c.3 are computational artifacts.

We emphasize three features in figure 5. First, though the planner responds to increases in the excess return on a satellite by launching more satellites and tolerating more debris, the increase is smaller than under open access and the planner can maintain the same stable basin. Thus, increases in the excess return on a satellite may not only make Kessler Syndrome more likely under open access, but also less efficient in that there are more states where open access causes Kessler Syndrome while the planner avoids it.[25]

[25] Note that the debris nullclines—the curve in 5a.1 labeled as *Dno* for open access, curve *Dnp* for the planner—overlap once both plans launch no satellites since the physical dynamics are the same.

Second, all else equal as the discount rate increases both the planner and open-access operators launch fewer satellites. At high discount rates the planner may prefer never launching over causing Kessler Syndrome. The contrast with biological resources like fisheries is noteworthy. Whereas high discount rates may incentivize a profit-maximizing fishery manager to drive a population to extinction, profit-maximizing orbit managers and open-access operators do not face incentives to render an orbit unusable due to high rates of time preference. This reflects the difference in how investment relates to biological and artificial population levels. Biological populations can reproduce without human investment, allowing a user to profit today at the expense of tomorrow by investing and harvesting many members of the species. Artificial populations require upfront investment and only generate profits over time—investing more today may reduce tomorrow's profits due to collisions and debris, but won't increase the profits today. Increases in the discount rate which reduce the rate of excess return only serve to lengthen the payback period required before the investment is profitable, making debris risks more salient.[26]

Third, the discount rate affects the optimal launch policy independent of the excess return on a satellite. While higher discount rates (holding the excess return constant) may not change the optimal stable steady state, it does change the optimal launch policy by making the planner willing to launch more at higher debris levels. At very low discount rates (panels c.2-3) an optimal unstable steady state emerges, creating a region where it is optimal to cause Kessler Syndrome (the blue shaded region between regions *Pb* and *Nk*). The interaction between the payback period effect of the discount rate and the debris cost effects of the discount rate suggest the planner's responses to changing outside investment options will be more complex than an open-access operator's.

Together, these results illustrate how the economic dynamics of orbit use differ substantially from previously-studied natural resources. Most importantly, they show that the inefficiencies in open-access orbit use are of two types: inefficient long-run stable satellite and debris levels, and inefficient acceptance of long-run instability. While the existence of Kessler Syndrome is not required for open-access orbit use to be inefficient, open-access operators also appear to cause Kessler Syndrome when the planner would avoid it.

6 Calibrated simulations

To assess the risk of open-access Kessler Syndrome in LEO, we calibrate our model to the physical and economic environment in the 600-650 km shell using data from 2006-2019, and

[26] We assume satellites are financed such that the launcher accrues profits immediately and pays an annuity for the life of the asset. But the intuition is the same: higher discount rates imply costlier financing, making satellite investments less attractive.

simulate open-access paths over the 2020-2520 horizon under historically-plausible variation in revenues and costs.[27] The majority of new satellites being launched and planned are intended for LEO, which has been described as "the New Space Race" (Ritchie and Seal, 2020). The 600-650 km shell is particularly interesting as it is the edge of the region where uncontrolled objects will naturally decay within 25 years. We find that under historical sectoral growth trends Kessler Syndrome is expected to occur in this shell around 2047. Higher mean growth rates for the space economy as a whole induce Kessler Syndrome sooner, though all scenarios considered indicate a greater than 50% chance of Kessler Syndrome occurring by 2050. Under growth rates consistent with optimistic industry and investment bank projections, the probability of Kessler Syndrome occurring by 2040 is over 75%. Consistent with Proposition 4, Kessler Syndrome will eventually occur with probability one in any scenario where growth in the net returns to satellite ownership is consistently positive, though the Kessler time may be centuries from now.[28]

Our approach involves three steps. First, we calibrate the physical model to the 600-650 km shell using previously-validated approaches from the engineering literature and a regression-based correction for deviations from the physical model assumptions. Second, we calibrate the economic parameters consistent with open access over 2006-2019 using regressions to account for unobserved scaling factors and frictions and obtain parameter uncertainty estimates. Third, we simulate the model forward for 500 years, 1000 times, using economic parameter uncertainty estimates to generate variation in the net returns to satellite ownership both within and across simulations. These simulated open-access paths enable us to estimate the probability of Kessler Syndrome occurring at different times. While our interest is in the relatively-near future (the 2020-2070 horizon), the very long-run dynamics allow us to distinguish between scenarios where Kessler Syndrome never occurs and those where it will only occur in the distant future.

[27] We use measured revenues as a proxy for payoffs broadly, and so refer to "satellite revenues" rather than "satellite payoffs" this section.

[28] Crane et al. (2020) survey recent space economy growth rate projections from industry associations and investment banks, including Morgan Stanley and Goldman Sachs, and also provide their own estimates based on more restrictive definitions of the space economy and alternate accounting conventions. Crane et al. (2020) argue that the growth rate estimates they survey incorporate an overly-expansive definition of the space economy and double-count revenues from government expenditures, with the double-counting roughly doubling the projected size of the space economy. Our approach to accounting for unobserved scaling factors (described below) is robust to this concern provided the measurement problems Crane et al. (2020) document are relatively constant over 2006-2019. We calculate the size of the space economy when the Kessler threshold is crossed using an approach consistent with the expansive definitions used by Morgan Stanley and Goldman Sachs. The slower-than-historical-average growth scenario is consistent with the more restrictive estimates in Crane et al. (2020), the historical-average growth scenario is consistent with growth rates projected by Morgan Stanley, and the faster-than-historical-average growth scenario is consistent with growth rates projected by Goldman Sachs. The Morgan Stanley estimates imply a total space economy value of roughly $1 trillion (nominal) USD in 2040 while the Goldman Sachs estimates imply a total space economy value on the order of $3 trillion (nominal) USD in 2040 (Crane et al., 2020).

The "25-year rule" is a guideline for satellite operators promoted by the Inter-Agency Space Debris Coordination Committee, NASA, and other space agencies since the early 1990s, asking that operators ensure their satellites will safely deorbit within 25 years of the end of their productive life (IADC, 2007; Krage, 2020). Satellites placed below 650 km are viewed as "naturally compliant with the 25-year rule because once their mission is over, they will decay within 25 years without any additional maneuvers. Many current policy approaches to orbital-use management are being designed with the 25-year rule in mind. For example, in a recent Notice of Proposed Rulemaking the Federal Communications Commission (which manages radio spectrum for satellite operators transmitting to and from the US) suggested that satellite spectrum applicants would receive greater scrutiny if their planned orbit was above 650 km since they would not be naturally compliant with the 25-year rule (Federal Communications Commission, 2020). If open access will cause Kessler Syndrome below 650 km, existing policy approaches will need to be reconsidered.

The 25-year rule is non-binding (i.e. a guideline rather than a legal requirement), and recent studies have suggested that even full compliance with the rule would be insufficient to prevent Kessler Syndrome in the coming decades and centuries (Lewis, 2020). While much attention has been focused on the physical properties of complying the 25-year rule over long time horizons, most of the extant analysis ignores behavioral responses and assumes that launch patterns of the last 7 years repeat indefinitely. Rao and Letizia (2021) use random utility models of orbital demand to develop an integrated assessment model of LEO with entry and sorting margins. They find that sorting across altitude shells in response to greater 25-year rule compliance can induce clustering of active satellites just above the naturally compliant region. However, they focus on modeling heterogeneous responses by different types of operators in the short run (no farther than 2030), do not enforce an open-access condition, and do not consider Kessler Syndrome. To keep our model tractable and theoretically consistent, we focus on a single shell and aggregate across operator types while enforcing an open-access condition.

6.1 Data

We calibrate the economic parameters of our model using data collected by The Space Report (Space Foundation, 2021) on the annual revenues accruing to each sector of the space economy from 2006-2019. These data have been used in other economic analyses of space and orbit use (Wienzierl, 2018; Rao, Burgess, and Kaffine, 2020; Crane et al., 2020; Rao and Letizia, 2021). The data are not ideal for our purpose as they are aggregates covering the entire space sector, but more granular datasets describing specific LEO satellite operators' revenues and costs are not available. To focus on revenues and costs relevant to LEO satellite oper-

ators, we use only the variables which are plausibly attributable to LEO satellite activities. We calculate total LEO satellite operator revenues as the sum of the "Satellite communications" and "Earth observation" variables, and total LEO satellite operator costs as the sum of the "Ground stations and equipment", "Space Situational Awareness" (SSA), "Insurance premiums", "Commercial satellite launch", and "Commercial satellite manufacturing" variables. We display these variables in table 1. We discard variables representing revenues to the direct-to-home television, GNT (Geolocation, Navigation, and Timing), and satellite radio sectors, as these are provided by satellites in higher orbits beyond LEO. We also exclude suborbital commercial human spaceflight deposits as they are by definition for transit to regions below orbital altitudes (e.g. 50-80 km above mean sea level). Since our data is recorded annually, we set the period length to 1 year.

Table 1: Economic data. Figures are in nominal billion USD.

Year	Satellite communications	Earth observation	Ground stations and equipment	SSA	Insurance premiums	Satellite launches (commercial)	Satellite manufacturing (commercial)	Total LEO operator revenues	Total LEO operator costs
2006	13.800	0	75.620	0	0.900	1.400	2.920	13.800	80.840
2007	15.100	1.268	86.870	0	0.736	1.550	3.800	16.368	92.956
2008	16.700	1.404	77.230	0	0.941	2	5.200	18.104	85.371
2009	17.070	1.625	61.860	0	0.970	2.410	4.030	18.695	69.270
2010	17.670	1.900	61.713	0	0.887	2.450	3.410	19.570	68.460
2011	19.322	2.102	76.806	0	0.877	1.930	4.240	21.424	83.853
2012	20.558	2.189	84.117	0	0.982	2.500	6.180	22.747	93.779
2013	21.550	2.133	101.252	0	0.778	1.809	4.360	23.683	108.199
2014	21.702	2.300	119.602	0	0.829	2.386	4.750	24.002	127.567
2015	23.200	2.684	77.832	0	0.727	2.613	6.050	25.884	87.222
2016	23	3.087	81.695	0	0.632	2.045	4.829	26.087	89.201
2017	23.195	3.350	85.839	0	0.712	2.489	6.817	26.545	95.857
2018	24.970	3.450	92.700	0	0.460	1.490	5.280	28.420	99.930
2019	23.740	3.580	112.450	1.200	0.500	1.210	3.800	27.320	119.160

We calibrate physical parameters of our model using a kinetic gas-like approximation of orbital mechanics and data from DISCOS (Letizia et al., 2017; European Space Agency, 2021). These data describe the launch traffic, active satellites, and tracked debris objects (i.e larger than 10 cm diameter) in the 600-650 km shell over the 2006-2020 period. These data aggregate over different types of operators (e.g. commercial operators, civil government operators, defense operators). We display these data in table 2, along with the collision probability calculated from the kinetic gas approximation assuming satellite operators avoid 99% of all

collisions between satellites and 95% of all collisions between satellites and tracked debris. Letting the avoidance success rates be κ_{SS} and κ_{DD}, the probability of an unavoidable collision becomes

$$L(S,D) = (1-\kappa_{SS})(1-e^{-\alpha_{SS}S}) + (1-\kappa_{SD})(1-e^{-\alpha_{SD}D}) - (1-\kappa_{SS})(1-\kappa_{SD})(1-e^{-\alpha_{SS}S})(1-e^{-\alpha_{SD}D}). \tag{33}$$

Many ostensibly-non-commercial satellites are operated as joint ventures with commercial enterprises and many commercial satellite operators serve primarily civil government or defense customers, so we do not separate the satellite data by operator type. Further, since all satellites contribute to debris and collision probability regardless of their operator type, non-commercial operators' satellites ought to be included in the state vector. Non-commercial operators may also contribute to the observed "occupancy elasticity" (described precisely in the following section), further complicating efforts to properly disentangle payoffs to different operator types from the available data.

The DISCOS physical data also provide object characteristics such as mass and cross-sectional area, which are necessary for the kinetic gas approximation. We describe the details of the kinetic gas approximation of orbital mechanics in Appendix A.3.

Table 2: Orbital traffic in the 600-650 km shell. Collision probability is rounded to two decimal places.

Year	Satellites launched	Active satellites	Tracked debris	Collision probability
2006	15	25	211	2.95e-06
2007	84	31	275	3.84e-06
2008	168	47	273	3.85e-06
2009	72	43	393	5.48e-06
2010	156	53	444	6.20e-06
2011	30	56	411	5.76e-06
2012	73	53	429	6.00e-06
2013	213	64	454	6.37e-06
2014	261	97	484	6.87e-06
2015	175	122	495	7.09e-06
2016	15	114	494	7.05e-06
2017	26	122	525	7.49e-06
2018	36	139	506	7.28e-06
2019	33	155	543	7.83e-06
2020	9	158	626	8.97e-06

6.2 Calibration approach

To calibrate our model, we make three modifications to the open-access equilibrium condition in equation 14. First, we allow the per-period satellite payoff and cost to vary over time, i.e $\pi \to \pi_t$ and $F \to F_t$. As described in Appendix B and in Rao, Burgess, and Kaffine (2020), this changes the equilibrium condition to

$$\pi_{t+1} = (1+r)F_t - (1 - L(S_{t+1}, D_{t+1}))F_{t+1} \tag{34}$$

$$\implies L(S_{t+1}, D_{t+1}) = 1 + \frac{\pi_{t+1}}{F_{t+1}} - (1+r)\frac{F_t}{F_{t+1}}. \tag{35}$$

This form is similar to the one described in Proposition 1 but for the time subscripts and term $1-(1+r)\frac{F_t}{F_{t+1}}$. This term represents capital gains accruing to a period t launcher from increases in the cost of building and launching a satellite in period $t+1$. We abstract from operators' expectations over economic variables and assume they perfectly forecast all $t+1$ objects.

Second, we allow the per-period satellite payoff to depend on the current stock of satellites in orbit, i.e $\pi_t \to \pi_t(S_t)$. We use a constant elasticity form, $\pi_t = p_t S_t^{\varepsilon}$, where ε is the "orbital occupancy elasticity of per-period satellite payoffs". The occupancy elasticity is a reduced-form measure of the net degree of competition and returns to scale from active satellites occupying the same shell. If $\varepsilon < 0$, satellites in the same shell are gross substitutes in output and the occupancy elasticity primarily reflects competitive effects, such as the price elasticity of demand or spectrum congestion elasticity of satellite output. If $\varepsilon > 0$, satellites in the same shell are gross complements in output and the occupancy elasticity primarily reflects scale effects. There are at least two sources of scale effects: improvements in output quality from satellites being able to coordinate signal transmissions between each other, and improvements in SSA due to the greater number of operators in the shell. Quality-driven revenue increases are possible when multiple satellites bounce signals between each other to ensure better service quality on the ground, while improved SSA reduces the marginal cost of collision avoidance maneuvers. While competitive effects may dominate in the long run (i.e. eventually $\varepsilon < 0$), scale effects are likely dominant in the short run (i.e. initially $\varepsilon > 0$) as the industry establishes itself. We assume that the downstream market for satellite outputs is competitive such that operators do not internalize $\frac{\partial \pi_t}{\partial S_t}$, ruling out the radio spectrum coordination interpretation of any scale effects. The equilibrium condition in equation 14 becomes

$$L(S_{t+1}, D_{t+1}) = 1 + \frac{\pi_{t+1}(S_{t+1})}{F_{t+1}} - (1+r)\frac{F_t}{F_{t+1}}. \tag{36}$$

We assume the occupancy elasticity varies much slower than satellite payoffs and costs, and treat the occupancy elasticity as constant within each simulation.[29]

[29] Specifically, we assume the occupancy elasticity is constant until at least 2070.

Finally, we incorporate exogenous limited satellite lifespans to allow for natural depreciation and replacement of satellites. We calibrate this value to the average active LEO satellite lifetime of roughly 6.71 years based on data from the European Space Agency's DISCOS database (European Space Agency, 2021). This implies roughly 15% of active satellites in LEO turn over every year on average, i.e the fraction remaining is $\mu = 0.85$. Though this introduces an additional term in the equilibrium condition, we describe below why it does not affect our calibration approach.

For simulation in future periods, we estimate the growth rates of total LEO satellite operator revenues and costs. For revenues, we estimate

$$\log(\pi_t) = \eta_0^{\pi} + \eta_1^{\pi} t + \eta_2^{\pi} \log(S_t) + \nu_t^{\pi}, \tag{37}$$

where $\log(\pi_t)$ is the natural logarithm of total LEO satellite operator revenues, t is the year, the growth rate is $g = \exp\left(\eta_1^{\pi}\right) - 1$, the occupancy elasticity is η_2^{π}, and the regression error is ν_t^{π}. For costs, we estimate

$$\log(F_t) = \eta_0^{F} + \eta_1^{F} t + \nu_t^{F}, \tag{38}$$

with variables and parameters defined similarly.

Regression results for equations 37 and 38 are shown in table 3, implying annual total revenue and cost growth rates of roughly 3% and 2.5%. Our central growth rate estimates are within the range calculated in Crane et al. (2020) and most consistent with space economy growth projections by Morgan Stanley. Given our small sample size and interest in drawing from the joint parameter distributions for simulations, we use a residual bootstrap with 100,000 draws to compute standard errors (MacKinnon, 2006). We show the bootstrapped distributions of occupancy elasticity, revenue growth, and cost growth parameter estimates in Appendix A.5, figure 9.

The competition and scale effects determining the sign of ε cannot be separately identified without more granular data on revenues and costs for individual LEO satellite operators or a plausible instrumental variable. To the best of our knowledge the former is not available, and the latter will require further research.

Calibrating π_t and F_t directly from the data in table 1 to reflect only operators in the 600-650 km shell is challenging for two reasons. First, the data in table 1 cover all satellite operators—our variable selection step is the only thing restricting the set of operators included in the data.

Even if we were successful in removing all operators outside of LEO through variable selection when calculating total LEO operator revenues and costs, the revenue and cost variables will still include operators outside the 600-650 km shell. Thus, there is an unmeasured "LEO-share" coefficient $l \in [0,1]$ attached to the measured total revenues and costs shown in table 1. Second, even if we had data on operators in the 600-650 km shell, we would need individual operator-level data to compute π_t and F_t. As far as we are aware, such granular data on LEO satellite operators is not publicly available. Consequently, there is also an unmeasured "shell-share" coefficient $s \in [0,1]$ attached to the measured total revenues and costs in table 1.

Fortunately, equation 35 offers a way to address both challenges. Letting π_t be the total LEO satellite operator revenues and F_t be the total LEO satellite operator costs from table 1, and L_t be the collision probability shown in table 2, we estimate the following regression on data from 2006-2019:

$$L_t = \gamma_0 + \gamma_1 \frac{\pi_t}{F_t} + \gamma_2 \frac{F_{t-1}}{F_t} + e_t. \tag{39}$$

The estimated "adjustment coefficients" $(\gamma_0, \gamma_1, \gamma_2)$ reflect the LEO-share and shell-share coefficients as well as the satellite turnover rate. Though these three parameters are not separately identified, we use the coefficient estimates to simulate the model in future periods given projected growth in π_t and F_t.[30] A similar approach was used in Rao, Burgess, and Kaffine (2020) to calculate the time path of an optimal Pigouvian tax on satellites.

We calibrate the debris decay rate δ based on residence times by object altitude, cross-sectional area, and average share of each object type over 2006-2019 from DISCOS, finding that approximately 7% of debris objects in the 600-650 km shell decay every year.[31] We calibrate the parameters of L and G in two steps. First, we compute the collision probability and new fragment formation parameters using a kinetic gas approximation similar to the one used in Letizia et al. (2017) and Letizia, Lemmens, and Krag (2018) as well as analytical fragmentation formulas from Krisko (2011) and Letizia (2016) calibrated to the NASA standard breakup model. These formulas require data on object mass and cross-sectional area, which we obtain from DISCOS. The DISCOS parameters describe average values across different types of active satellites and debris objects, so we compute share-weighted averages for active satellites

[30] If the shares are common to revenues and costs, e.g. $\pi \to s\pi, F \to sF$, the coefficients will cancel out of the ratios we use in equation 39 and our estimated adjustment coefficients would only reflect satellite turnover. Our estimation results suggest these shares are not common to revenues and costs, i.e. $\pi \to s^{\pi}\pi, F \to s^{F}F$, and may be varying over time. This is not the only interpretation of our estimates—as described in Rao, Burgess, and Kaffine (2020), the coefficients may also reflect unmodeled frictions in satellite launching and operation.

[31] At these altitudes, the decay rates from higher shells rapidly approach zero. For the 650-700 km shell, the share-weighted average decay rate is roughly 5%, and for the 700-750 km shell the decay rate is 3%. We therefore neglect objects entering the 600-650 km shell from higher altitudes as they are unlikely to significantly change our results.

Table 3: Parameter estimates from equations 37, 38, and 39. Estimates are rounded to 2 decimal places. Standard errors shown in parentheses. Standard errors for equations 37 and 38 are bootstrapped for use in simulations.

	Dependent variable:		
	$\log(\pi_t)$	$\log(F_t)$	L_t
	(1)	(2)	(3)
time	0.031^{*}	0.025^{***}	
	(0.016)	(0.009)	
$\log(S_t)$	0.134		
	(0.115)		
$\frac{\pi_t}{F_t}$			$2.22\text{e-}05^{**}$
			(9.01e-06)
$\frac{F_{t-1}}{F_t}$			$-2.67\text{e-}06$
			(1.98e-06)
Constant	2.315^{***}	4.357^{***}	3.35e-06
	(0.372)	(0.079)	(2.13e-06)
Observations	14	14	13
Note:		*p<0.1; **p<0.05; ***p<0.01	

and debris objects. The kinetic gas approximation implies that objects within the shell are moving randomly, leading to our next step. Second, to adjust for the non-random motion of objects in the shell, we regularize the expected fragmentation components of G by estimating a ridge regression on the debris law of motion using data in table 2 and the analytically-computed parameter values. We also use this second step to jointly estimate the launch debris parameter m from the ridge regression. We describe our procedure for calibrating the physical model parameters in more detail in Appendix section A.3.2. Table 4 summarizes the calibrated parameters used for simulations, including standard errors where relevant.

Table 4: Summary of calibrated parameter values for the 600-650 km shell. Values are rounded to the second non-zero decimal place.

Parameter	Value	Notes
η_1^{π}	0.031	Total revenues growth parameter. Standard error is 0.016.
η_1^{F}	0.025	Total costs growth parameter. Standard error is 0.009.
γ_0	3.35e-06	Equilibrium adjustment coefficient 1 (open-access capital gains). Standard error is 2.13e-06.
γ_1	2.22e-05	Equilibrium adjustment coefficient 2 (gross satellite rate of return). Standard error is 9.01e-06.
γ_2	-2.67e-06	Equilibrium adjustment coefficient 3 (open-access capital gains). Standard error is 1.98e-06.
ε	0.134	Occupancy elasticity. Standard error is 0.115.
δ	0.074	Annual fraction of debris decaying to lower shell.
μ	0.85	Annual fraction of satellites not reaching (natural) end-of-life. Equivalently, the natural satellite turnover rate is 0.15.
α_{SS}	2.73e-07	Satellite-satellite collision rate parameter.
α_{SD}	2.73e-07	Satellite-debris collision rate parameter.
α_{DD}	2.78e-07	Debris-debris collision rate parameter.
κ_{SS}	0.99	Fraction of satellite-satellite collisions successfully avoided.
κ_{SD}	0.95	Fraction of satellite-debris collisions successfully avoided.
$\tilde{\beta}_{SS}$	53,282	Expected number of fragments from satellite-satellite collision. (regularized).
$\tilde{\beta}_{SD}$	2,102	Expected number of fragments from satellite-debris collision. (regularized).
$\tilde{\beta}_{DD}$	103	Expected number of fragments from debris-debris collision (regularized).
m	0.013	Expected number of launch debris remaining in shell after 1 year (regularized).

6.3 Simulation results

We simulate the open-access model of the 600-650 km shell forward for 500 years from the 2020 initial condition ($(S_{2020}, D_{2020}) = (158, 626)$) 1000 times. Each simulation draws a different fixed occupancy elasticity. Within each simulation, the growth rates of annual costs and

returns vary randomly about their trends. This approach is motivated by our assumption that the occupancy elasticity varies more slowly than the costs of and returns to satellite ownership.[32]

We generate annual variation in the returns and costs to operating a LEO satellite by drawing annual growth rates from the estimated distributions of η_1^π and η_1^F. We assume that operators perfectly forecast these changes and treat them as exogenous when making launch decisions. We construct the slower-than-historical-average growth scenario by halving the mean growth rates for revenues and costs, and the faster-than-historical-average growth scenario by doubling the mean growth rates. We set the launch constraint $\bar{X}$ to 261, the maximum launch rate to the 600-650 km shell observed over 2006-2019. The launch constraint binds in the majority of years with positive launch rates, leading to launch patterns that are typically maximal when returns are high and zero otherwise. We describe our simulation procedure detail in Appendix A.5.

Table 5 shows summary statistics of key economic parameters, state variables, and Kessler times from our simulations. 90% of simulations cross the Kessler threshold within 500 years, accounting for the difference in sample sizes for Kessler time metrics. We show simulated time paths over the 2020-2070 horizon of the launch rate, satellite stock, debris stock, and collision probability until the year when the Kessler threshold is crossed, along with the simulated empirical distribution of Kessler times, in figure 6. Many paths begin with sequences of no launch activity to allow the satellite and debris stocks to draw down. We omit years after the threshold is crossed since exponential growth makes the debris dynamics hard to see. Consequently, the fan of lines thins as time progresses and Kessler Syndrome occurs along simulation paths. The distribution of Kessler times shows that the probability of Kessler Syndrome peaks within 25 years.

Nevertheless, open-access launch activity need not stop immediately after the Kessler time. Figure 7 shows an example of an open access path with a Kessler time of 21 years (i.e. the Kessler threshold is crossed in 2041) over the 2020-2070 horizon. Operators continue to launch to the 600-650 km shell after the Kessler time—indeed, the maximum satellite stock is not reached until a few years after the Kessler time. Though collision probability does not exceed 1% by 2065, by that point operators have already begun to reduce launch activity and the satellite stock is drawing down. Exponential growth in the debris stock means this is too little, too late.

[32] While the error from holding ε constant may be large for long-time simulations, it is likely small for the 2020-2070 horizon which we focus on. Given the short timeseries data available, tracing the likely evolution of the occupancy elasticity is an interesting challenge for future research.

Table 5: Orbit-use simulation summary statistics. Column means are over time within a simulation, row means are over simulation means. Satellite and debris stocks and Kessler times are rounded to nearest integer.

	Mean aggregate growth rate	Mean returns growth rate	Mean cost growth rate	Occupancy elasticity	Maximum satellite stock	Debris stock at Kessler time	Kessler time
Obs.	1,000	1,000	1,000	1,000	1,000	901	901
Mean	0.062	0.031	0.025	0.136	1,090	910	28
St. Dev.	0.026	0.016	0.009	0.114	151	56	35
Min	-0.026	−0.020	−0.002	−0.211	407	751	8
Median	0.061	0.031	0.025	0.136	1,091	915	20
Max	0.146	0.079	0.051	0.512	1,525	1,020	437

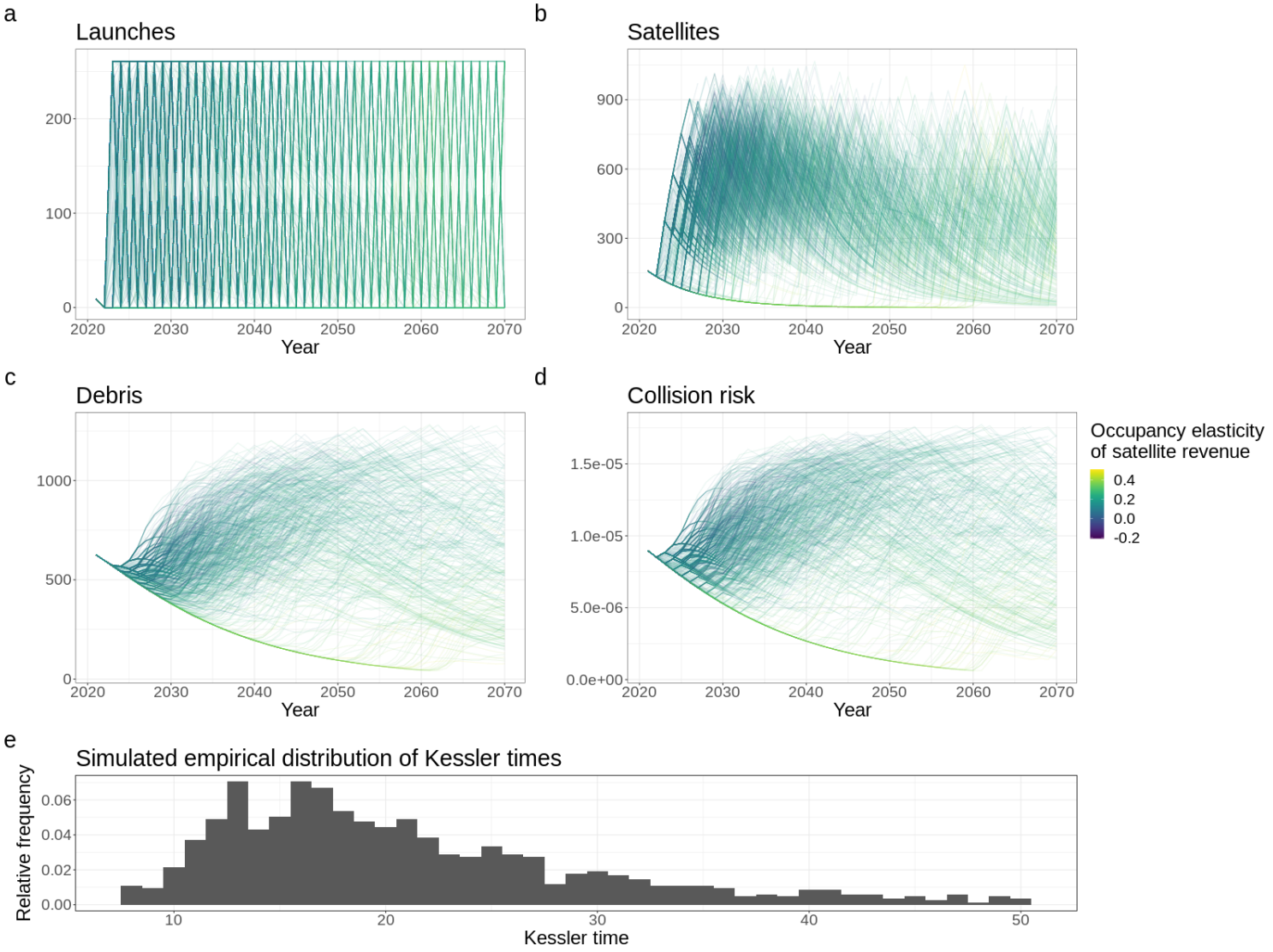

Figure 6: Simulated open-access paths of launches, satellites, debris, collision probability, and simulated empirical distribution of Kessler times, in the 600-650 km shell over the 2020-2070 horizon. Paths in panels a-d are truncated after they cross the Kessler threshold to avoid scaling issues, causing the fan of lines to thin over time.

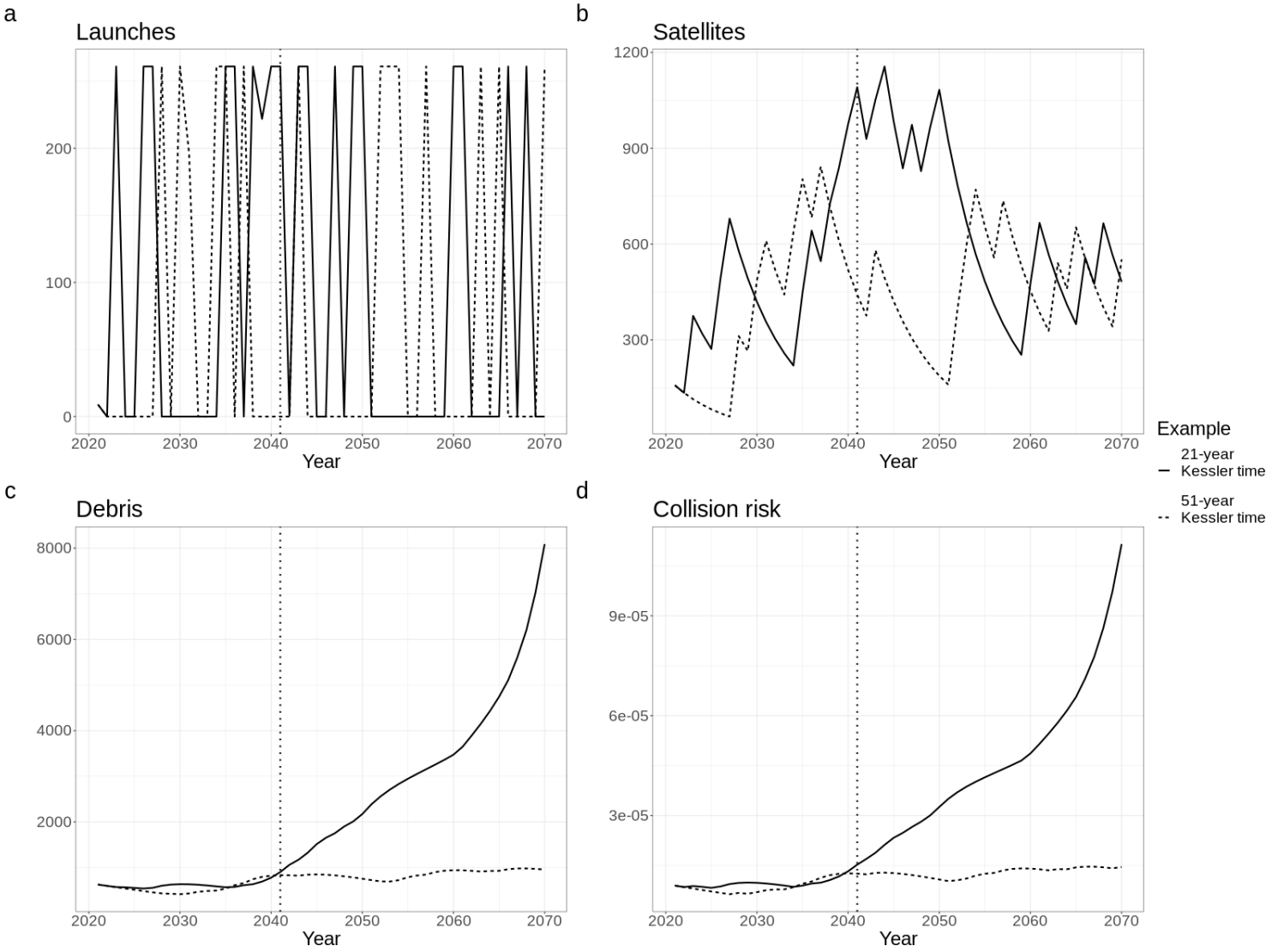

Figure 7: Examples of simulated open-access paths of launches, satellites, debris, and collision probability in the 600-650 km shell over the 2020-2070 horizon, along paths where growth in satellite revenues exceeds growth in costs. Kessler Syndrome occurs along the solid-line path in 2041 (marked by the dotted vertical line), while Kessler Syndrome doesn't occur along the dashed-line path until 2071.

Figure 8 shows the conditional distribution of Kessler times under different parameter sets, along with 95% confidence bands reflecting uncertainty due to variation in industry economics. Figure 8a shows the distribution under the main parameter set listed in table 4, while figures 8b and 8c show the distribution under alternative low-growth and high-growth parameter sets drawn from their bootstrapped joint distributions. The conditional distribution of Kessler times is a hazard curve for the occurrence of Kessler Syndrome. We estimate this functional and its confidence bands using distribution regression and the confidence band algorithm described in Chernozhukov, Fernández-Val, and Melly (2013).

The high-growth free-elasticity parameter set corresponds to projections by Goldman Sachs where the global space economy grows to $3 trillion (nominal) USD by 2040, while the low-growth free-elasticity parameter set corresponds to adjusted historical estimates of the nominal growth of the space economy from Crane et al. (2020).[33,34] The mean-growth, low-elasticity parameter set takes the main estimates and reduces the occupancy elasticity by 50%, while the mean-growth, high-elasticity parameter set takes the same values and increases the occupancy elasticity by 50%. These parameter sets are collected in table 6.

Table 6: Economic parameters for scenarios in figure 8.

Scenario	Mean space economy growth rate	Mean returns growth rate	Mean cost growth rate	Occupancy elasticity
Main	6.13%	3.11%	2.48%	0.136
Low growth, free elasticity	2%	0.535%	1.89%	0.299
High growth, free elasticity	9.5%	5.05%	3.06%	-0.00445
Mean growth, low elasticity	6.13%	3.11%	2.48%	0.0679
Mean growth, high elasticity	6.13%	3.11%	2.48%	0.204

[33]The satellite industry growth projections listed in Crane et al. (2020) do not describe their assumptions regarding occupancy elasticity. We therefore select the bootstrap draw with the growth rate closest to the listed projection and use the associated occupancy elasticity and growth rates for returns and costs.

[34]We compute the growth rate of the space economy as a whole by regressing the size of the excluded sectors (sub-orbital commercial human spaceflight deposits, guidance and positioning, direct-to-home television, and satellite radio) on the sectors we model in equations 37 and 38 and then projecting the size of the space economy as a function of the modeled returns to operating a LEO satellite. We report these regression results in Appendix A.5.

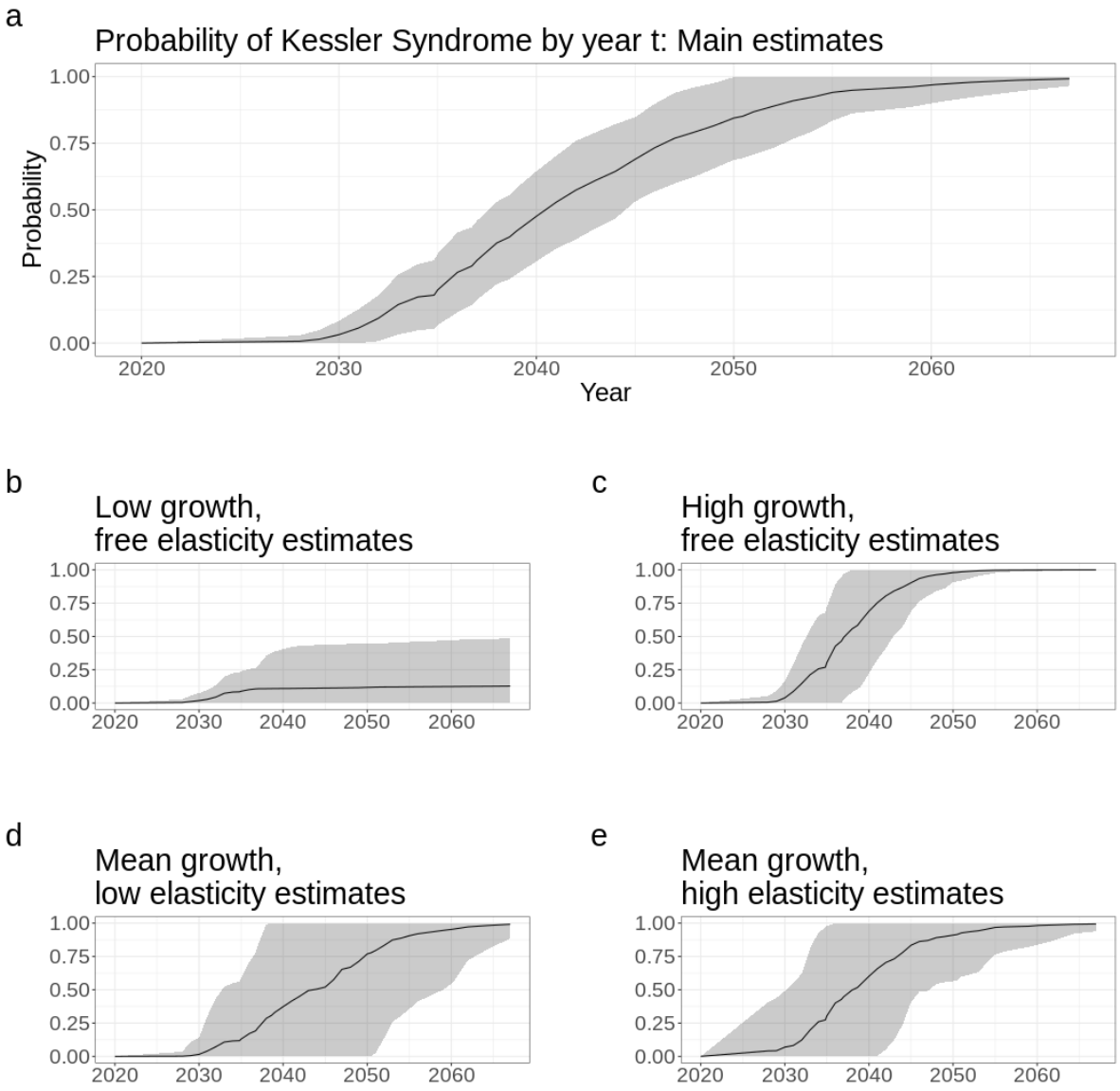

Figure 8: Estimated probability of crossing the Kessler threshold in the 600-650 km shell under open access over the 2020-2070 horizon. Shading shows 95% confidence bands. Panel a shows estimates under the main parameter set. Panel b shows estimates under a "low growth" parameter set with the occupancy elasticity free. Panel c shows estimates under a "high growth" parameter set with the occupancy elasticity free. Panel d shows estimates under a "low elasticity" parameter set near the main growth estimates. Panel e shows estimates under a "high elasticity" parameter set near the main growth estimates.

Under all but the low growth, free elasticity parameter sets, we find it more likely than not that Kessler Syndrome will occur by 2050 given open access and historically-plausible annual variation in sectoral costs and revenues. The low growth, free elasticity parameter set is the only case where the costs of operating a satellite grow faster than the revenues. As might be

expected, the the probability of Kessler Syndrome is uniformly lower at any given time under the low-growth parameter set than under the main set, and vice versa for the high-growth parameter set. All else equal, higher occupancy elasticities uniformly increase the probability of Kessler Syndrome at any given time. In the main parameter set, the probability of Kessler Syndrome occurring exceeds 0.5 shortly after 2040. In the low-growth parameter set, the upper 95% confidence band of the probability of Kessler Syndrome occurring does not approach 0.5 until 2070, while under the high-growth parameter set the probability is nearly 1 by 2045.

7 Discussion

Natural resource collapse is not an unusual possibility in many contexts (e.g. Clark (1973); Mäler, Xepapadeas, and de Zeeuw (2003); Costello, Gaines, and Lynham (2008); Gars and Spiro (2018); Costello and Grainger (2018); Berry, Fenichel, and Robinson (2019)), but the way it manifests in orbit use is unique. In particular, the role of the discount rate in orbit use is quite different from its role in biological resource use. Rather than higher discount rates inducing resource collapse, all else equal higher discount rates will reduce the excess return on a satellite, thus reducing open-access and optimal orbit use and potentially staving off resource collapse. This result may seem counterintuitive—shouldn't higher discount rates induce less consideration for outcomes in the future?—but is a natural consequence of rent dissipation. Higher discount rates reduce the excess return on a satellite (i.e lengthen the payback period), reducing incentives to launch.

It is important to note that open-access rent dissipation in orbit is fundamentally the same as in other settings. Launchers and operators do not benefit from self-restraint because they have no reason to expect others to follow suit. The excess launching generated by this behavior is similar to overexploitation in other common resource contexts. In orbit, autocatalytic debris production creates multiple steady states. As in other resources with nonlinear dynamics, e.g. May (1974); Clark and Munro (1975); Wagener (2003), this multiplicity creates a tipping point.

As in biological contexts, once resource collapse in orbit has been initiated it will continue unless the population levels are altered. While in fisheries and other biological contexts this often amounts to introducing new members of the harvested species, the reverse is true for orbit use: to prevent or stop Kessler Syndrome, the satellite or debris populations (or both) must be reduced. This is driven by the difference between biological reproduction and "reproduction" of debris. Since any mass on orbit can be a source of new debris, lowering the rate at which debris "reproduces" requires reducing the mass on orbit. Combined with equation 3, framing the result in terms of "debris reproduction" clarifies the role of the new fragment formation

function, G, in determining whether Kessler Syndrome is possible and why it might occur. If the new fragment function is not coupled with the debris stock ($G_D \equiv 0$), then equation 3 is always negative and Kessler Syndrome is impossible. Intuitively, $G_D \equiv 0$ means new fragments can only form due to active satellites. Thus, as the debris stock grows, collision probability also increases, eventually leading firms to stop launching satellites. If $G_D \equiv 0$ then the debris stock will shrink as the number of active satellites dwindles, until firms can begin launching again and the stable steady state is reached. But if $G_D > 0$, debris can reproduce without active satellites. Since multiple combinations of satellites and debris can produce the level of collision probability required for rent dissipation, firms may stop launching only after there is enough mass on orbit for "debris reproduction" without additional human input. The new fragment debris coupling is considered a key factor in long-run debris population dynamics even ignoring the economic incentives to launch satellites (Liou, 2006a; Lewis, 2020).

Recent research also indicates that the natural rate of debris decay in LEO is decreasing in atmospheric CO_2 concentrations, with a 1.5°C warming target projected to cause a 30% increase in orbital residence times relative to the year 2000 (Brown et al., 2021). Terrestrial economic activity thus affects orbit-use dynamics through an additional channel not modeled here. Given that near-collisions between debris objects are already occurring and the likelihood that warming in coming decades will exceed 1.5°C, it seems only a matter of time before this coupling acquires greater empirical significance (Davenport, 2020; Masson-Delmotte et al., 2021).

Indeed, our analysis suggests that an important region of LEO may experience Kessler Syndrome within the next few decades. While our Kessler time calculations should be taken with a grain of salt since we assume no active debris removal technology and do not incorporate the substitution possibilities afforded by multiple shells (biasing our estimates upward), we also assume perfect compliance with satellite disposal guidelines and extremely successful active collision avoidance measures (biasing our estimates downward). While the net effect of these assumptions is unclear, our results suggest that the economic returns to satellite ownership will be a key factor determining whether and when Kessler Syndrome occurs.

One, perhaps less alarming, way to interpret these estimates is with analogy to the ratio of proven fossil fuel reserves to production. Since the 1980s, such estimates have indicated that there are roughly 50 years worth of proven reserves of natural gas remaining (Dale et al., 2021). Despite production increases, new discoveries and innovations have thus far consistently maintained this roughly 50-year time till depletion of proven fossil fuel resources. If a similar story holds for orbit use, perhaps Kessler Syndrome is not actually imminent in LEO. Yet the physical and institutional differences between orbit use and fossil fuel extraction give

some cause for concern. Nonlinear dynamics and the difficulty of clearing small hazardous fragments from orbit suggest at lease some portions of the debris population will continue to grow in the near future, as the active debris removal technologies nearing commercial readiness are focused only on large objects. The institutional picture is even bleaker: open access to orbit, dispersed property rights over debris objects, and the public good nature of debris removal all suggest privately-demanded debris removal will be inefficient and subject to free-rider problems (Klima et al., 2016, 2018). Additionally, military activity in space presents a novel challenge relative to other resource contexts, as kinetic anti-satellite missile tests can be significant sources of small debris fragments (Liou and Johnson, 2009a). Thus, technological advances in orbit use must not only address the current physical state of the environment, but must also counter institutional features which make Kessler Syndrome more likely.

8 Conclusion

In this paper we present a dynamic physico-economic model of orbit use under rational expectations with endogenous collision probability and Kessler Syndrome. We show how both economic and physical parameters drive equilibrium short- and long-run orbital-use patterns, derive the marginal external cost of a satellite, explore the multiplicity and stability of open-access steady states, and examine the relationships between open-access orbit use, optimal orbit use, and Kessler Syndrome. We then calibrate the model to an important region of LEO and estimate the likely times when Kessler Syndrome will occur under different patterns of satellite industry economics. We highlight three messages regarding orbital-use management.

First, under open access too many firms will launch satellites because they won't internalize the risks they impose on other orbit users. Though profit maximizing satellite owners have incentives to reduce launches as the risk of a collision grows, they do not respond to debris growth or collision risk optimally. This inefficiency is independent of whether Kessler Syndrome is possible or not. Unlike many other bioeconomic commons problems, higher discount rates can induce less (rather than more) open-access overexploitation.

Second, Kessler Syndrome is possible as long as debris objects can collide with each other and generate new fragments, i.e the new fragment formation debris coupling exists. Engineering studies indicate that this coupling does in fact exist. Due to open access, even profit-maximizing firms with rational expectations may continue to launch satellites despite recognizing their role in causing Kessler Syndrome and even after the Kessler threshold has been crossed.

Third, under open access Kessler Syndrome is more likely as the excess return on a satellite

rises, even if firms will respond to orbital congestion by launching fewer satellites. As launch costs fall and new commercial satellite applications become viable, LEO is thus increasingly and inefficiently likely to experience Kessler Syndrome. While it may seem paradoxical that the very changes which make orbit use profitable can also increase the risk of resource collapse, such dynamics occur frequently in bioeconomic commons problems. Calibrated simulations reveal that space economy growth rates projected by investment banks and industry associations are consistent with Kessler Syndrome occurring as early as 2035. Our results suggest that, absent institutional reform, continued growth of the space economy may trigger Kessler Syndrome in the near future. This can occur even in regions perceived to have relatively high rates of natural renewability, providing new evidence that compliance with the 25-year rule is insufficient to ensure sustainable orbit use.

Commons management is one of the oldest problems in economics. Economists tend to favor property rights, corrective taxes, or other market-based mechanisms to solve such problems. While these mechanisms can ensure efficient orbit use, more data collection and research are needed to understand how orbital-use management policies should be designed in light of the unique physical and institutional features of this environment. Whether they are enforced by states, structured as self-enforcing agreements between private actors, or some combination of the two, effective orbital-use management policies must address the open access problem.

References

Adilov, Nodir, Peter J. Alexander, and Brendan M. Cunningham. 2015. "Earth Orbit Debris: An Economic Model." *Environmental and Resource Economics* 60:81–98.

Adilov, Nodir, Peter J Alexander, and Brendan M Cunningham. 2018. "An economic "Kessler Syndrome": A dynamic model of earth orbit debris." *Economics Letters* 166:79–82.

Adilov, Nodir, Brendan M Cunningham, Peter J Alexander, Jerry Duvall, and Daniel R Shiman. 2019. "Left For Dead: Anti-Competitive Behavior In Orbital Space." *Economic Inquiry* 57 (3):1497–1509.

Ailor, William, James Womack, Glenn Peterson, and Norman Lao. 2010. "Effects of Space Debris on the Cost of Space Operations." Tech. Rep. IAC-10.A6.2.10.

Baragwanath, Kathryn, Ran Goldblatt, Gordon Hanson, and Amit K Khandelwal. 2019. "Detecting urban markets with satellite imagery: An application to India." *Journal of Urban Economics* :103173.

Beaudry, Paul, Dana Galizia, and Franck Portier. 2020. "Putting the cycle back into business cycle analysis." *American Economic Review* 110 (1):1–47.

Bernknopf, Richard, Andrew Steinkruger, and Yusuke Kuwayama. 2021. "Earth Observations Can Enable Cost-Effective Conservation of Eastern North Pacific Blue Whales: A Value of Information Analysis." *UMBC Faculty Collection* .

Berry, Kevin, Eli P. Fenichel, and Brian E. Robinson. 2019. "The ecological insurance trap." *Journal of Environmental Economics and Management* 98:102251. URL http://www.sciencedirect.com/science/article/pii/S0095069618300275.

Bohn, Henning and Robert T Deacon. 2000. "Ownership risk, investment, and the use of natural resources." *American Economic Review* 90 (3):526–549.

Boldrin, Michele. 1992. "Dynamic externalities, multiple equilibria, and growth." *Journal of Economic Theory* 58 (2):198–218.

Bradley, Andrew M. and Lawrence M. Wein. 2009. "Space debris: Assessing risk and responsibility." *Advances in Space Research* 43:1372–1390.

Brodkin, Jon. 2017. "With latency as low as 25ms, SpaceX to launch broadband satellites in 2019." *Ars Technica* .

Brown, Matthew Kenneth, HG Lewis, AJ Kavanagh, and Ingrid Cnossen. 2021. "Future decreases in thermospheric neutral density in low Earth orbit due to carbon dioxide emissions." *Journal of Geophysical Research: Atmospheres* 126 (8):e2021JD034589.

Brown Jr, Gardner. 1974. "An optimal program for managing common property resources with congestion externalities." *Journal of Political Economy* 82 (1):163–173.

Béal, Sylvain, Marc Deschamps, and Hervé Moulin. 2020. "Taxing congestion of the space commons." *Acta Astronautica* 177:313 – 319. URL http://www.sciencedirect.com/science/article/pii/S009457652030463X.

Chavas, Jean-Paul, Corbett Grainger, and Nicholas Hudson. 2016. "How should economists model climate? Tipping points and nonlinear dynamics of carbon dioxide concentrations." *Journal of economic behavior & organization* 132:56–65.

Chernozhukov, Victor, Iván Fernández-Val, and Blaise Melly. 2013. "Inference on counterfactual distributions." *Econometrica* 81 (6):2205–2268.

Clark, Colin W. 1973. "The economics of overexploitation." *Science* 181 (4100):630–634.

Clark, Colin W and Gordon R Munro. 1975. "The economics of fishing and modern capital theory: A simplified approach." *Journal of Environmental Economics and Management* 2 (2):92 – 106. URL http://www.sciencedirect.com/science/article/pii/0095069675900029.

Cooke, Roger and Alexander Golub. 2020. "Market-based methods for monetizing uncertainty reduction." *Environment Systems and Decisions* 40 (1):3–13.

Costello, Christopher, Steven D Gaines, and John Lynham. 2008. "Can catch shares prevent fisheries collapse?" *Science* 321 (5896):1678–1681.

Costello, Christopher and Corbett A Grainger. 2018. "Property rights, regulatory capture, and exploitation of natural resources." *Journal of the Association of Environmental and Resource Economists* 5 (2):441–479.

Crane, Keith W, Evan Linck, Bhavya Lal, and Rachel Y Wei. 2020. "Measuring the Space Economy: Estimating the Value of Economic Activities in and for Space." Tech. Rep. AD1122153, Institute for Defense Analyses, Alexandria VA.

Dale, Spencer et al. 2021. "BP statistical review of world energy." *BP Statistical Review, London, UK* (70).

Daniel, Kent D, Robert B Litterman, and Gernot Wagner. 2019. "Declining CO2 price paths." *Proceedings of the National Academy of Sciences* 116 (42):20886–20891.

Davenport, Christian. 2020. "A rocket booster and a dead satellite avoided a collision Thursday, illustrating the 'ticking time bomb' of space debris." *The Washington Post* .

Dietz, Simon, James Rising, Thomas Stoerk, and Gernot Wagner. 2021a. "Economic impacts of tipping points in the climate system." *Proceedings of the National Academy of Sciences* 118 (34). URL https://www.pnas.org/content/118/34/e2103081118.

Dietz, Simon, Rick van der Ploeg, Arman Rezai, and Frank Venmans. 2021b. "Are economists getting climate dynamics right and does it matter?" *Journal of the Association of Environmental and Resource Economists* .

Donaldson, Dave and Adam Storeygard. 2016. "The view from above: Applications of satellite data in economics." *Journal of Economic Perspectives* 30 (4):171–98.

Duranton, Gilles and Matthew A Turner. 2011. "The fundamental law of road congestion: Evidence from US cities." *American Economic Review* 101 (6):2616–52.

European Space Agency. 2021. "Database and information system characterising objects in space." https://discosweb.esoc.esa.int/. Accessed: 2021-03-19.

Farzin, Y Hossein. 1996. "Optimal pricing of environmental and natural resource use with stock externalities." *Journal of Public Economics* 62 (1-2):31–57.

Federal Communications Commission. 2020. "Report and Order and Further Notice of Proposed Rulemaking in the matter of Mitigation of Orbital Debris in the New Space Age." Tech. Rep. IB Docket No. 18-313. FCC-FIRC2004-03.

Fons, Jerome S. 1987. "The default premium and corporate bond experience." *The Journal of Finance* 42 (1):81–97.

Gars, Johan and Daniel Spiro. 2018. "Trade and the risk of renewable-resource collapse." *Journal of the Association of Environmental and Resource Economists* 5 (1):155–206.

Gordon, H. Scott. 1954. "The Economic Theory of a Common-Property Resource: The Fishery." *Journal of Political Economy* 62.

Gorove, Stephen. 1969. "Interpreting Article II of the Outer Space Treaty." *Fordham Law Review* 37.

Grzelka, Zachary and Jeffrey Wagner. 2019. "Managing Satellite Debris in Low-Earth Orbit: Incentivizing Ex Ante Satellite Quality and Ex Post Take-Back Programs." *Environmental and Resource Economics* :1–18.

Guyot, Julien, Sébastien Rouillon et al. 2021. "Designing satellites to cope with orbital debris." Tech. rep., Groupe de Recherche en Economie Théorique et Appliquée (GREThA).

Haveman, Robert H. 1973. "Common Property, Congestion, and Environmental Pollution." *The Quarterly Journal of Economics* 87:278–287.

Hein, Lars. 2006. "Cost-efficient eutrophication control in a shallow lake ecosystem subject to two steady states." *Ecological Economics* 15:429–439.

Henderson, Vernon. 1997. "Externalities and industrial development." *Journal of urban economics* 42 (3):449–470.

Hoerl, Arthur E, Robert W Kennard, and Roger W Hoerl. 1985. "Practical use of ridge regression: A challenge met." *Journal of the Royal Statistical Society: Series C (Applied Statistics)* 34 (2):114–120.

Huang, Ling and Martin D Smith. 2014. "The dynamic efficiency costs of common-pool resource exploitation." *American Economic Review* 104 (12):4071–4103.

IADC. 2007. "IADC Space Debris Mitigation Guidelines." Tech. Rep. IADC-02-01.

Jain, Meha. 2020. "The benefits and pitfalls of using satellite data for causal inference." *Review of Environmental Economics and Policy* 14 (1):157–169.

Kessler, Donald J and Burton G Cour-Palais. 1978. "Collision Frequency of Artificial Satellites: The Creation of a Debris Belt." *Journal of Geophysical Research* 83:2637–2646.

Kessler, Donald J, Nicholas L Johnson, J-C Liou, and Mark Matney. 2010. "The Kessler Syndrome: Implications to Future Space Operations." *33rd Annual AAS Guidance and Control Conference* .

Klima, Richard, Daan Bloembergen, Rahul Savani, Karl Tuyls, Daniel Hennes, and Dario Izzo. 2016. "Space debris removal: A game theoretic analysis." *Games* 7 (3):20.

Klima, Richard, Daan Bloembergen, Rahul Savani, Karl Tuyls, Alexander Wittig, Andrei Sapera, and Dario Izzo. 2018. "Space debris removal: Learning to cooperate and the price of anarchy." *Frontiers in Robotics and AI* 5:54.

Krage, Frederic Joshua. 2020. "NASA Spacecraft Conjunction Assessment and Collision Avoidance Best Practices Handbook." .

Krisko, PH. 2011. "Proper implementation of the 1998 NASA breakup model." *Orbital Debris Quarterly News* 15 (4):1–10.

Lemoine, Derek and Christian Traeger. 2014. "Watch your step: optimal policy in a tipping climate." *American Economic Journal: Economic Policy* 6 (1):137–66.

Lemoine, Derek and Christian P Traeger. 2016. "Economics of tipping the climate dominoes." *Nature Climate Change* 6 (5):514–519.

Letizia, F., S. Lemmens, and H. Krag. 2018. "Application of a debris index for global evaluation of mitigation strategies." 69th International Astronautical Congress.

Letizia, Francesca. 2016. *Space debris cloud evolution in Low Earth Orbit*. Ph.D. thesis, University of Southampton.

Letizia, Francesca, Camilla Colombo, Hugh Lewis, and Holger Krag. 2017. "Extending the ECOB space debris index with fragmentation risk estimation." .

Levhari, David and Leonard J Mirman. 1980. "The great fish war: an example using a dynamic Cournot-Nash solution." *The Bell Journal of Economics* :322–334.

Lewis, Hugh G. 2020. "Understanding long-term orbital debris population dynamics." *Journal of Space Safety Engineering* 7 (3):164–170.

Libecap, Gary D and Steven N Wiggins. 1985. "The influence of private contractual failure on regulation: the case of oil field unitization." *Journal of Political Economy* 93 (4):690–714.

Liou, J.C. 2006a. "Collision activities in the future orbital debris environment." *Advances in Space Research* 38:2102–2106.

———. 2006b. "A statistical analysis of the future debris environment." *Acta Astronautica* 62:264–271.

Liou, J.C., D.T. Hall, P.H. Krisko, and J.N. Opiela. 2004. "LEGEND - a three-dimensional LEO-to-GEO debris evolutionary model." *Advances in Space Research* 34:981–986.

Liou, J.C. and N.L. Johnson. 2008. "Instability of the present LEO satellite populations." *Advances in Space Research* 41:1046–1053.

———. 2009a. "Characterization of the catalogued Fengyun-1C fragments and their long-term effect on the LEO environment." *Advances in Space Research* 43:1407–1415.

———. 2009b. "A sensitivity study of the effectiveness of active debris removal in LEO." *Acta Astronautica* 64:236–243.

Macauley, Molly K. 2015. "The economics of space debris: Estimating the costs and benefits of debris mitigation." *Acta Astronautica* 115:160–164.

MacKinnon, James G. 2006. "Bootstrap methods in econometrics." *Economic Record* 82:S2–S18.

Mäler, Karl-Göran, Anastasios Xepapadeas, and Aart de Zeeuw. 2003. "The Economics of Shallow Lakes." *Environmental and Resource Economics* 26:603–624.

Masson-Delmotte, V., P. Zhai, A. Pirani, S. L. Connors, C. Péan, S. Berger, N. Caud, Y. Chen, L. Goldfarb, M. I. Gomis, M. Huang, K. Leitzell, E. Lonnoy, J. B. R. Matthews, T. K. Maycock, T. Waterfield, O. Yelekçi, R. Yu, and B. Zhou. 2021. "Climate Change 2021: The Physical Science Basis. Contribution of Working Group I to the Sixth Assessment Report of the Intergovernmental Panel on Climate Change." Tech. rep.

May, Robert M. 1974. "Biological populations with nonoverlapping generations: stable points, stable cycles, and chaos." *Science* 186 (4164):645–647.

Nordhaus, William. 1982. "How fast should we graze the global commons?" *The American Economic Review* 72 (2):242–246.

O'Connor, Alan C, Michael P Gallaher, Kyle Clark-Sutton, Daniel Lapidus, Zack T Oliver, Troy J Scott, Dallas W Wood, Manuel A Gonzalez, Elizabeth G Brown, and Joshua Fletcher. 2019. "Economic Benefits of the Global Positioning System." Tech. Rep. 0215471, RTI International. Sponsored by National Institute of Standards and Technology.

Ostrom, Elinor, Joanna Burger, Christopher B Field, Richard B Norgaard, and David Policansky. 1999. "Revisiting the commons: local lessons, global challenges." *science* 284 (5412):278–282.

Rao, Akhil. 2018. "Economic Principles of Space Traffic Control." *Job mar-*

ket paper URL https://akhilrao.github.io/assets/working_papers/Economic_Principles_of_Space_Traffic_Control.pdf.

Rao, Akhil, Matthew G. Burgess, and Daniel Kaffine. 2020. "Orbital-use fees could more than quadruple the value of the space industry." *Proceedings of the National Academy of Sciences* 117 (23):12756–12762. URL https://www.pnas.org/content/117/23/12756.

Rao, Akhil and Francesca Letizia. 2021. "An Integrated Debris Environment Assessment Model." In *Proceedings of the 8th European Conference on Space Debris (virtual)*. ESA Space Debris Office. URL ttp://conference.sdo.esoc.esa.int.

Reinganum, Jennifer F and Nancy L Stokey. 1985. "Oligopoly extraction of a common property natural resource: The importance of the period of commitment in dynamic games." *International Economic Review* :161–173.

Ritchie, Greg and Thomas Seal. 2020. "Why Low-Earth Orbit Satellites Are the New Space Race." *The Washington Post* .

Rossi, A., L. Anselmo, A. Cordelli, P. Farinella, and C. Pardini. 1998. "Modelling the evolution of the space debris population." *Planetary Space Science* 46:1583–1596.

Rouillon, Sébastien. 2020. "A Physico-Economic Model of Low Earth Orbit Management." *Environmental and Resource Economics* :1–29.

Sandler, Todd and William Schulze. 1981. "The Economics of Outer Space." *Natural Resources Journal* 21:371–393.

Schaub, Hanspeter, Lee E.Z. Jasper, Paul V. Anderson, and Darren S. McKnight. 2015. "Cost and risk assessment for spacecraft operation decisions caused by the space debris environment." *Acta Astronautica* 113:66–79.

Scott, Anthony. 1955. "The Fishery: The Objectives of Sole Ownership." *Journal of Political Economy* 62.

Selk, Avi. 2017. "Thousands of tiny satellites are about to go into space and possibly ruin it forever." *The Washington Post* .

Sherstyuk, Katerina, Nori Tarui, Majah-Leah V Ravago, and Tatsuyoshi Saijo. 2016. "Intergenerational games with dynamic externalities and climate change experiments." *Journal of the Association of Environmental and Resource Economists* 3 (2):247–281.

Simaan, Marwan and JB Cruz. 1975. "Formulation of Richardson's model of arms race from a differential game viewpoint." *The Review of Economic Studies* 42 (1):67–77.

Somma, Gian Luigi. 2019. *Adaptive remediation of the space debris environment using feedback control*. Ph.D. thesis, University of Southampton.

Somma, Gian Luigi, Camilla Colombo, HG Lewis et al. 2017. "A statistical LEO model to investigate adaptable debris control strategies." In *7th European Conference on Space Debris, ESA/ESOC*. ESA, 1–12.

Space Foundation. 2021. "The Space Report." https://www.thespacereport.org.

Stavins, Robert N. 2011. "The problem of the commons: still unsettled after 100 years." *American Economic Review* 101 (1):81–108.

Stroming, Signe, Molly Robertson, Bethany Mabee, Yusuke Kuwayama, and Blake Schaeffer. 2020. "Quantifying the human health benefits of using satellite information to detect cyanobacterial harmful algal blooms and manage recreational advisories in US Lakes." *GeoHealth* 4 (9):e2020GH000254.

Sullivan, Daniel M and Alan Krupnick. 2018. "Using satellite data to fill the gaps in the US air pollution monitoring network." *Resources for the Future Working Paper* :18–21.

TelAstra, Inc. 2017. "Communications Satellite Databases." Available from TelAstra, Inc. at http://telastra.com/ . The data shown here are from the 2017 edition, which is available through the CU Boulder Libraries.

Union of Concerned Scientists. 2020. "UCS Satellite Database." Available from UCS at https://www.ucsusa.org/nuclear-weapons/space-weapons/satellite-database . The data shown here run through the December 2020 update.

———. 2021. "UCS Satellite Database."

Wagener, F O O. 2003. "Skiba points and heteroclinic bifurcations, with applications to the shallow lake system." *Journal of Economic Dynamics and Control* 27:1533–1561.

Weeden, Brian C. 2010. "Overview of the Legal and Policy Challenges of Orbital Debris Removal." Tech. Rep. IAC-10.A6.2.10.

Weeden, Brian C and Tiffany Chow. 2012. "Taking a common-pool resources approach to space sustainability: A framework and potential policies." *Space Policy* 28:166–172.

Wienzierl, Matthew. 2018. "Space, the Final Economic Frontier." *Journal of Economic Perspectives* 32:173–192.

Zou, Hui and Trevor Hastie. 2005. "Regularization and variable selection via the elastic net." *Journal of the royal statistical society: series B (statistical methodology)* 67 (2):301–320.

Appendices

A Proofs and derivations

A.1 Proofs

Proposition 1 (Equilibrium collision probability)**.** *Given that an open-access equilibrium exists and the collision probability function is coupled with both the satellite and debris stocks, there are multiple vectors* (X_t, S_t, D_t) *such that*

$$L(S_{t+1}, D_{t+1}) = r_s - r.$$

Increases in the excess return on a satellite cause S_{t+1}*,* D_{t+1}*, and* $L(S_{t+1}, D_{t+1})$ *to increase.*

Proof. Taking equation 14 and dividing by F, the equilibrium collision probability in $t+1$ can be written as

$$L(S_{t+1}, D_{t+1}) = r_s - r, \tag{40}$$

where $r_s - r$ is the excess return on a satellite. By inspection, increases in the excess return will also increase the equilibrium collision probability.

Since L is continuous and increasing in both arguments, there is a continuum of points (S, D) such that equation 14 holds—the level set of L equal to $r_s - r$.

To see the effect of increases in the excess return on the launch rate in t and the debris stock in $t+1$, we apply the Implicit Function Theorem to equation 14:

$$\begin{aligned}
\frac{\partial X_t}{\partial (r_s - r)} &= \frac{1}{L_S(S_{t+1}, D_{t+1}) + mL_D(S_{t+1}, D_{t+1})} > 0 \\
\frac{\partial D_{t+1}}{\partial (r_s - r)} &= \frac{1}{L_D(S_{t+1}, D_{t+1})} > 0 \\
\frac{\partial S_{t+1}}{\partial (r_s - r)} &= \frac{1}{L_S(S_{t+1}, D_{t+1})} > 0,
\end{aligned}$$

where variable-subscripts indicate partial derivatives, i.e. $L_S \equiv \frac{\partial L}{\partial S}$, and $L_S, L_D > 0$ by assumption. □

Lemma 1 (Reduction)**.** *Given a fully-coupled collision probability function, the steady states of an open-access equilibrium are defined by solutions to*

$$\mathscr{Y}(D) = -\delta D + G(\hat{S}, D) + m(r_s - r)\hat{S} = 0, \tag{20}$$

where $\hat{S} = S(r_s - r, D) \geq 0$ *is defined from*

$$L(\hat{S}, D) = r_s - r \tag{21}$$

when such an S exists and 0 *otherwise.*

Proof. The open-access steady states are defined by equations 17, 18, and 19. Equation 17 implicitly determines the number of satellites as a function of the amount of debris, the excess return on a satellite, and the collision rate function,

$$L(S, D) = r_s - r \implies S = S(r_s - r, D). \tag{41}$$

Since L is monotone increasing in each argument, $S(r_s - r, D)$ is monotone decreasing in D. Since S must be nonnegative, there exists a nonnegative $D^S : S(r_s - r, D) = 0 \; \forall D \geq D^S$. So we have

$$\hat{S} = \begin{cases} S(r_s - r, D) \text{ if } D \in [0, D^S) \\ 0 \text{ if } D \geq D^S \end{cases} \tag{42}$$

Using $\hat{S}$ we can reduce equations 17, 18, and 19 to a single equation in debris,

$$\mathscr{Y}(D) = -\delta D + G(\hat{S}, D) + m(r_s - r)\hat{S},$$

with

$$\{\hat{D} \geq 0 : \delta \hat{D} = G(\hat{S}, \hat{D}) + m(r_s - r)\hat{S}\} \tag{43}$$

being the open-access steady states.

□

Proposition 2 (Multiplicity)**.** *Given a positive excess return on a satellite and a fully-coupled collision probability function, multiple open-access steady states can exist if the new-fragment-debris coupling exists (i.e.* $G = G(S, D)$*).*

Proof. Using the reduction to equation 20 from Lemma 1, we focus our attention on solutions to

$$\mathscr{Y}(D) = -\delta D + G(\hat{S}, D) + m(r_s - r)\hat{S}.$$

δD is monotonically increasing in D with $\delta D = 0$ when $D = 0$, and $m(r_s - r)\hat{S}$ is monotonically decreasing in D with $\hat{S} > 0$ when $D = 0$, but $\hat{G} \equiv G(\hat{S}, D)$ is nonmonotone in D. To

see this, note

$$\frac{d\hat{G}}{dD}(\hat{S},D) = \underbrace{\frac{\partial G}{\partial S}}_{\geq 0}\underbrace{\frac{\partial \hat{S}}{\partial D}}_{\leq 0} + \underbrace{\frac{\partial G}{\partial D}}_{\geq 0}, \text{ with} \tag{44}$$

$$\frac{d\hat{G}}{dD}(\hat{S},0) = \frac{\partial G}{\partial S}\frac{\partial \hat{S}}{\partial D} < 0 \text{ and} \tag{45}$$

$$\frac{d\hat{G}}{dD}(0,D^S) = \frac{\partial G}{\partial D} > 0, \tag{46}$$

where $\frac{\partial \hat{S}}{\partial D} = -\frac{L_D}{L_S} \leq 0$ by application of the Implicit Function Theorem on equation 14.

Let $\hat{D}$ be a solution to equation 20. If $G_D > 0$, then $\hat{G}$ is nonmonotone in D and the existence or uniqueness of $\hat{D}$ cannot be guaranteed. If G_D is large enough, $\hat{D}$ will not exist; if G_D is not too small, multiple $\hat{D}$ will exist. If $G_D = 0$, then the existence of $\hat{D}$ also ensures its uniqueness. If G_D is strictly convex in both arguments, at most two $\hat{D}$ can exist. □

Proposition 3 (Local stability)**.** *Given a positive excess return on a satellite, new fragment satellite coupling, and launch debris coupling, open-access steady states will be locally stable if and only if the fragment autocatalysis rate is small enough, or the marginal rate of technical substitution of satellites for debris in collision probability is high enough, i.e.*

$$(G_D(S^*,D^*) - \delta) < \frac{L_D(S^*,D^*)}{L_S(S^*,D^*)}(G_S(S^*,D^*) + m(r_s - r)). \tag{22}$$

When G is strictly convex in both arguments and two steady states exist, the higher-debris steady state is unstable.

Proof. We use the reduction from Lemma 1 to simplify the proof. The open access steady states are solutions to equation 20, and the sign of $\frac{\partial \mathscr{Y}}{\partial D}$ at the solutions allows us to classify the stability of the system. Applying the Implicit Function Theorem to equation 17 to calculate S_D, then differentiating $\mathscr{Y}$ in the neighborhood of an arbitrary solution D^*,

$$\frac{\partial \mathscr{Y}}{\partial D}(D^*) = (G_D(S^*,D^*) - \delta) - \frac{L_D(S^*,D^*)}{L_S(S^*,D^*)}(G_S(S^*,D^*) + m(r_s - r)), \tag{47}$$

where $S^* \equiv S(r_s - r, D^*)$. $(G_D(S^*,D^*) - \delta)$ is the fragment autocatalysis rate and $\frac{L_D(S^*,D^*)}{L_S(S^*,D^*)}$ is the MRTS of satellites for debris in collision probability. Both $G_S(S^*,D^*)$ and $m(r_s - r)$ are positive by assumption. So $\frac{\partial \mathscr{Y}}{\partial D}(D^*) < 0$ can hold if and only if the fragment autocatalysis rate is small enough, or the MRTS of satellites for debris in collision probability is large enough. □

Lemma 2 (Open-access Kessler threshold)**.** *When G is strictly convex in both arguments and two steady states exist, let*

$$\underline{D} = \min\{D : \mathscr{Y}(D) = 0\}$$

be the stable steady state, and

$$\bar{D} = \max\{D : \mathscr{Y}(D) = 0\}$$

be the unstable steady state. Then

$$\bar{D} = D_X^{\kappa}.$$

Proof. When G is stictly convex in both arguments and two steady states exist, the reduction

$$\mathscr{Y}(D) = -\delta D + G(\hat{S}, D) + m(r_s - r)\hat{S} = 0$$

has two solutions. The curve $G(\hat{S}, D) + m(r_s - r)\hat{S}$ is above δD when $D = 0$ and again as $D \to \infty$, as shown in Proposition 2 and illustrated in panel a of figure 2. So the first solution,

$$\underline{D} = \min\{D : \mathscr{Y}(D) = 0\},$$

must occur when $G(\hat{S}, D) + m(r_s - r)\hat{S}$ approaches δD from above, and the second,

$$\bar{D} = \max\{D : \mathscr{Y}(D) = 0\},$$

when $G(\hat{S}, D) + m(r_s - r)\hat{S}$ approaches δD from below.

This implies that at the first solution, $\underline{D}$,

$$\frac{\partial \mathscr{Y}}{\partial D}(\underline{D}) = (G_D(\underline{S}, \underline{D}) - \delta) - \frac{L_D(\underline{S}, \underline{D})}{L_S(\underline{S}, \underline{D})}(G_S(\underline{S}, \underline{D}) + m(r_s - r)) < 0 \tag{48}$$

and at the second solution, $\bar{D}$,

$$\frac{\partial \mathscr{Y}}{\partial D}(\bar{D}) = (G_D(\bar{S}, \bar{D}) - \delta) - \frac{L_D(\bar{S}, \bar{D})}{L_S(\bar{S}, \bar{D})}(G_S(\bar{S}, \bar{D}) + m(r_s - r)) > 0 \tag{49}$$

where $\underline{S} = \hat{S}(\underline{D})$ and $\bar{S} = \hat{S}(\bar{D})$.

Since $\bar{D}$ is an unstable fixed point of $\mathscr{Y}(D) = 0$, initial conditions $D \geq \bar{D}$ must diverge from $\bar{D}$. But $\bar{D}$ is the largest fixed point of $\mathscr{Y}(D) = 0$, so such trajectories must diverge to $+\infty$.

The Kessler region and threshold are defined as

$$\kappa_X \equiv \{(S,D) : \lim_{t\to\infty} D_{t+1} = \infty \mid S_0 = S, D_0 = D, X_t = X(S_t, D_t)\}$$
$$D_X^\kappa \equiv \sup\{D : (S,D) \notin \kappa_X\}.$$

So from the definition of D_X^κ and the properties of $\bar{D}$, we have that $\bar{D} = D_X^\kappa$.

□

Proposition 4 (Open-access Kessler Syndrome)**.** *When the rate of excess return is positive and the new fragment function is fully coupled and strictly convex in both arguments,*

1. *open access will cause Kessler Syndrome if the excess return on a satellite exceeds the maximum sustainable excess return R^{max};*
2. *the open-access Kessler region will expand as the excess return approaches R^{max}.*

Proof. We begin with the single-equation reduction from Lemma 1:

$$\mathscr{Y}(D) = -\delta D + G(\hat{S}, D) + m(r_s - r)\hat{S}. \tag{50}$$

If the new fragment formation function G is strictly convex in both arguments, there are up to two solutions to the above equation.[35] From Lemma 2 we have that the smaller (attracting) solution is $\underline{D}$ and the larger (repelling) solution is D_X^κ. The basin of attraction for $\underline{D}$ in the D dimension is thus at most $[0, D_X^\kappa)$. We say "at most" because, as figure 3 illustrates, in two dimensions the basin depends on both S and D.

Next, consider how open-access steady-state debris levels change as the excess return on a satellite changes. We suppress function arguments to reduce notation; all functions are evaluated at an arbitrary open-access steady state. Applying the Implicit Function Theorem to equation 20, and applying it again to equation 17 to calculate $\frac{\partial S}{\partial(r_s - r)}$, we get:

$$\frac{\partial D}{\partial(r_s - r)} = -\frac{\frac{G_S}{L_S} + m(S(r_s - r, D) + \frac{r_s - r}{L_S})}{(G_D - \delta) - \frac{L_D}{L_S}(G_S + m(r_s - r))} \lessgtr 0$$

Given our assumptions, the numerator is always positive. From Proposition 3, an open-access steady state is locally stable if and only if the denominator is negative. So if the steady state is stable, increases in the excess rate of return on a satellite will cause the debris level to increase. If the steady state is unstable, increases in the excess rate of return on a satellite will cause the

[35] Strict convexity of G is a sufficient but not necessary condition for this result. However, it is a reasonable physical assumption and simplifies the proof.

debris level to decrease. So we have

$$\frac{\partial \underline{D}}{\partial(r_s - r)} > 0, \quad \frac{\partial D_X^\kappa}{\partial(r_s - r)} < 0,$$

so as $r_s - r$ increases, $\underline{D}$ and D_X^κ are squeezed closer together. As this happens, the basin of attraction for $\underline{D}$ must shrink under any non-atomic measure applied to $[0, D_X^\kappa)$. Since the open-access Kessler region is the complement of the stable steady state's basin of attraction, as the basin shrinks, the open-access Kessler region must expand.

Eventually, increases in $r_s - r$ will result in $\underline{D} = D_X^\kappa = D^*$. This is because increases in $r_s - r$ shift the curve $G(\hat{S}, D) + m(r_s - r)\hat{S}$ upwards through both the coefficient on $\hat{S}$ and the value of $\hat{S}$ itself—recall from Proposition 1 that increases in $r_s - r$ shift the equilibrium isoquant outwards, and from Lemma 1 that $\hat{S}$ is the equilibrium satellite stock given D.

Thus there exists a threshold value R^{max} for $r_s - r$ such that

1. there is a single solution to $\mathscr{Y}(D) = 0$, and
2. for $r_s - r > R^{max}$ there is no solution to $\mathscr{Y}(D) = 0$.

Defining this threshold as R^{max} and letting that single solution be D^* (with $S^* \equiv \hat{S}(D^*)$), the first condition can be formalized as

$$R^{max} : \mathscr{Y}(D^*; R^{max}) = -\delta D^* + G(S^*, D^*) + mR^{max}S^* = 0. \tag{51}$$

The second condition implies that R^{max} is such that $G(\hat{S}, D) + mR^{max}\hat{S}$ is tangent to δD at D^*, so that when $r_s - r > R^{max}$, $G(\hat{S}, D) + mR^{max}\hat{S}$ and δD do not intersect. The second condition can therefore be formalized as

$$R^{max} : G_D(S^*, D^*) - \frac{L_D(S^*, D^*)}{L_S(S^*, D^*)}(G_S(S^*, D^*) + mR^{\max}) = \delta. \tag{52}$$

The tangency condition in equation 52 combined with the properties of the curve $G(S^*, D^*) + mR^{max}S^*$ imply that $G(S^*, D^*) + mR^{max}S^*$ approaches and departs the point of tangency from above. For any $\mu > 0$, $\mathscr{Y}_D(D^*; R^{max} - \mu) < 0$ and $\mathscr{Y}_D(D^*; R^{max} - \mu) > 0$. So trajectories under R^{max} which approach D^* will be driven away from D^* if they receive any small positive perturbation. Consequently, the steady state induced by R^{max} must be an unstable one, i.e. $D^* = D_X^\kappa$. Finally, combining equations 51 and 52 yields

$$R^{max} : -\delta D_X^\kappa + G(S_X^\kappa, D_X^\kappa) + mR^{max}S_X^\kappa = G_D(S_X^\kappa, D_X^\kappa) - \frac{L_D(S_X^\kappa, D_X^\kappa)}{L_S(S_X^\kappa, D_X^\kappa)}(G_S(S_X^\kappa, D_X^\kappa) + mR^{max}) - \delta. \tag{53}$$

□

Proposition 5 (Overshooting)**.** *Suppose the new fragment formation function is strictly convex in both arguments and the launch rate constraint does not bind. Except on a set of measure zero, open access paths from initial conditions with positive launch rates will overshoot the stable open-access steady state in at least one state variable.*

Proof. We first define the following sets and functions, where $S, D \geq 0$ is assumed:

- The action region: the set of states with positive open-access launch rates,

$$A \equiv \left\{(S,D) : r_s - r - L(S',D') \geq 0\right\}, \tag{54}$$

  where

$$\begin{aligned} S' &= S(1-L(S,D)) + X \\ D' &= D(1-\delta) + G(S,D) + mX, \end{aligned}$$

- The equilibrium manifold:

$$E \equiv \left\{(S,D) : r_s - r - L(S,D) = 0\right\}. \tag{55}$$

- The stable open-access steady state: following the reduction to equation 20 from Lemma 1,

$$E_s \equiv \left\{ \begin{aligned} &(\hat{S},D) : \mathscr{Y}(D) = -\delta D + G(\hat{S},D) + m(r_s - r)\hat{S} = 0, \\ &\hat{S} : L(\hat{S},D) = r_s - r, \;\; \mathscr{Y}'(D) < 0 \end{aligned} \right\}. \tag{56}$$

- The physical dynamics: the mapping $P_{SD} : \mathbb{R}^2_+ \to \mathbb{R}^2_+$ which describes the effect of orbital mechanics on the satellite and debris stocks in one period,

$$P_{SD}(S,D) \equiv \left(S(1-L(S,D)),\;\; D(1-\delta) + G(S,D)\right). \tag{57}$$

- The one-step set: the set of states from which one period's physical dynamics, followed by launching, will read an open-access steady state,

$$A_{P1} \equiv \{(S,D) : P_{SD}(S,D) + (X,mX) \in E_s,\;\; X \in (0,\bar{X}]\}. \tag{58}$$

- The one-step ray: the set of states from which one period of launching will reach an open-access steady state,

$$A_1 \equiv \left\{(S,D) : (S+X, D+mX) \in E_s,\;\; X \in (0,\bar{X}]\right\}, \tag{59}$$

where m is the same as in the debris law of motion. The one-step ray can be viewed as part of a decomposition of the satellite and debris laws of motion: after a period's physical dynamics have been applied, launches to the stable steady state occur from the one-step ray. The one-step set encompasses both of these components.

Our proof proceeds in three steps. First, we show that initial conditions in the action region A reaching points on the equilibrium manifold $E \setminus E_S$ must overshoot an open-access steady state. Second, we establish the bijectivity of the physical dynamics P_{SD}. Third, we show that these results imply that the one-step set A_{P1} has zero Lebesgue measure on A.

1. Initial conditions in the action region A reaching points on the equilibrium manifold $E \setminus E_S$ must overshoot an open-access steady state: Since the launch rate constraint does not bind, any point in A will by definition reach a point in E. Since E_s contains at most one element given the strict convexity of G while E is a manifold, $E_s \subset E$. Given that L is increasing in both arguments, points in $E \setminus E_s$ must therefore have either larger S and smaller D than E_s, or vice versa. Consequently, reaching points in $E \setminus E_s$ constitutes overshooting E_s in one state variable and undershooting in the other.

2. Bijectivity of the physical dynamics P_{SD}: To show that P_{SD} is a bijection on $\mathbb{R}^2_+$, we separate the physical dynamics into two functions $P_S, P_D : \mathbb{R}^2_+ \to \mathbb{R}_+$,

$$P_S(S,D) = S(1 - L(S,D)), \tag{60}$$

$$P_D(S,D) = D(1-\delta) + G(S,D). \tag{61}$$

P_D is a sum of strictly monotone increasing functions, so is strictly monotone increasing as well. Strictly monotone functions are bijections, so P_D is a bijection. So for two arbitrary pairs (S_1,D_1) and (S_2,D_2) we have

$$P_{SD}(S_1,D_1) = P_{SD}(S_2,D_2) \iff P_S(S_1,D_1) = P_S(S_2,D_2) \;\&\; P_D(S_1,D_1) = P_D(S_2,D_2) \tag{62}$$

P_S is a function, so we have $(S_1,D_1) = (S_2,D_2) \implies P_S(S_1,D_1) = P_S(S_2,D_2)$, but since $SL(S,D)$ may be non-monotone the other direction may not hold. Since P_D is a bijection, $P_D(S_1,D_1) = P_D(S_2,D_2) \iff (S_1,D_1) = (S_2,D_2)$. Putting this together we have the following:

- If $(S_1,D_1) = (S_2,D_2)$, then $P_{SD}(S_1,D_1) = P_{SD}(S_2,D_2)$.
- If $P_{SD}(S_1,D_1) = P_{SD}(S_2,D_2)$, then $P_S(S_1,D_1) = P_S(S_2,D_2)$ and $P_D(S_1,D_1) = P_D(S_2,D_2)$. While there may exist a pair $(S_1,D_1) \neq (S_2,D_2)$ such that $P_S(S_1,D_1) = P_S(S_2,D_2)$, the bijectivity of P_D means $P_D(S_1,D_1) \neq P_D(S_2,D_2)$.

Consequently, $P_{SD}(S_1,D_1) = P_{SD}(S_2,D_2)$ if and only if $(S_1,D_1) = (S_2,D_2)$, i.e. P_SD is a

bijection on $\mathbb{R}^2_+$.

3. The one-step set A_{P1} has zero Lebesgue measure on A:

By definition, $A_1 \subseteq A$. Since E_s contains at most one element, A_1 is a single line segment, so $A_1 \subset A$. The Lebesgue measure on A of A_1 is therefore zero.

Since P_{SD} is a bijection, the Lebesgue measure of the pre-image of A_1 under P_{SD},

$$P_{SD}^{-1}(A_1) \equiv \left\{(S,D) : P_{SD}(S,D) \in A_1\right\},$$

is the same as the Lebesgue measure of A_1. Since $P_{SD}^{-1}(A_1) = A_{P1}$, the Lebesgue measure on A of A_{P1} is also zero. Lebesgue measure is isomorphic to any non-atomic probability measure, so the one-step set is measure zero under any non-atomic probability measure. This gives the desired result: initial conditions with positive open-access launch rates will overshoot the stable open-access steady state except on a set of measure zero.

□

Proposition 6 (Negative externality)**.** *If the excess rate of return on a satellite weakly exceeds the collision probability and marginal rate of congestion costs in an optimal interior steady state, then the marginal external cost is weakly positive and the optimal collision probability is weakly lower than the open-access collision probability, i.e.*

$$r_s - r \geq L(S,D) + L_S(S,D)S \implies \xi(S,D) \geq 0, \tag{31}$$

and

$$\xi(S,D) \geq 0 \implies L(S^*,D^*) \leq L(\hat{S},\hat{D}). \tag{32}$$

Proof. Let $r_s - r \geq L(S,D) + L_S(S,D)S$ at an interior optimal steady state (S,D). Suppressing function arguments, the marginal external cost is

$$\begin{aligned}\xi = L_S SF + \frac{1}{1+r}\left(G_S + m(L+SL_S)\right)L_D SF + (1-\frac{1}{1+r})mL_D SF \\ + (1-\delta+G_D)\left(\frac{1}{1+r}(\pi-(L+L_S S)F) - (1-\frac{1}{1+r})F\right)\end{aligned} \tag{63}$$

All terms in this equation are weakly positive for all S and D, and the first two terms on the right-hand side add non-negative components separately or in a convex combination weighted by $\frac{1}{1+r}$. To see that $r_s - r \geq L(S,D) + L_S(S,D)S$ is equivalent to the third term being weakly

positive, note that

$$\frac{1}{1+r}(\pi-(L+L_S S)F)-(1-\frac{1}{1+r})F \geq 0 \tag{64}$$

$$\iff \frac{\pi-(L+L_S S)F}{F} \geq r \tag{65}$$

$$\iff r_s-(L+L_S S) \geq r \tag{66}$$

$$\iff r_s - r \geq L+L_S S. \tag{67}$$

Since all the components of $\xi(S,D)$ are weakly positive, $\xi(S,D) \geq 0$ at an optimal interior steady state.

Next, consider the open-access interior steady-state launch rate, $\hat{X}$, and the optimal interior steady-state launch rate, X^*. An interior open-access steady state, $(\hat{S},\hat{D})$, is such that

$$\pi = rF + L(\hat{S},\hat{D})F \tag{68}$$

and an interior optimal steady state, (S^*,D^*), is such that

$$\pi = rF + L(S^*,D^*)F + \xi(S^*,D^*). \tag{69}$$

Since ξ is weakly positive at an optimal interior steady state, it must be that $L(S^*,D^*) \leq L(\hat{S},\hat{D})$.

□

A.2 Optimal launch policy and the marginal external cost

The sequence version of the fleet planner's problem is

$$\max_{\{X_t,S_{t+1},D_{t+1}\}_{t=0}^{\infty}} S_t Q(S_t,D_t,X_t) + \frac{1}{1+r}\sum_{\tau=t}^{\infty}\frac{1}{1+r}^{\tau-t-1} X_\tau(\frac{1}{1+r}Q(S_{\tau+1},D_{\tau+1},X_{\tau+1})-F) \tag{70}$$

$$\text{s.t. } Q(S_t,D_t,X_t) = \pi + \frac{1}{1+r}(1-L(S_t,D_t))Q(S_{t+1},D_{t+1},X_{t+1}) \tag{71}$$

$$S_{t+1} \leq S_t(1-L(S_t,D_t))+X_t \tag{72}$$

$$D_{t+1} \geq D_t(1-\delta)+G(S_t,D_t)+mX_t \tag{73}$$

$$X_t \in [0,\bar{X}] \ \ \forall t \tag{74}$$

$$S_{t+1} \geq 0, D_{t+1} \geq 0 \tag{75}$$

$$S_0 = s_0, D_0 = d_0 \tag{76}$$

The planner's Lagrangian is

$$\mathscr{L}(X,S,D,\lambda,\gamma) = \sum_{t=0}^{\infty}\left(\frac{1}{1+r}\right)^t \Big\{ \pi S_t - FX_t + \lambda_{S_t}\left(S_t(1-L(S_t,D_t)) + X_t - S_{t+1}\right) \tag{77}$$

$$+ \lambda_{D_t}\left(D_{t+1} - D_t(1-\delta) - G(S_t,D_t) - mX_t\right) \tag{78}$$

$$+ \gamma_{X_t}X_t + \gamma_{\bar{X}_t}(\bar{X} - X_t) + \gamma_{S_t}S_{t+1} + \gamma_{D_t}D_{t+1} \Big\} \tag{79}$$

The first-order necessary conditions for an optimal launch path are, $\forall t$ up to T,

$$\mathscr{L}_{X_t} = -F + \lambda_{S_t} - m\lambda_{D_t} + \gamma_{X_t} - \gamma_{\bar{X}_t} = 0 \tag{80}$$

$$\mathscr{L}_{S_{t+1}} = \frac{1}{1+r}\{\pi + \lambda_{S_{t+1}}(1 - L(S_{t+1},D_{t+1}) - S_{t+1}L_S(S_{t+1},D_{t+1})) \tag{81}$$

$$- \lambda_{D_{t+1}}G_S(S_{t+1},D_{t+1})\} + \gamma_{S_t} - \lambda_{S_t} = 0 \tag{82}$$

$$\mathscr{L}_{D_{t+1}} = \frac{1}{1+r}\{\lambda_{D_{t+1}}(\delta - 1 - G_D(S_{t+1},D_{t+1})) - \lambda_{S_{t+1}}S_{t+1}L_D(S_{t+1},D_{t+1})\} + \lambda_{D_t} + \gamma_{D_t} = 0 \tag{83}$$

$$\mathscr{L}_{S_{T+1}} = \gamma_{S_T} - \lambda_{S_T} = 0 \tag{84}$$

$$\mathscr{L}_{D_{T+1}} = \lambda_{D_T} + \gamma_{D_T} = 0 \tag{85}$$

with complementary slackness and transversality conditions

$$\lambda_{St}\left(S_t(1 - L_t + X_t - S_{t+1}\right) = 0 \tag{86}$$

$$\lambda_{Dt}\left(D_{t+1} - D_t(1-\delta) - G_t - mX_t\right) = 0 \tag{87}$$

$$\gamma_{Xt}X_t = 0, \tag{88}$$

$$\gamma_{\bar{X}t}(\bar{X} - X_t) = 0, \tag{89}$$

$$\gamma_{St}S_{t+1} = 0, \tag{90}$$

$$\gamma_{Dt}D_{t+1} = 0 \tag{91}$$

$$\lim_{T\to\infty}\left(\frac{1}{1+r}\right)^T \lambda_{ST}S_{T+1} = 0 \tag{92}$$

$$\lim_{T\to\infty} -\left(\frac{1}{1+r}\right)^T \lambda_{DT}D_{T+1} = 0. \tag{93}$$

In what follows we drop time subscripts to reduce notational clutter. Period t values are shown with no subscript, period $t+1$ values are marked with a $'$ after the variable, and period $t-1$ values are marked with a $'$ before the variable e.g. $S_{t-1} \equiv {}'S$, $S_t \equiv S$, $S_{t+1} \equiv S'$. By (80),

$$\lambda_S = (1+r)(F + \frac{1}{1+r}m\lambda_D - \gamma_X + \gamma_{\bar{X}}). \tag{94}$$

In the next period, this becomes

$$\lambda_S' = (1+r)(F + \left(\frac{1}{1+r}\right) m\lambda_D' - \gamma_X' + \gamma_{\bar{X}}'). \tag{95}$$

By (82) and (83),

$$\lambda_S = \pi + (1+r)\gamma_S + \frac{1}{1+r}\{\lambda_S'(1 - L(S',D') - S'L_S(S',D')) - \lambda_D' G_S(S',D')\} \tag{96}$$

$$\lambda_D = \frac{1}{1+r}\{\lambda_D'(1 + G_D(S',D') - \delta) + \lambda_S' S' L_D(S',D')\} - (1+r)\gamma_D. \tag{97}$$

Using (95),

$$\lambda_S = \pi + (1+r)\gamma_S - F(L(S',D') + S'L_S(S',D') - 1) - \frac{1}{1+r}\lambda_D G_S(S',D') \tag{98}$$

$$- \frac{1}{1+r} m\lambda_D(L(S',D') + S'L_S(S',D') - 1) + (L(S',D') + S'L_S(S',D') - 1)(\gamma_X' - \gamma_{\bar{X}}') \tag{99}$$

$$\lambda_D = FS'L_D(S',D') + \frac{1}{1+r} W_D(S',D')(1 + G_D(S',D') - \delta) + \frac{1}{1+r} m\lambda_D S'L_D(S',D') \tag{100}$$

$$- \left((1+r)\gamma_D + S'L_D(S',D')(\gamma_X' - \gamma_{\bar{X}}'\right) \tag{101}$$

Define,

$$\alpha_1' = \pi + (1 - L(S',D') - S'L_S(S',D'))F \tag{102}$$

$$\alpha_2' = S'L_D(S',D')F \tag{103}$$

$$\Gamma_1' = G_S(S',D') - m(1 - L(S',D') - S'L_S(S',D')) \tag{104}$$

$$\Gamma_2' = 1 - \delta + G_D(S',D') + mS'L_D(S',D') \tag{105}$$

$$\kappa_1' = (1+r)\gamma_S - (\gamma_{X'} - \gamma_{\bar{X}'})(1 - L(S',D') - S'L_S(S',D')) \tag{106}$$

$$\kappa_2' = (1+r)\gamma_D + S'L_D(S',D')(\gamma_{X'} - \gamma_{\bar{X}'}) \tag{107}$$

so that

$$\lambda_S = \alpha_1' - \frac{1}{1+r}\lambda_D'\Gamma_1' + \kappa_1' \tag{108}$$

$$\lambda_D = \alpha_2' + \frac{1}{1+r}\lambda_S'\Gamma_2' - \kappa_2' \tag{109}$$

Then,

$$\lambda_D' = \frac{\lambda_D - \alpha_2' + \kappa_2'}{\frac{1}{1+r}\Gamma_2'} \tag{110}$$

Substitute (94) and (110) in (108) to get the following expression for $W_D(S,D)$

$$\frac{\frac{1}{1+r}\{\Gamma_1'(\alpha_2'-\kappa_2')+\Gamma_2'(\alpha_1'+\kappa_1')\}+\Gamma_2'(\gamma_X-\gamma_{\bar{X}}-F)}{\frac{1}{1+r}(\Gamma_1'+m\Gamma_2')} \tag{111}$$

Iterate 111 to period $t+1$ and substitute into 110 to obtain

$$\lambda_D'=\frac{\frac{1}{1+r}\{\Gamma_1''(\alpha_2''-\kappa_2'')+\Gamma_2''(\alpha_1''+\kappa_1'')\}+\Gamma_2''(\gamma_X'-\gamma_{\bar{X}}'-F)}{\frac{1}{1+r}(\Gamma_1''+m\Gamma_2'')} \tag{112}$$

Use (111) and (112) in (109) to get

$$\alpha_1'=m(\alpha_2'-\kappa_2')-\kappa_1'+\frac{1}{\frac{1}{1+r}}(\gamma_{\bar{X}}-\gamma_X+F)+\frac{\Gamma_1'+m\Gamma_2'}{\Gamma_1''+m\Gamma_2''}\left(\Gamma_1''\frac{1}{1+r}(\alpha_2''-\kappa_2'')+\Gamma_2''(\frac{1}{1+r}(\alpha_1''+\kappa_1'')-F+\gamma_X'-\gamma_{\bar{X}}')\right) \tag{113}$$

Evaluate (113) in the previous time period as:

$$\alpha_1=m(\alpha_2-\kappa_2)-\kappa_1+\frac{1}{\frac{1}{1+r}}({}'\gamma_{\bar{X}}-{}'\gamma_X+F)+\frac{\Gamma_1+m\Gamma_2}{\Gamma_1'+m\Gamma_2'}\left(\Gamma_1'\frac{1}{1+r}(\alpha_2'-\kappa_2')+\Gamma_2'(\frac{1}{1+r}(\alpha_1'+\kappa_1')-F+\gamma_X-\gamma_{\bar{X}})\right) \tag{114}$$

Subtract $F(\frac{1}{\frac{1}{1+r}}+L')$ from both sides and add $F(L+SL_S)$ to both sides to obtain

$$\begin{aligned}\pi-rF-FL(S',D')=F(L(S,D)+SL_S(S,D)-L(S',D'))+m(\alpha_2-\kappa_2)-\kappa_1+\frac{1}{\frac{1}{1+r}}({}'\gamma_{\bar{X}}-{}'\gamma_X)+\frac{\Gamma_1+m\Gamma_2}{\Gamma_1'+m\Gamma_2'}\\ \left(\Gamma_1'\frac{1}{1+r}(\alpha_2'-\kappa_2')+\Gamma_2'(\frac{1}{1+r}(\alpha_1'+\kappa_1')-F+\gamma_X-\gamma_{\bar{X}})\right) \qquad (115)\\ \implies \xi(S',D')=L_S(S,D)SF+\big(L(S,D)-L(S',D')\big)F+\frac{\Gamma_1+m\Gamma_2}{\Gamma_1'+m\Gamma_2'}\Gamma_2'(\frac{1}{1+r}\alpha_1'-F)+\frac{1}{1+r}\frac{\Gamma_1+m\Gamma_2}{\Gamma_1'+m\Gamma_2'}\Gamma_1'\alpha_2'\\ +m\alpha_2+\frac{\Gamma_1+m\Gamma_2}{\Gamma_1'+m\Gamma_2'}\left(\Gamma_2'(\frac{1}{1+r}\kappa_1'+\gamma_X-\gamma_{\bar{X}})-\frac{1}{1+r}\Gamma_1'\kappa_2'\right)-(m\kappa_2+\kappa_1)+\frac{1}{\frac{1}{1+r}}(\gamma_{\bar{X}}-\gamma_X).\\ (116)\end{aligned}$$

Along an interior launch path, the MEC $\xi(S',D')$ reduces to

$$\xi(S',D')=L_S(S,D)SF+\big(L(S,D)-L(S',D')\big)F+\frac{\Gamma_1+m\Gamma_2}{\Gamma_1'+m\Gamma_2'}\Gamma_2'(\frac{1}{1+r}\alpha_1'-F)+\frac{1}{1+r}\frac{\Gamma_1+m\Gamma_2}{\Gamma_1'+m\Gamma_2'}\Gamma_1'\alpha_2'+m\alpha_2, \tag{117}$$

and in an interior steady state the MEC further reduces to

$$\xi(S,D)=L_S(S,D)SF+\Gamma_2(\frac{1}{1+r}\alpha_1-F)+\frac{1}{1+r}(\Gamma_1+m)\alpha_2. \tag{118}$$

A.3 The collision probability and new fragment formation functions

In this section we derive the functional forms of the collision probability and new fragment functions, discuss the physical assumptions they encode, and describe our process for calibrating the physical model in more detail.

A.3.1 Functional forms

For numerical simulations, we model the probability that objects of type j are struck by objects of type k as

$$p_{jk}(k_t) = 1 - e^{-\alpha_{jk} k_t}, \tag{119}$$

where $\alpha_{jk} > 0$ is a physical parameter ("intrinsic collision probability") reflecting the relative mean sizes, speeds, and inclinations of the object types (see Letizia (2016) for a derivation of the physical content of α_{jk}). The probability a satellite is destroyed is the sum of the probabilities it is struck by debris and by other satellites, adjusted for the probability it is struck by both. For satellite-satellite and satellite-debris collisions, equation 119 gives us

$$\begin{aligned} L(S,D) &= p_{SS}(S) + p_{SD}(D) - p_{SS}(S)p_{SD}(D) \qquad (120)\\ &= (1 - e^{-\alpha_{SS}S}) + (1 - e^{-\alpha_{SD}D}) - (1 - e^{-\alpha_{SS}S})(1 - e^{-\alpha_{SD}D}) \\ \implies L(S,D) &= 1 - e^{-\alpha_{SS}S - \alpha_{SD}D}. \qquad (121) \end{aligned}$$

We write the new fragment formation function as

$$G(S,D) = F_{SD}p_{SD}(D) + F_{SS}p_{SS}(S) + F_{DD}p_{DD}(D), \tag{122}$$

where F_{jk} is the number of fragments produced in a collision between objects of type j and k. Letting $F_{SS} = \beta_{SS}S$, $F_{SD} = \beta_{SD}S$, and $F_{DD} = \beta_{DD}D$ where $\beta_{jk} > 0$ is a physical parameter reflecting the physical compositions and masses of the colliding objects, and using the forms in equation 119, we obtain

$$G(S,D) = \beta_S S(1 - e^{-\alpha_{SS}S})S + \beta_{SD}(1 - e^{-\alpha_{SD}D})S + \beta_{DD}(1 - e^{-\alpha_{DD}D})D. \tag{123}$$

The form in equation 121 is convenient as it allows us to solve explicitly for the open access launch rate and is easy to manipulate. Similar forms have been used in engineering studies of the orbital debris environment, and are currently used by the European Space agency in developing indices to study the long-term evolution of the orbital environment (Letizia, 2016; Letizia et al., 2017; Letizia, Lemmens, and Krag, 2018).

To derive equation 121, we consider balls (satellites and debris) being placed into bins (the set of all possible orbital paths within the shell of interest). The probability of a specific satellite being struck by another object is then equivalent to the probability that a randomly-placed ball ends up in a bin containing the specific ball we are focusing on. This is a version of the "pigeonhole principle", used in Béal, Deschamps, and Moulin (2020) to derive a similar form for satellite-satellite collisions.

Suppose we have b equally-sized bins and $n+1$ balls in total, where $b \geq n+1$. Without loss of generality, we label the ball we are interested in as i. We will first place i into an arbitrary bin, and then drop the remaining N balls into the b bins with equal probability over bins. The probability a ball is dropped into a given bin is $\frac{1}{b}$, and the probability a ball is not dropped into a given bin is then $\frac{b-1}{b} = 1 - \frac{1}{b}$. As we drop the remaining n balls, the probability that none of the balls is dropped in the same bin containing j is

$$Pr(\text{no collision with } i) = \left(1 - \frac{1}{b}\right)^n \tag{124}$$

Consequently, the probability that any of the n balls are dropped into i's bin is

$$Pr(\text{collision with } i) = 1 - \left(1 - \frac{1}{b}\right)^n. \tag{125}$$

Now suppose we are interested in the probability that members of a collection of j balls, $1 \leq j < b$, end up in a bin with one of the remaining $n+1-j$ balls. The probability that any of the remaining balls end up in a bin with any of the j balls we are interested in is then

$$Pr(\text{collision with } i) = 1 - \left(1 - \frac{j}{b}\right)^{n+1-j}. \tag{126}$$

As the number of bins and balls grow large ($\lim_{b,n\to\infty}$), we obtain

$$Pr(\text{collision with } i) = 1 - e^{-j}. \tag{127}$$

Though neither the number of objects in orbits nor the possible positions they could occupy is infinite, the negative natural exponential form is likely a reasonable approximation. If we suppose that we have two types of balls j and k of different sizes and bins the size of the smallest type of ball, we get that the probability a ball of type k is dropped into in a bin with a

ball of type j as

$$Pr(k\text{–}j \text{ collision}) = 1 - \left(1 - \frac{\alpha_{jk} k}{b}\right)^{n+1-k} \tag{128}$$

$$\implies \lim_{b,n\to\infty} Pr(k\text{–}j \text{ collision}) = 1 - e^{-\alpha_{jk} k}, \tag{129}$$

which is the form in equation 119, where α_{jk} is a nonnegative parameter indexing the relative sizes of objects j and k. In the orbital context, α_{jk} reflects not only the sizes of the objects but also their relative speeds and inclinations. From here we obtain the form of L by applying standard rules of probability to satellite-satellite and satellite-debris collisions. Equation 123 follows from the form of L.

This "kinetic gas-like" approximation is used extensively in the space debris modeling literature as a tractable approximation of results from more complex and computationally-intensive orbital mechanics simulators. It is most suitable for long-term modeling studies with "large" (relative to the timescale of orbital interactions) time steps. As described in Letizia (2016), this approximation is equivalent to modeling collisions as a Poisson process. The Poisson assumption that the number of events occurring in non-overlapping time intervals are independent is equivalent to assuming that objects move randomly throughout the shell volume. This assumption is clearly not true, leading to our regularization approach described below. The assumption that the probability of an event is proportional to the length of the interval implies that fragment clouds are dispersed enough, and contain enough fragments, to be considered a continuum. Since our model is solved at annual timesteps while debris clouds evolve at much smaller timescales, this assumption is reasonable for our purposes.

A.3.2 Calibrating the physical model

We draw on methods applied in Rao, Burgess, and Kaffine (2020) and Rao and Letizia (2021) to calibrate our model. Here we describe key equations and the ridge regression approach to correcting for non-random object paths. Readers interested in detailed explanations of the physics-based elements of our calibration approach, including derivations and validation, are referred to Letizia (2016).

We require physically-appropriate values for the following parameters: δ, μ, α_{SS}, α_{SD}, α_{DD}, β_{SS}, β_{SD}, β_{DD}. Calibrating δ and μ (the mean debris decay rate and mean satellite active lifetime time) are the most straightforward. We take data from ESA regarding the residence time δ_r of debris objects and lifetime of active satellites μ_r at different altitudes, and set the decay rate for debris objects as $\delta = \min\{1 - \delta_r^{-1}, 1\}$ and the natural turnover rate for satellites as as $\mu = \min\{1 - \mu_r^{-1}, 1\}$. All calibrated values are shown in table 4.

To calculate the intrinsic collision probabilities $\alpha_{SS}, \alpha_{SD}, \alpha_{DD}$, we start with data regarding object cross-sectional areas for active satellites (commercial, military, civil government, and other) and intact debris objects. We assume debris fragments are uniform aluminium spheres of diameter 10 cm, and treat all other objects as uniform spheres as well. We compute the cross-sectional areas of active satellites and debris within each shell as share-weighted averages over 2006 2019 across the types of objects within each class, e.g. if 20% of the debris objects are intact and 80% are fragments we calculate the area as $0.2 * (intact\ area) + 0.8 * (fragment\ area)$. Under these assumptions the rate at which a reference object moving randomly at speed s in a closed space of volume V is struck by an object of cross-sectional area a is

$$\frac{sa}{V}, \tag{130}$$

where the volume is determined by the altitude and our assumption of that the space is a spherical shell, and the speed is determined by the altitude, the Earth's gravitational constant, and our assumption that the objects are uniform spheres.

To calculate the unadjusted fragmentation rates, we use data on average object masses from ESA along with a formula found to fit the high-fidelity NASA standard breakup model described in Krisko (2011). Letting the mass of the object struck be M, and assuming the object is shattered into uniform 10 cm spheres, the number of fragments from a catastrophic collision n is

$$n = 0.1 M^{0.75} 0.1^{-1.71}. \tag{131}$$

The only steps remaining are to adjust our estimate of the expected number of fragments from collisions for the non-random motion of objects in the shell, and to set the value of the launch debris parameter m. ODE-based engineering models of the debris environment use such adjustment coefficients based fitting the ODE model to results from many computationally-costly runs of high-fidelity orbital environment models, e.g. as in Somma et al. (2017); Somma (2019). This approach would be even costlier for our model, as the launch rate is endogenous, and would not provide a useful estimate of the launch debris parameter m. We instead perform the adjustment and estimate m jointly using historical data and ridge regression, a regularization technique used to improve out-of-sample predictive performance at the expense of in-sample fit. Ridge regression achieves this goal by exploiting the bias-variance trade-off, shrinking parameter values toward zero in exchange for reduced prediction variance (Hoerl, Kennard, and Hoerl, 1985; Zou and Hastie, 2005).

Since satellites are specifically coordinated to reduce collisions, the adjustment for non-

random motion should involve shrinking the expected number of fragments from a collision (with the expectation taken over the probability of a collision) toward zero. Ridge regression achieves this goal. Additionally, ridge regression is often used when the number of variables is "large" relative to the number of observations or when parameter estimates are known to be noisy due to (for example) high degrees of collinearity. Our model and data satisfy the former condition (with 4 parameters to estimate from 14 observations), and our physical calibration approach (specifically the assumption that all objects are uniform spheres) causes collinearity in our collision probability values. Since our collision model prescribes the functional form of the collision probability as $(1-\exp(-\alpha_{jk}k))$, the effect of non-random motion on new debris growth cannot be separately identified from α_{jk} and β_{jk}. This is convenient for our regression-based adjustment, since it allows us to pose the ridge regression as a linear model. Specifically, letting $\bar{x}$ denote a physically-calibrated parameter value, we estimate the following regression:

$$D_{t+1}-(1-\delta)D_t = \rho_{SS}\beta_{SS}(1-\exp(-\alpha_{SS}S_t))+\rho_{SD}\beta_{SD}(1-\exp(-\alpha_{SD}S_t))+\rho_{DD}\beta_{DD}(1-\exp(-\alpha_{DD}D_t))+m+\nu_t^D, \tag{132}$$

where $\rho_{SS},\rho_{SD},\rho_{DD},m$ are parameters to be estimated and ν_t^D is the error term. The final regularized estimates of the fragmentation and launch debris parameters are shown in table 4 as $\tilde{\beta}_{SS}$, $\tilde{\beta}_{SD}$, $\tilde{\beta}_{DD}$, m. Since ridge regression estimates are biased toward zero to reduce variance, we do not report standard errors.

A.4 Limited lifetimes, time-varying returns and costs, and occupancy elasticity

In this section we give some more details on the key extensions of the economic model necessary for calibration and simulation.

A.4.1 Limited lifetimes

Like all forms of reproducible capital, satellites depreciate over time—they do not produce payoffs forever until destroyed in a collision. Over 1967-2015, planned satellite lifetimes ranged from 3 months to 20 years, with longer lifetimes being more representative of larger and more expensive GEO satellites.[36] How would finite lifetimes affect the collision probability and debris growth?

Suppose satellite lifetimes are finite and exogenously distributed with mean μ^{-1}. Satellites live at least one time period in this setting, so that $\mu^{-1}>1$. The probability that a satellite will

[36]These numbers are taken from the Union of Concerned Scientists' publicly available data on satellites. The data are available at https://www.ucsusa.org/nuclear-weapons/space-weapons/satellite-database.

exogenously "die" in any given period is then μ. The value of a single satellite becomes

$$Q(S_t, D_t, X_t) = \pi + \frac{1}{1+r}(1-\mu)(1-L(S_t, D_t))Q(S_{t+1}, D_{t+1}, X_{t+1}), \tag{133}$$

and the equilibrium condition becomes

$$\frac{1}{1+r}Q(S_{t+1}, D_{t+1}, X_{t+1}) = F \tag{134}$$

$$\implies L(S_{t+1}, D_{t+1}) = \frac{r_s - r - \mu}{1-\mu}, \tag{135}$$

which is lower than the equilibrium collision probability when satellites are infinitely lived ($\mu = 0$), i.e. $\frac{\partial L}{\partial \mu} < 0$. Intuitively, the fact that the satellite will stop generating payoffs at some point reduces its expected present value, and with it the incentive to launch. All else equal, shorter lifetimes reduce the equilibrium collision probability. The rest of the analysis in this paper goes through with minor modifications. Equation 135 is the non-stationary discrete-time analog of the physico-economic equilibrium condition in Definition 2 of Rouillon (2020).

Satellites built for GEO tend to be longer lived than satellites launched for LEO. If shorter lifetimes tend to reduce satellite costs, then the downward shift in the collision probability isoquant from the shorter lifetimes will be balanced against the upward shift caused by higher rates of return. The net effect may be higher or lower equilibrium rates of collisions.

The distinction between exogenous and endogenous lifetimes is relevant here. The above analysis hinges on satellite lifetimes being exogenously set. This is not the case in reality. Satellite lifetimes are determined by cost minimization concerns, technological constraints, expectations of component failures, and expectations of future technological change. Incorporating all these features to realistically model the choice of satellite life along with launch decisions and their effects on orbital stock dynamics is beyond our scope in this paper, though it is an interesting area for future research. See Guyot, Rouillon et al. (2021) for an exploration of endogenous choice of satellite characteristics. The assumption that the end-of-life is random simplifies the analysis, but does not change any conclusions over imposing a pre-specified end date in this model.[37]

A.4.2 Time-varying returns and costs

Though it simplifies the analysis, the rate of return on a satellite is not constant over time. How would changes over time in these economic parameters affect our conclusions? For simplicity,

[37] This simplification could matter in a model where firms own multiple satellites and have to plan replacements.

suppose that costs, payoffs, and discount rate vary exogenously and are known in advance.[38] The open access equilibrium condition is then

$$\pi_{t+1} = (1+r_t)F_t - (1-L(S_{t+1},D_{t+1}))F_{t+1} \tag{136}$$

Equation 136 can be rewritten as

$$L(S_{t+1},D_{t+1}) = 1 + \frac{\pi_{t+1} - (1+r_t)F_t}{F_{t+1}} \tag{137}$$

$$\implies L(S_{t+1},D_{t+1}) = 1 + r_{s,t+1} - (1+r_t)\frac{F_t}{F_{t+1}} \tag{138}$$

$$\text{Letting } r_t = r \ \ \forall t \text{ and rearranging,} \tag{139}$$

$$L(S_{t+1},D_{t+1}) = \underbrace{\left(r_{s,t+1} - r\frac{F_t}{F_{t+1}}\right)}_{\substack{\text{excess return from} \\ \text{satellite ownership}}} + \underbrace{\left(1 - \frac{F_t}{F_{t+1}}\right)}_{\substack{\text{capital gains} \\ \text{from changes in} \\ \text{satellite launch cost}}} . \tag{140}$$

If $\pi_{t+1} > (1+r)F_t$, then the one period return on a satellite is greater than the gross return on the launch cost from the safe asset, and the collision probability will be 1. Ignoring that corner case, the equilibrium collision probability is decreasing in the current cost of launching a satellite, but increasing in the future cost of launching a satellite. All else equal, the collision probability in $t+1$ will be lower when F_{t+1} increases. This highlights the role of the launch cost under open access: if firms enter until zero profits in each period, future increases in the cost deter firms from entering in the future, increasing the value of satellites already in orbit. Alternately, the equilibrium collision probability can be decomposed into two components: one representing the excess returns of satellite ownership, and the other representing the capital gains from changes in the cost of launching a satellite under open access.

When the costs and payoffs are time-varying, the equilibrium set is still a collision probability isoquant, though the isoquant selected may vary over time. These changes do not affect the physical dynamics or the Kessler threshold, though they may affect how close the selected equilibrium is to the threshold. If the parameters vary so that the ratio $\frac{\pi_{t+1}-(1+r)F_t}{F_{t+1}}$ is stationary, then the equilibrium set will stay on the same isoquant.

A.4.3 Occupancy elasticity of satellite revenues

Satellite applications generally require transmissions to and from the Earth. These transmissions may be the satellite's main output or incidental to its operation. In both cases, satellite

[38] Uncertainty over costs, payoffs, and discount rates doesn't change the qualitative results, though it introduces expectations over the changes. Endogeneity in the changes, for example due to investment in R&D or marketing, may have more significant consequences which are beyond the scope of this paper.

operators must secure spectrum use rights from the appropriate national authorities for their broadcast and receiving locations. How will spectrum management affect collisions and debris growth?

Spectrum congestion degrades signal quality, making the per-period output of a satellite decreasing in the number of satellites in orbit, i.e. $\pi = \pi(S), \pi'(S) < 0$. A similar form can result from the costs of maneuvering to avoid collisions with other satellites. If satellites are launched only when they have appropriate spectrum rights and spectrum use is optimally managed, then firms will be forced to account for their marginal effects on spectrum congestion in their decision to launch or not. The equilibrium condition would then become

$$L(S_{t+1}, D_{t+1}) = r_s(S_{t+1}) + r_s'(S_{t+1}) - r, \tag{141}$$

where $r_s'(S_{t+1}) = \pi'(S_{t+1})/F < 0$ by assumption. The equilibrium set would no longer be a collision probability isoquant, although it would still be a manifold in the state space. Even if it is not managed optimally, spectrum congestion will reduce the equilibrium collision probability by reducing the rate of excess return on a satellite.[39] For tractability, we do not incorporate this feature into our model.

Open access orbit use will still be inefficient. Although spectrum congestion can reduce the chance of Kessler Syndrome, efficient spectrum management will not incorporate the marginal external cost of collisions and debris growth, $\xi(S_{t+1}, D_{t+1})$. Collision and debris growth management policies could be implemented through spectrum pricing. The rest of the analysis in this paper still goes through when spectrum congestion is considered, though some proofs become more complicated since the equilibrium set is no longer a collision probability isoquant.

Mathematically, this modification would also apply to price effects induced by additional firms entering a particular orbit. Such effects may be relevant for orbits where the dominant satellite application does not face terrestrial competition, such as satellite imaging in sun-synchronous orbits. In orbits where the price of the service provided by satellites is pinned down by terrestrial applications, such as LEO or GEO internet or television service provided to urban areas, either the baseline model where r_s is constant or the interpretation of $r_s'(S)$ as spectrum congestion is appropriate. Both spectrum and price effects may be relevant for applications which require substantial spectrum use and face little terrestrial competition, such as satellite telecom service to remote areas. We put the spectrum congestion interpretation first since all satellites require some spectrum and could interfere with each other regardless of application, whereas price effects are application-specific. Price effects, however, can be

[39] If spectrum use were also under open access then the marginal congestion effect ($r_s'(S_{t+1})$) would not be in the equilibrium condition, but the equilibrium set would still not be a collision probability isoquant.

orbit-agnostic in the sense that satellite systems in different physical orbits may have price effects on each other if they compete in the same market.

A.5 Simulation and estimation methods

In this section we describe how we simulate our model and compute the growth of the space economy as a whole.

A.5.1 Simulating a single open access path

Given the theoretical ambiguity of the sign of ε and the statistically insignificant estimate of η_2, we conduct our simulations using values of ε and *mean* values of η_1^{π} sampled from their bootstrapped joint distribution, and *mean* values of η_1^{F} sampled from their bootstrapped joint distribution. To generate annual variation in π_t and F_t, we then draw from their conditional distributions given the mean values drawn for the simulation as a whole. We show the bootstrapped distributions of the occupancy elasticity, revenue growth, and cost growth parameters in figure 9. We describe our procedure for a single simulated open-access path more precisely in algorithm 1. We run this procedure 1000 times to generate an ensemble of open-access paths. We set the launch constraint $\bar{X} = 261$, the maximum number of total launches to the 600-650 km shell observed over the 2006-2019 horizon.

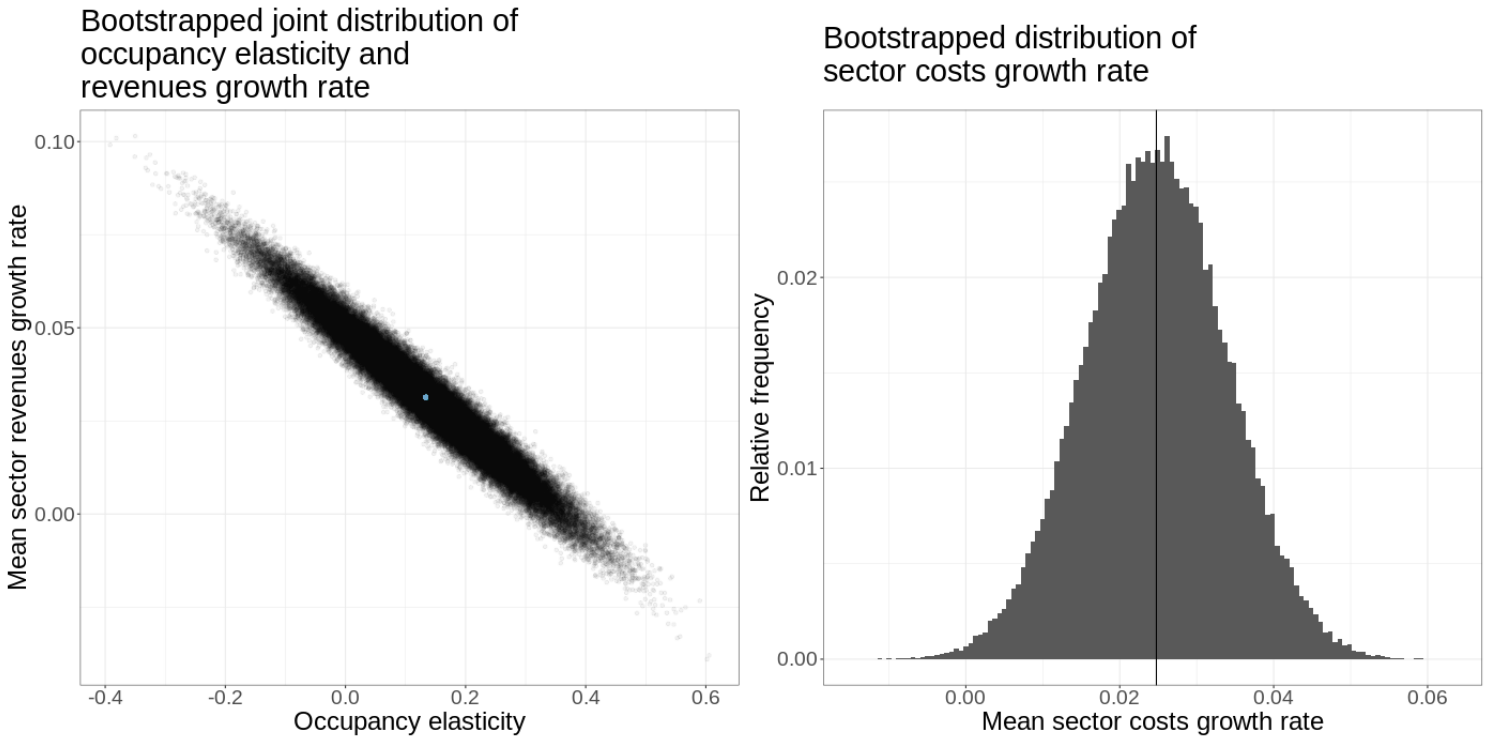

Figure 9: Bootstrapped distributions of occupancy elasticity, revenue growth, and cost growth parameters. Panel a shows the joint distribution of occupancy elasticity and revenue growth parameter estimates, and the blue dot marks the main model estimates. Panel b shows the distribution of cost growth parameter estimates, and the vertical line marks the main model estimate.

A.5.2 Calculating the growth of the space economy

To calculate the size of the space economy during simulations, we regress the size of the excluded sectors (suborbital commercial human spaceflight deposits, direct-to-home television) on the remaining sectors modeled in equations 37 and 38 using historical data from 2006-2019. The regression equation is

$$y_t = \alpha + \beta_1 \pi_t + \beta_2 F_t + \nu_t. \tag{142}$$

Regression results are reported below in table 7. Since our goal is prediction rather than inference, we report summary measures of model fit along with parameter estimates. We then measure the space economy in each simulation s, period t, as $\hat{y}_{st} + \pi_{st}(S_t) + F_{st}$, and compute the CAGR as the coefficient on time in a log-linear regression of the form

$$\log(y_t) = \alpha_0 + \alpha_1 t + \nu_t^y. \tag{143}$$

Algorithm 1: Simulate an open-access path

For simulated path s, draw

$$(\eta_0^{\pi}{}_s, \eta_1^{\pi}{}_s, \varepsilon_s),\ (\eta_1^{F}{}_s, \eta_0^{F}{}_s)$$

from their respective bootstrapped distributions.

Calculate $(\gamma_{0s}, \gamma_{1s}, \gamma_{2s})$ from the regression

$$L_t = \gamma_{0s} + \gamma_{1s}\frac{\pi_{t+1}(S_t)_s}{F_t} + \gamma_{2s}\frac{F_{t-1}}{F_t} + e_t$$

using historical data from 2006-2019.

Set $(S_0, D_0) = (158, 626)$, i.e. the 2020 initial condition for the 600-650 km shell.

for $t \in \{1, \ldots, T\}$ **do**

  Draw $\eta_1^{\pi}{}_{st}$ and $\eta_1^{F}{}_{st}$ from their conditional distributions given $(\eta_0^{\pi}{}_s, \varepsilon_s)$ and $\eta_0^{F}{}_s$, respectively.

  Calculate the open-access launch rate $X_{st} \in [0, \bar{X}]$ such that

$$L(S_{t+1}, D_{t+1}) = \gamma_{0s} + \gamma_{1s}\frac{\pi_{st+1}(S_{t+1})}{F_{t+1}} + \gamma_{2s}\frac{F_t}{F_{t+1}},$$

  if such an X_{st} exists and 0 or $\bar{X}$ otherwise as per Definition 5.

  Compute summary statistics for period t.

  Propagate S_t, D_t to S_{t+1}, D_{t+1}.

  t ← t+1

end

Table 7: Results from estimating equation 142.

	Dependent variable:
	y_t
β_1	12.661^{***}
	(1.684)
β_2	0.569
	(0.447)
α	-104.922^{**}
	(38.599)
Observations	14
R^2	0.898
Adjusted R^2	0.879
Residual Std. Error	22.799 (df = 11)
F Statistic	48.408^{***} (df = 2; 11)
Note:	*p<0.1; **p<0.05; ***p<0.01

B Multiple shells and space weather

In this section we describe two physical extensions to the core theoretical model. While these are likely important in practice, data challenges limit our ability to incorporate these features in our calibrated simulations.

B.1 Open access equilibrium between multiple shells

We have so far focused on a single orbital shell in isolation. While we can expand the "shell of interest" to cover a large region, in practice this is unlikely to yield accurate results over heterogeneous regions and use cases. Consider two orbital shells, H and L, with access costs $F^H > F^L$ and equal payoffs π. What would open access imply for the collision risks between the shells? Letting H superscripts index the higher orbit and L superscripts index the lower one, the new laws of motion are

$$
\begin{aligned}
S^H_{t+1} &= S^H_t(1 - L^H(S^H_t, D^H_t)) + X^H_t \\
D^H_{t+1} &= D^H_t(1 - \delta^{HE} - \delta^{HL}) + G(S^H_t, D^H_t) + \mu_L X^H_t + \delta^{LH} D^L_t \\
S^L_{t+1} &= S^L_t(1 - L^L(S^L_t, D^L_t)) + X^L_t \\
D^L_{t+1} &= D^L_t(1 - \delta^{LE} - \delta^{LH}) + G(S^L_t, D^L_t) + \mu_L X^L_t + \delta^{HL} D^H_t
\end{aligned}
$$

with the debris transport matrix

$$\mathbf{D} = \begin{array}{c} \\ H \\ L \\ E \end{array} \begin{array}{c} \begin{array}{ccc} H & L & E \end{array} \\ \left\| \begin{array}{ccc} 1-\delta^{HL}-\delta^{HE} & \delta^{HL} & \delta^{HE} \\ \delta^{LH} & 1-\delta^{LH}-\delta^{LE} & \delta^{LE} \\ 0 & 0 & 1 \end{array} \right\| \end{array},$$

where E represents the Earth. All transport coefficients are bounded in $[0,1]$ and sum to 1 across rows, with row labels indexing the source of debris and column labels indexing the destination.

The Bellman equations for the launch decision are now

$$Q_t^H = \pi + \frac{1}{1+r}(1-L_t^H)Q_{t+1}^H \tag{144}$$

$$Q_t^L = \pi + \frac{1}{1+r}(1-L_t^L)Q_{t+1}^L \tag{145}$$

$$V_{it} = \max_{x_{it}\in\{0,L,H\}} \{\mathbb{1}(x_{it}=0)\beta V_{t+1} + \mathbb{1}(x_{it}=H)[\frac{1}{1+r}Q_{t+1}^H - F^H] \tag{146}$$

$$+ \mathbb{1}(x_{it}=L)[\frac{1}{1+r}Q_{t+1}^L - F^L]\}, \tag{147}$$

where we suppress function arguments and use time subscripts for brevity (though these are still infinite-horizon Bellman equations). In an open-access equilibrium, the payoffs from owning a satellite in either shell should be zero, i.e.

$$(X_t^H, X_t^L) : V_{it} = 0 \implies \frac{1}{1+r}Q_{t+1}^H - F^H = 0,\ \frac{1}{1+r}Q_{t+1}^L - F^L = 0 \tag{148}$$

$$\implies \frac{1}{1+r}[\pi + (1-L_{t+1}^H)F^H] - F^H = 0,\ \frac{1}{1+r}[\pi + (1-L_{t+1}^L)F^L] - F^L = 0 \tag{149}$$

$$\implies \pi = rF^H + L_{t+1}^H F^H,\ \pi = rF^L + L_{t+1}^L F^L \tag{150}$$

$$\implies rF^H + L_{t+1}^H F^H = rF^L + L_{t+1}^L F^L \tag{151}$$

$$\implies \frac{F^L}{F^H} = \frac{r + L_{t+1}^H}{r + L_{t+1}^L} \tag{152}$$

In this case the cheaper orbit will have higher equilibrium collision risk, e.g. if the lower orbit is cheaper to access then the higher orbit will have lower equilibrium collision risk:

$$F^L < F^H \implies L_{t+1}^H < L_{t+1}^L. \tag{153}$$

If the payoffs earned by satellites in either shell are not identical, but rather π^H and π^L with

$\pi^H = \pi^L + \gamma$, then we have

$$\frac{F^L}{F^H} = \frac{r + L^H_{t+1} - \frac{\gamma}{F^H}}{r + L^L_{t+1}} \tag{154}$$

If the lower orbit is cheaper to access, $F^L < F^H \implies L^H_{t+1} - \frac{\gamma}{F^H} < L^L_{t+1}$. This gives us two possibilities:

- If the higher orbit generates greater payoffs, either orbit may be riskier in equilibrium depending on how big the return premium to the higher orbit is: $\gamma > 0 \implies L^H_{t+1} \lesseqgtr L^L_{t+1}$.
- If the lower orbit generates greater payoffs, then the higher orbit will have lower equilibrium collision risk: $\gamma < 0 \implies L^H_{t+1} < L^L_{t+1}$.

The physical and economic dynamics in the multi-shell setting are likely richer than those of the single-shell setting. Rao and Letizia (2021) describe a roadmap for how multiple shells could be incorporated in integrated assessment models of orbit use, noting that economic data limitations greatly impede the scope of model applications. Given these challenges, we do not consider multiple shells in this paper.

B.2 The effects of space weather

Proposition 5 suggests parameter changes which lower the open-access steady-state debris level may still cause short-run rebound effects. Sunspot activity ("space weather") is a driver of environmental processes in orbit which can cause such parameter changes. Sunspots induce differential heating of the Earth's atmosphere, causing it to expand and contract over time and changing the radiation pressure exerted on satellites. These changes increase the debris decay rate, and force satellites to expend more fuel to remain in their intended orbit. Formally, suppose sunspots cause decay rates to vary periodically with mean $\bar{\delta}$, making the laws of motion

$$\begin{aligned} S_{t+1} &= S_t(1 - L(S_t, D_t)) + X_t \\ D_{t+1} &= D_t(1 - \delta_t) + G(S_t, D_t) + mX_t \end{aligned}$$

If the variations are exogenous and publicly known, there are no further changes to the firm or planner's Bellman equations. Figure 10 shows an example of debris rebound effects under discrete changes to the decay rate.

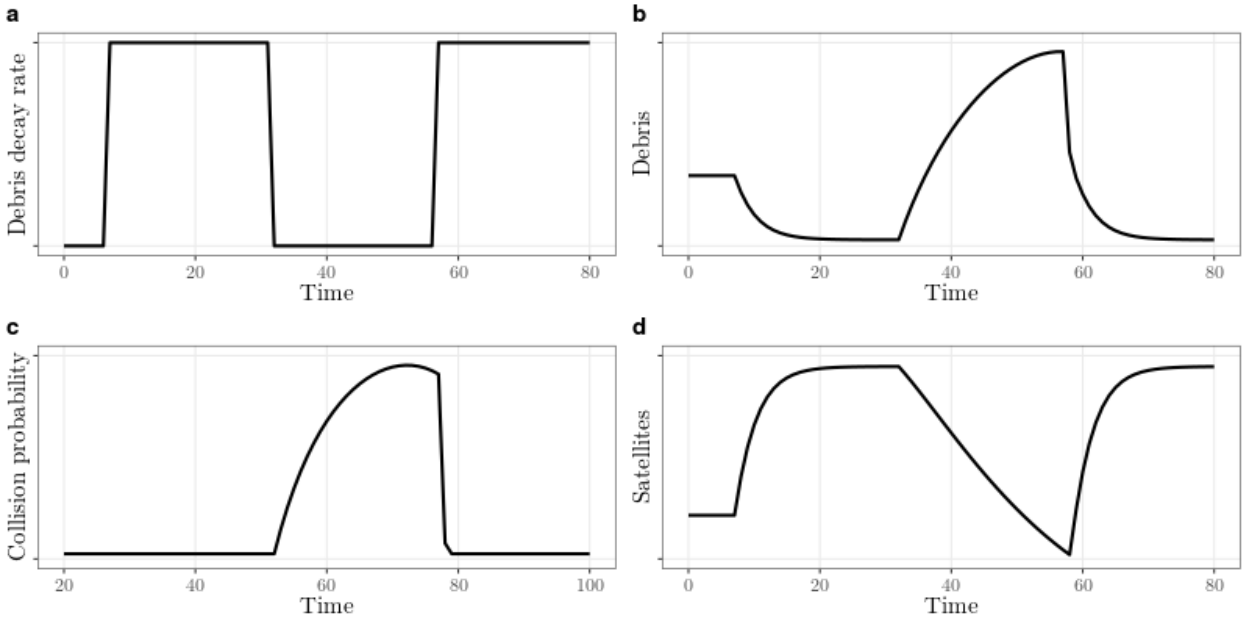

Figure 10: Panel a shows the debris decay rate varying over time. Panels b-d show equilibrium debris stock, equilibrium collision probability, and equilibrium satellite stock responding to the changes in the decay rate. The initial increase in the decay rate reduces the debris stock and allows more satellites to be sustained. When the decay rate falls, the debris stock grows rapidly and the satellite stock falls. This growth in debris causes the collision probability to rise above the equilibrium level, which stops launch activity. The growth in debris is halted only by the decay rate once again increasing. Once the collision probability is back in equilibrium, new satellites are again launched to take advantage of the higher decay rate.

Such variability in the decay rate will make the basin of attraction to the stable steady state expand (high sunspot activity) and contract (low sunspot activity), potentially leading to Kessler Syndrome. To see how this can occur, suppose we begin from the stable steady state during a period of low sunspot activity. When sunspot activity increases, it raises the debris decay rate and expands the stable basin to cover more of the equilibrium isoquant. The equilibrium isoquant itself remains unchanged but the stable steady state moves along it to a point where the debris stock is lower and the satellite stock is higher. When the sunspot activity dies down again, the stable steady state moves back to its original location and the stable basin contracts back to its original size. However, if the newly-contracted basin no longer covers the high-sunspot-activity steady state, Kessler Syndrome will occur. Similar paths which cause Kessler Syndrome are possible if periods of overshooting coincide with periods of reduced sunspot activity. Launch rate caps which control overshooting and limit the reachable portions of the equilibrium isoquant can help manage these dynamics.

As the sunspot activity increases, firms will have incentives to take advantage of the increased renewal by launching more satellites. The net effect may be an increase or decrease the equilibrium amount of debris. As the activity decreases, firms will reduce the launch rate,

again with ambiguous effects on the equilibrium amount of debris. These effects will be offset by the extent to which sunspot activity increases the cost of operating a satellite, e.g. by increasing the necessary fuel expenditures on stationkeeping.

Increases in the decay rate have the benefit of shifting the Kessler threshold up. If the net increase in debris due to the launch response is not too large, then increased sunspot activity may stabilize orbit use. On the other hand, if the rebound effect for decay rates is strong enough, sunspot activity may push the equilibrium debris level into the basin of the Kessler region. Even when the rebound effect is not very strong, a decrease in the decay rate at the end of a period of extra sunspot activity may make the original open-access steady state locally unstable given the increase in debris due to the rebound effect. Given the lack of data regarding radiation shielding and maneuvering capabilities for current and future satellites, and to keep the model relatively simple, we do not incorporate these features in our simulations.